Defense Nuclear Agency
Alexandria, VA 22310-3398

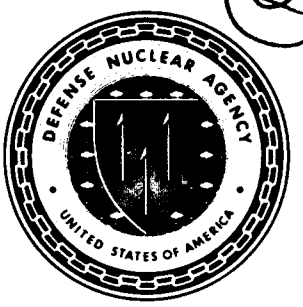

DNA-TR-89-193

Wind-Aided Firespread Across Arrays of Discrete Fuel Elements

Francis E. Fendell
George F. Carrier
Michael F. Wolff
TRW, Inc.
TRW Space and Defense
One Space Park
Redondo Beach, CA 90278-1071

October 1990

Technical Report

CONTRACT No. DNA 001-86-C-0297

Destroy this report when it is no longer needed. Do not return to sender.

PLEASE NOTIFY THE DEFENSE NUCLEAR AGENCY, ATTN: CSTI, 6801 TELEGRAPH ROAD, ALEXANDRIA, VA 22310-3398, IF YOUR ADDRESS IS INCORRECT, IF YOU WISH IT DELETED FROM THE DISTRIBUTION LIST, OR IF THE ADDRESSEE IS NO LONGER EMPLOYED BY YOUR ORGANIZATION.

DISTRIBUTION LIST UPDATE

This mailer is provided to enable DNA to maintain current distribution lists for reports. We would appreciate your providing the requested information.

NOTE:
Please return the mailing label from the document so that any additions, changes, corrections or deletions can be made more easily.

☐ Add the individual listed to your distribution list.

☐ Delete the cited organization/individual.

☐ Change of address.

NAME: _____

ORGANIZATION: _____

OLD ADDRESS	CURRENT ADDRESS
_____	_____
_____	_____
_____	_____

TELEPHONE NUMBER: ( ) _____

SUBJECT AREA(s) OF INTEREST:

_____	_____
_____	_____
_____	_____

DNA OR OTHER GOVERNMENT CONTRACT NUMBER: _____

CERTIFICATION OF NEED-TO-KNOW BY GOVERNMENT SPONSOR (if other than DNA):

SPONSORING ORGANIZATION: _____

CONTRACTING OFFICER OR REPRESENTATIVE: _____

SIGNATURE _____

CUT HERE AND RETURN

Director
Defense Nuclear Agency
ATTN: TITL
Washington, DC 20305-1000

Director
Defense Nuclear Agency
ATTN: TITL
Washington, DC 20305-1000

REPORT DOCUMENTATION PAGE

Form Approved
OMB No. 0704-0188

1. AGENCY USE ONLY (Leave blank)	2. REPORT DATE	3. REPORT TYPE AND DATES COVERED
	901001	Technical - 860926-890831

4. TITLE AND SUBTITLE
Wind-Aided Firespread Across Arrays of Discrete Fuel Elements

5. FUNDING NUMBERS
C - DNA 001-86-C-0297
PE - 62715H
PR - RG
TA - RR
WU - DH012980

6. AUTHOR(S)
Francis E. Fendell, George F. Carrier and Michael F. Wolff

7. PERFORMING ORGANIZATION NAME(S) AND ADDRESS(ES)
TRW, Inc.
TRW Space and Defense
One Space Park
Redondo Beach, CA 90278-1071

8. PERFORMING ORGANIZATION REPORT NUMBER

9. SPONSORING/MONITORING AGENCY NAME(S) AND ADDRESS(ES)
Defense Nuclear Agency
6801 Telegraph Road
Alexandria, VA 22310-3398

RARP/Hartley

10. SPONSORING/MONITORING AGENCY REPORT NUMBER
DNA-TR-89-193

11. SUPPLEMENTARY NOTES
This work was sponsored by the Defense Nuclear Agency under RDT&E RMC Code B4662D RG RR 00004 SPTD 3450A 25904D.

12a. DISTRIBUTION/AVAILABILITY STATEMENT
Approved for public release; distribution is unlimited.

12b. DISTRIBUTION CODE

13. ABSTRACT *(Maximum 200 words)*

The rate v_f of wind-aided firespread across an array of very-small-diameter, discrete fuel elements is sought, as a step toward the objective of predicting the advance in time of a firefront through either strewn debris in a heavily-blast-damaged scenario or through brush-and-grass-type wildlands. Here, the quasisteady rate (if one exists) is sought for conditions under which there is both (1) a wind whose mean speed U is constant and whose direction is constant, and (2) a horizontal bed with a macroscopically uniform fuel distribution m. More precisely, m is the mass of fuel (per unit planform area of the bed) consumed with firefront passage; here the fuel elements are thin, so the fuel consumed is identical with the fuel loading initially present, if fire propagates at all. Laboratory-scale experiments in a specially dedicated fire-tunnel, with supplementary approximate analysis, are reported. Extensive testing suggests that v_f varies with $(U/m)^{1/2}$ over a wide, but obviously finite, range of the parameters U and m. Only if the thin-fuel loading m approaches the rather large value of very roughly 2 g/cm^2 is radiative transfer likely to play a role comparable to that of convection/diffusion for preheating. The next direction for research is suggested to be wind-aided firespread across more clumped fuel distributions.

14. SUBJECT TERMS
Fire Dynamics
Flamespread
Fire Propagation
Wind-aided Fire Spread

15. NUMBER OF PAGES
144

16. PRICE CODE

17. SECURITY CLASSIFICATION OF REPORT	18. SECURITY CLASSIFICATION OF THIS PAGE	19. SECURITY CLASSIFICATION OF ABSTRACT	20. LIMITATION OF ABSTRACT
UNCLASSIFIED	UNCLASSIFIED	UNCLASSIFIED	SAR

Wind velocity; Fire storms; Nuclear explosion
Simulation; Flame propagation. (MM)

CLASSIFIED BY:

N/A since Unclassified

DECLASSIFY ON:

N/A since Unclassified

PREFACE

The technical suggestions, cooperation, and encouragement in the early stages of this work by Michael Frankel are very gratefully acknowledged. This work was helpfully guided in its later stages as a result of many informative discussions with Randy Rohr, Cliff McFarland, and George Ullrich. The authors also wish to thank Nahum Gat for overseeing the experimental effort; Ethel Johnson and Gail Takahashi for the editing and processing of the manuscript; and Barbara Hetzel and Darren Way for the preparation of the fuel beds for testing.

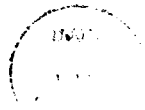

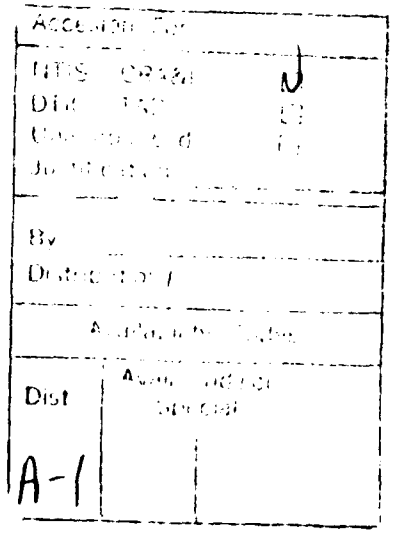

TABLE OF CONTENTS

LIST OF ILLUSTRATIONS

LIST OF ILLUSTRATIONS (Continued)

LIST OF ILLUSTRATIONS (Continued)

LIST OF ILLUSTRATIONS (Continued)

LIST OF ILLUSTRATIONS (Continued)

LIST OF TABLES

SECTION 1

FIRE EFFECTS IN A THERMONUCLEAR AFTERMATH

Relative to what is known concerning the consequences of blast, prompt radiation, and radioactive-material fallout, comparatively little is known about fire effects in a thermonuclear aftermath (Glasstone and Dolan 1977). This limited predictive capability seems at least partially attributable to the dedication of comparatively limited resources to the investigation of fire effects. Because no canonical, standard fire behavior seems identifiable, and because fire effects seem particularly meteorologically dependent, this limited effort is understandable. In fact, however, aside from very-short-term thermonuclear effects, other postexplosion events also can be meteorologically dependent (witness the role of thermal layers, which can result in highly nonideal blast-wave structure and soil scouring, or the role of tropospheric winds and stratification on dry and wet deposition of fallout). If fire effects are to be knowledgeably included with other post-thermonuclear effects for purposes of strategic-weapon targeting, a stronger technical base for decision making seems desirable.

A fundamental goal in assessing post-thermonuclear fire effects is achieving an estimate of what matter burns how soon (if it burns at all), given the areal density of the combustible and inert material (the "loading"), the meteorological environment, and the topography of the vicinity of the target. This goal may be restated as seeking an estimate of the rate and direction of firespread (i.e., the rate and direction of fire propagation from combustible material already alight to combustible material not yet involved with burning).

Assigning the phenomenon of firespread this priority is not without alternatives. For example, preliminary to firespread is the phenomenon of ignition, effected in a thermonuclear context by (1) preblast arrival and postblast-arrival radiative heating of combustible matter, and (2) the consequences of blast effects, which can knock down power lines, disrupt gas mains and liquid-fuel-storage facilities, etc. Of course, the interaction of blast arrival with fires initiated by blast-precursive radiation is varied, since an ignited object may be broken into many pieces

(some serving as torches, some too small for burning to be sustained), and forced-convective extinction of fire sustained by noncharring fuels may occur--though most burning synthetic and natural polymers form near-surface heat-retaining char layers that sustain the outgassing of combustible vapor, and hence the polymers typically relight after the brief (few-second) interval of high blast-associated winds. The point of view adopted here is that, within the range of free-burning fire phenomena, ignition criteria are relatively well investigated, understood, and quantified (Glasstone and Dolan 1977). Furthermore, many ignitions arise from difficult-to-anticipate circumstances dependent on the time of day or season of the year or meteorological conditions or extent of preparedness or whether fire-safety infractions are incurring, etc. It seems reasonable to anticipate that ignitions inevitably will occur in a thermonuclear aftermath. The key issue is whether fire spreads from the sites of ignition, and, if so, how quickly and in what directions. Knowledge of firespread is essential to assessing the viability of fire-fighting countermeasures (the pertinent parameters include available time, manpower, equipment, communication, transport, water distribution, and visibility), to assessing the adequacy of natural or man-made firebreaks, and, in general, to anticipating what the fire effects will be.

Predictive capability concerning the structure-to-structure spread of fire in an urban or suburban setting is in a primitive state because, aside from incendiary or thermonuclear bombing, such spread is a rare event associated with natural disasters (earthquakes, hurricanes) or violent accidents (huge explosions and detonations, usually of munitions or propellants). The fire-safety regulations and fire-fighting capabilities of technologically advanced countries tend to limit large-area fires in the twentieth century to wildlands or to portions of communities at the wildlands/suburban interface, though counterexamples certainly can be cited (Pyne 1985). To the knowledge of the authors, there is no agency (other than the Defense Nuclear Agency) supporting investigations into block-scale or neighborhood-scale burning, and the modeling of the dynamics of very large wildland fires seems not to be a major undertaking of even the Forest Service. The rudimentary state of the topic is suggested by the current uncertainty concerning the quantitative criteria for the relative

importance of radiative transfer and of convection/conduction in the preheating of uninvolved combustible matter (henceforth referred to as fuel) to its pyrolysis condition. It was in this context that the present firespread investigation, combining laboratory-scale experiment and approximate simplistic theoretical modeling, was undertaken. (A discussion of methodology for the investigation of urban-scale firespread is undertaken in Section 2.)

Although the present investigation is concerned with firespread in an urban/suburban setting, there are parameter ranges in which wildland-firespread experience is pertinent. In wildlands, a multisized (by diameter and height) fuel loading is perennially present, hot and dry spells of weather periodically arise in many geographic areas, and unwanted ignitions frequently occur (owing to lightning, arson, accidents in commercial activity such as logging, carelessness in recreational use, etc.). In fact, the greatness of the fire danger is intermittently such that fuel-loading reduction and/or elimination by so-called prescribed burning is practiced in many areas of the globe; furthermore, intentional burning is used to remove residual organic matter from harvested forests and tilled areas, both as a low-cost convenience and/or as a promoter of regeneration. However, it is only with the arising of strong sustained winds in conjunction with drought, heavy accumulation, and ignitions that routine fire events, normally unreported, become front-page episodes, even historical watersheds (Noble 1977; Pyne 1982; Simpson 1989). The relatively rapid spread of fire under wind aiding may arise via buoyancy-induced flow during upslope runs. So-called active crown fires arise only in connection with high winds (Fendell 1986). Such "blowups" persist as long as the winds are sustained, unless a firebreak, effective against even firebrands, along the path of spread is encountered. For a large complex of fires, generally only a prolonged interval of cool moist weather, including significant precipitation, terminates the spread, or at least facilitates containment and control. Accordingly, on the basis of wildlands experience, emphasis in the work to be reported is on flow-assisted firespread across beds of discrete fuel elements.

Wildlands fuels include live vegetation with appreciable moisture content (typically equal to, or exceeding, the dry weight, for thin-diameter fuels), whereas the dead wood used in construction is typified by appreciably lower moisture content (even shortly after rainfall, since there is fairly rapid adjustment of dead wood to ambient conditions). Thus, the moisture content of the fuel tends to be important for wildlands firespread, because the fuel is virtually fully desiccated even of "bound" water before it is pyrolyzed, and an often nontrivial heat requirement is associated with the desiccation. But with respect to the importance of the role of moisture content on the rate of firespread in the urban-suburban context, the wildlands experience may be misleading.

Finally, in the aftermath of a large thermonuclear explosion, one expects particularly strong blast effects close to the hypocenter, and diminished blast damage at greater lateral distances from the hypocenter. One also anticipates more ignitions in the strewn debris in close to the hypocenter, and fewer ignitions at greater lateral distances, where the fuel distribution is more "clumped." In fact, in close to the hypocenter the fire serves mainly to transform heavily damaged homes and structures into carbonaceous residue; this vigorous burning in the early hours after the thermonuclear event is primarily of interest in conjunction with the rapid lofting of smoke, soot, and other combustion products (including water vapor), into a tall central convective column. The convectively induced advection retards laterally outward firespread from the sites of ignition because such spread is against the wind. This central-buoyant-column-dominated, early stage of the post-thermonuclear fires is mainly of specialized interest in connection with (1) hypothesized long-term, global effects related to climatic cooling and reduction of incoming solar radiation, and (2) shorter-term, more localized consequences of lofted dust and smoke (the so-called "fog of war"), whereby the efficacy of high-altitude sensors operating in the infrared and visible portions of the electromagnetic spectrum is significantly reduced. As the fire intensity is mitigated after a few hours, laterally outward propagation in the direction of the prevailing ambient winds occurs. The fires in the distributed, small-diameter rubble closer to the hypocenter center serve to sustain and propagate burning that later may inflict damage at large

distances from the hypocenter, at sites at which blast damage is slight or virtually negligible. Thus, the fires in the more closely spaced, thin fuel elements typical of strewn debris give the locus of the burning front at an earlier time, a prerequisite to inferring the position of the firefront locus at some later time. In this way it seems reasonable (in a systematic approach linked to the sequence of events in a thermonuclear aftermath) to treat firespread across beds of closely spaced, thin fuel elements as a first step, and only then to proceed on to firespread among the larger, more isolated fuel elements with "internal structure" (i.e., fuel elements simulating houses and buildings, with hollow cores, ceilings, and internal fuel loading representative of furniture, finishing materials, etc.). Accordingly, attention is focused here on flow-assisted firespread across beds of close-proximity, thin-diameter wooden fuel elements, as a prerequisite to treating firespread across clumped fuel distributions typifying sites mostly unaltered by blast damage. For completeness, it is noted that, in wildlands, the thermally thin, leaf-and-twig-type component of the fuel distribution [that is, the fraction (of the total fuel loading) which is of less than (say) one-centimeter thickness, and hence more readily desiccated and pyrolyzed] often is consumed with firefront passage. The thicker fuel elements mainly serve (as do rocks and other inert matter) as heat sinks during firefront passage; thicker fuel elements are burned after firefront passage, if ever burned at all. Thus, for estimation of the rate of firespread, the emphasis on the amount and the properties of small-diameter fuel elements in multisized fuel distributions seems appropriate.

SECTION 2

METHODOLOGY

Fire experiments on an urban scale are prohibitive for reasons of cost, and perhaps prohibited for reasons of environmental concern. Predictions ultimately must be made by a computer-code simulation. (Engineering judgment must be exercised in assessing the plausibility of predictions made by a computer code for a scale of phenomena for which it has never been tested.) To the knowledge of the authors, a candidate fire-effects computer code does not exist. One goal of near-term research is to help determine the desired characteristics of such a computer code, and to establish a systematic procedure for validating the code. However, in view of the present state of limited understanding of needs and capabilities, it may be premature even to initiate the development of an urban-scale fire-effects "hydrocode".

An alternate approach is to undertake jointly experimental and theoretical projects that pursue fire effects over a sequence of spatial scales, by proceeding from small laboratory scale to large enclosed-facility scale to small field scale to large field scale. The reasons for commencing on smaller scale and proceeding subsequently to larger scale are many. On smaller scale, there is more control of test conditions [so that the prescribed experiment can be executed without delay and without change (during a test) of nominally fixed constraints, and the experiment can be repeated], relatively small cost per test, rapid turnaround time (so that relatively little calendar time need elapse between tests), and relatively complete and delicate instrumentation is feasible. In fact, the development, hardening, calibration, and siting of instrumentation can be advanced on laboratory scale, for later use in larger-scale tests. Some phenomena important at large scale are not readily reproduced in a laboratory-scale, wind-aided-firespread experiment, such as wind gustiness, (prescribed) air-stream relative humidity, and radiative transfer. However, this circumstance may be an asset in that only a subset of the total range of concerns need be addressed at early stages of an investigation. Attention may later be concentrated on the initially

underplayed effects, since understanding of the initially present subset of effects presumably by then will be well in hand. In any case, since larger-scale tests are more costly, executable only at longer calendar intervals, and harder to control and instrument, there typically will be fewer of such tests, and the need for each one to be informative if programmatic objectives are to be achieved is more critical. Therefore, seeking insight at the outset via experimentation at smaller scale seems judicious. A frequently incremented bank of experimental data, that often can be extended (on request) to any of a wide range of parametric assignments, seems advantageous for the development and upgrading of a concomitant theoretical-prediction capability. Again, because only a subset of the total number of ultimately relevant phenomena may enter significantly at the smaller scales for which laboratory-scale experimental testing is executed, there is greater probability that the theoretical model will not be overwhelmed at the outset of its development. Rather, the opportunity for the theoretical model to be evolved in tractable stages (i.e., levels of sophistication) is enhanced.

Ultimately, it is clearly indispensable that preliminary insights achieved on the basis of laboratory-scale and small-field-scale experiments be tested on the scale of the event of interest (or, in the context of urban-scale fire, on as large a scale as feasible). The factor of the unexpected furnishes a major motivation for proceeding to tests on larger scale. However, for firespread across a bed of thin discrete fuel elements, no very large extrapolation may be necessary. It is indicated in the text to follow that, for thin fuels, the rate of propagation of the flaming front is primarily a function of two parameters, the ambient wind speed U and the fuel loading m, where m is the mass of fuel (consumed with firefront passage) per unit planform area of the fuel bed. The wind speeds attainable in the TRW laboratory facility (Fleeter et al. 1984; Beach et al. 1986) approach 5 m/s and fuel loadings approach 0.3 g/cm^2. Thus, the wind speeds are comparable to values of interest in commonplace situations. The fuel loadings are comparable to the total thin-fuel loading (both in the canopy and in the understory) in a typical Canadian conifer stand (B. Stocks, private communication); are within a factor of ten of loadings in typical American urban/suburban areas; and are within a factor of 50 of

the extraordinarily high fuel loadings that characterized the Hammerbrook section of Hamburg, Germany, in which a firestorm was induced by massive incendiary/high-explosive bombing on 27-28 July 1943 (Carrier, Fendell, and Feldman 1985; Carrier and Fendell 1986). Hence, at least with respect to key parameters for wind-aided firespread across thin-fuel distributions, there is required no large extrapolation of observations from the parametric conditions attainable in a laboratory facility.

This section on methodology is concluded with the comment that the major impediment to the development of a hydrocode to predict the position of the locus of a propagating firefront at some later time, given its position at some earlier time, is probably not associated with the capacity of computer hardware to permit the user efficiently to store, retrieve, manipulate, and display data relating to fuel loading, meteorological conditions, and topography--although production of the required software would require a considerable investment of time, money, and effort. If the capacity existed to infer the fire-propagation rate and direction for a given postulated ignition pattern, the capacity could be exercised for an alternate ignition pattern, so that the sensitivity to the (difficult-to-anticipate) ignition pattern can be examined. What currently limits this capacity is uncertainty concerning the physically relevant "rules" by which the firefront position evolves in a given fuel bed under known wind aiding. [Incidentally, only that component of the wind perpendicular to the local tangent to the firefront locus serves to aid (or to oppose) spread; the component of the wind tangential to the front does not much alter firespread. For this reason, the ellipsoidal locus of a firefront evolving from a local ignition in a constant wind tends to develop ever-more-unequal axes in time, in plan view.] This project is dedicated to reducing this uncertainty concerning the physically pertinent rules for firespread.

SECTION 3

WIND-AIDED FIRESPREAD ACROSS ARRAYS OF DISCRETE FUEL ELEMENTS

3.1 INTRODUCTION.

Fire propagates through a mixed-size array of fuels at the rate at which the thermally thin fuels (i.e., the fuels well described as isothermal) are desiccated and heated to their onset-of-pyrolysis temperatures. Thicker fuels may act primarily as heat sinks during firefront passage, though these fuels may eventually burn well upwind of the firefront. Although a fire "jumps" forward discontinuously through discrete-element fuel beds, the rate of spread usually may be taken as effectively continuous for the time scales of practical interest.

Though spread can occur against the wind or in the absence of an ambient wind, attention here is focused on the faster rate of propagation observed under wind aiding. Well-defined (repeatable) arrays of identical, vertical, regularly arranged, small-equivalent-diameter, matchstick-like, wooden fuel elements are examined for the most part, though some tests with beds of elements of varied diameters (but generally uniform height), and with beds including inert as well as combustible elements, are undertaken. Reference to the wind speed is to the ambient values; the wind in the fuel bed may be comparable (as in grasslands) or quite distinct (as in tall forest)--though the burning of the upwind fuel may reduce the impedance to the ambient wind. The quasisteady rate of spread is sought, if a quasisteady rate exists, so that one envisions an experiment with a still-to-be-involved expanse of unburned fuel downwind, a flaming front (of finite streamwise extent) whose speed of translation is sought, and an expanse of burned fuel upwind (Figure 1).

Among the unresolved issues associated with wind-aided firespread across arrays of discrete fuel elements is the preheating mechanism by which fresh downwind fuel is raised from ambient temperature to pyrolysis temperature (~600 K), as distinct from the heat-transfer mechanism significant immediately at the flaming front (at which the bulk-gas temperature may reach 1000 K to 1200 K). Emmons (1965), Rothermel and Andersen (1966), Van Wagner (1968), Emmons and Shen (1971), Steward (1974a),

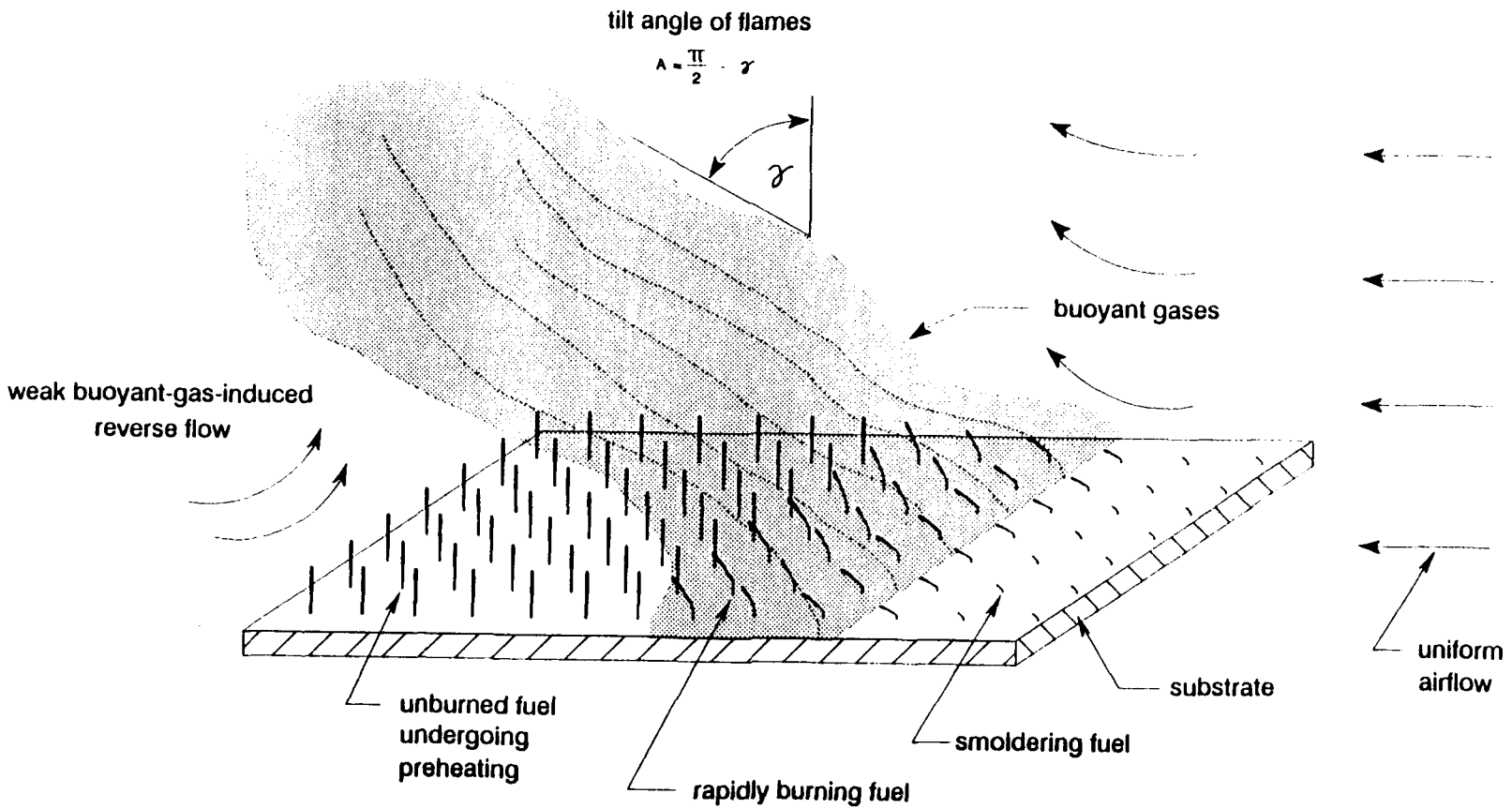

Figure 1. A schematic of the phenomenology of wind-aided firespread across a bed of identical, upright, regularly arranged, thin, wooden fuel elements, supported in holes in a substrate. Hot buoyant gases, generated at the firefront [which lies between the downwind fuel elements (undergoing preheating) and the essentially burned-out upwind fuel bed] are tilted downwind by the crosswind. Thin light strips of cloth often indicate a weak reverse flow toward the firefront from the downwind side. In the modeling, the upwind flow is idealized as uniform until arrival at the firefront.

Telisin (1974)--with some reservations, and Steward et al (1977) all take the preheating mechanism primarily to be radiative transfer, as opposed to convection, but without definitive experimental evidence. Also, Luke and McArthur (1977) and Cheney (1981) report that the rate of spread increases nearly linearly with the fuel loading, whereas Thomas (1971) reports that it varies inversely with loading--the same dependence on loading drawn theoretically by Fleeter et al. (1984) on the basis of a suggestion by Taylor (1961) that the rate of spread adjusts itself such that the entrainment requirements of a fire-generated line plume are just met by the ambient-wind crossflow. While the model may have relevance to crown fires, Taylor warns that the near-ground decrement in the ambient wind speed is overlooked in the simplistic model; furthermore, the use of weakly-buoyant-plume-type entrainment concepts in the flaming zone seems of uncertain accuracy. Also, Cheney (1981) notes that the rate of spread has been conjectured to increase linearly, quadratically, and even exponentially with the wind speed; the above-cited line-plume-in-a-crossflow model implies a cubic dependence of spread rate on wind speed (Fleeter et al. 1984).

Intuitively, it seems curious that convective-conductive preheating almost universally has been accorded a secondary role to radiative preheating, yet, almost invariably, rapid-firespread events are associated with enhanced wind-aiding (Davison 1931; Mushan 1941; Caidin 1960; Wells 1968; Noble 1977; Pyne 1982; Simpson 1989). The individual fuel elements maintain their separation in the presence of high sustained wind; however, convective transport may permit the hot "wash" (if not the flames themselves) from upwind burning fuel elements to span the distance to the nearest downwind fuel element, such that downwind element is brought to its onset-of-pyrolysis condition before the upwind elements burn out.

3.2 NOTES FROM THE LITERATURE TREATING WIND-AIDED FIRESPREAD ACROSS MATCHSTICK-TYPE FUEL ELEMENTS.

Hwang and Xie (1984) examine the increment in the firespread rate across vertical matchstick arrays for upslope orientation, and the decrement for downslope propagation, relative to the rate of spread for horizontal propagation. Upslope orientation induces a wind that aids spread, even if no ambient wind exists; upslope orientation also results in

the flame being closer to the fuel bed to abet the radiational view-factor and contact ignition. The effect of slope seems relatively modest for orientations of no more than 10° from horizontal. Steward (1974a) represents data for cribs, beds of needles, and matchsticks; the spread rate remains invariant with downslope up to 30° and more, whereas the spread rate doubles for an upslope of 20° (relative to the rate at zero slope). Cheney (1981) summarizes results of similar gist concerning the effect of slope on spread from field data gathered in Australia.

Prahl and T'ien (1973) consider wind-aided flame-spread phenomena for vertically oriented single lines of matchsticks, in the manner of Vogel and Williams (1970). However, Miller (1970) documents the need to consider sufficiently two-dimensional arrays of matchsticks in order to obtain rates of spread invariant with further increase in the number of parallel columns. Also, Prahl and T'ien engender the impressed wind via downstream suction, rather than via upwind blowing; this procedure precludes unconstrained action of the plume-type behavior, since the induction of low-level air into the plume from the downwind side is (artificially) opposed. The increment in spread rate with increasing wind (over wind-free tests) is found to level off at the higher wind speeds examined (~75 cm/s); the authors speculate that at still higher wind speed forced-convective extinction would be anticipated. [For thin fuel elements, extinction is effected by forced-convection-transport rates sufficiently in excess of chemical-exothermicity-release rates; for thicker fuel elements, surface reradiation of heat is responsible for extinction (Spalding 1955, pp. 208-211). For fuel beds composed of identical, upright, regularly arranged, discrete elements, it seems generally appropriate to discuss the fuel-bed extinction in terms of single-element extinction, since no elements are bypassed in a flame propagation: a downwind fuel element burns only if its upwind neighbor(s) burn(s) first.]

The effect of wind and moisture content on line-fire spread across reasonably uniform beds of ponderosa-pine needles (that burned with one-meter-high flames) and white-pine needles (that burned with one-third-meter-high flames) is such that less of the fuel is burned as the wind speed increases up to 2.2 m/s (Anderson and Rothermel 1965; Rothermel and

Anderson 1966). Above this speed the streamwise expanse of the flaming zone extended to the length of the fuel bed (2.4 m), and there is strong doubt that a steady rate of flame propagation was achieved. The less-than-complete consumption of matchstick-type fuel elements during firefront passage under higher winds is noted by Fang (1969).

Steward and Tennankore (1981) emphasize the longer length of run required to achieve a steady rate of flame propagation, or even a quasisteady rate, for the higher speed of spread under a higher ambient wind. (This behavior was also observed in the experiments to be reported below.) These investigators adopted a wind tunnel with a working section 1.22 m wide, 1.19 m high, and 7.1 m long, in which identical, vertically oriented, birch dowels arranged in a uniform matrix were burned. Center-to-center distances ranged from 0.82 cm to 3.8 cm, and the diameters of the circular-cross-section dowels ranged from 2.5 mm to 12.7 mm. "For the small diameter dowels with high rates of spread there was considerable doubt that a steady state was achieved even after 100 rows" (ibid., p. 642). The rate of fire spread was observed typically to increase by a factor of five as the wind was increased from 0.28 m/s to 2.8 m/s for 2.5-mm-diameter dowels; but the burning time of both large-diameter and small-diameter dowels was found to be independent of wind speed for a particular fuel bed, over the range of winds just discussed. Thus, "...the width of the active burning zone is directly proportional to the rate of fire spread which...increases rapidly with wind speed" (ibid., p. 645). [Byram et al. (1966), had reported quite similar results for cribs (i.e., for fuel beds consisting of layers of parallel pine sticks, with alternate layers parallel and perpendicular to the flow).] While the burning time of an individual birch dowel was independent of wind velocity, the burning time from 80% to 20% of initial weight was proportional to the dowel diameter to approximately the 3/2 power. Thus, whereas in a given test a 2.5-mm-diameter dowel burned in less than 20 s, a 12.7-mm-diameter dowel burned in about 200 s. "In a fuel bed with a mixture of two such diameters the 2.5 mm dowels would ignite and burn to completion before the 12.7 mm diameter dowels had virtually even started to burn" (ibid., p. 643). Such a large separation in fuel thicknesses does emphasize that flame-propagation rate is associated normally with the thin fuels present; however, in a more

general context in which a more continuous spectrum of fuel sizes is present, it may be worth remarking that fire-front propagation is expected to be associated with the thinner (probably not just the thinnest) fuels present, and these more easily ignited thinner fuels, in turn, do ignite the thicker, slower-to-burn-out fuels.

Steward et al. (1977) also emphasize the difficulty of attaining steady, reproducible rates of fire propagation with an aiding wind. Especially for winds in excess of 3 m/s, spread tends to be unstable and to be dependent on the details of ignition. Nevertheless, these investigators report wind-aided-firespread results for birch dowels (with 5% moisture content). For dowels 0.15 cm in diameter and 6.68 cm in length, the fire-spread speed is reduced to one-half if the center-to-center spacing of the array is reduced from 2.54 cm to 1.27 cm; the spread-rate increase with increase of the wind up to 2 m/s is appreciable for either spacing. (Other tests with dowels over twice as long indicated even faster spread than with shorter dowels, but these tests were cited as unstable.) However, for a wind in excess of 2 m/s, the increase of spread rate with increase of wind is much less. Indeed, at spacing of 3.81 cm, no fire would propagate over the range of wind speeds examined (0.5 m/s to 3.5 m/s). Furthermore, for dowels of 0.64 cm in diameter, for a center-to-center spacing of 2.54 cm, the increase of rate of spread with wind is rather modest and almost independent of an increase of dowel length from 6.68 cm to 13.97 cm. Again, there is suggestion that at wind of sufficient speed, in this case 3 m/s, the increase of spread rate with wind approaches zero. In brief, a decrease of flame-spread rate with increased loading (more particularly, with decreased porosity), and a (more pronounced) increase with increased wind speed at small wind speed (and a more modest increase with still higher wind speed), seem to summarize the results.

Fons (1946) systematically varied the ambient temperature, moisture content, wind, and spacing for 19-cm-long, 0.33-cm-to-1.0-cm-diameter twigs of dead ponderosa pine, set vertically and at regular intervals in fire-retardant-treated sawdust. The bed was 91 cm in width and almost 11 m in length; the upwindmost one-third of the length was set aside to permit the fire to reach an equilibrium rate of spread after line ignition of the

midregion (only) of the upwindmost row. In addition to noting the reduced spread rate under lower ambient temperature (longer preheating times) and higher moisture content, Fons reported that, for the thermally thin fuel, if U denotes ambient wind speed, ρ_s denotes solid-fuel density, and d denotes solid-fuel diameter, then

$$v_f \sim \frac{1}{\rho_s} \left(\frac{s}{d}\right) U^n,$$

where $n \simeq 1$ for winds under 2.25 m/s and $n \simeq 1.5$ for winds between 2.25 m/s and 9 m/s. Fons noted that spread must slow and desist for sufficiently large element-to-element spacing s.

While some general trends are evident, definitive insight is not available yet in the literature.

3.3 EXPERIMENTAL TESTS.

3.3.1 Test Facility.

The facility used in the present investigation has been described in detail previously (Fleeter et al. 1984), but brief comments are included here so that the presentation is self-contained and updated.

The facility consists of a blower which pushes ambient air through a flow-conditioning section upwind of the test section (Figure 2). Through the use of a sequence of honeycombs and fine screens, all at least several meters upwind of the test section, the flow-preparation section produces a uniform steady stream of low turbulence. Specifically, with the exclusion of near-wall layers, the time-averaged streamwise speed varies by less than $\pm$5% from the nominal cross-sectional mean wind velocity for a test-section-entrance speed of 4.2 m/s, and the rms turbulence level at this speed was about 0.6% (Beach et al. 1985). The wind tunnel has a movable ceiling, readily translatable downwind in its own plane, such that the leading edge of the ceiling can be made to trail just behind the downwind-propagating buoyant flaming upflux. The strongly buoyant gas is concentrated in the vicinity of the burning front, which separates uninvolved downwind fuel from whatever char remains of the fully outgassed upwind fuel. The movable

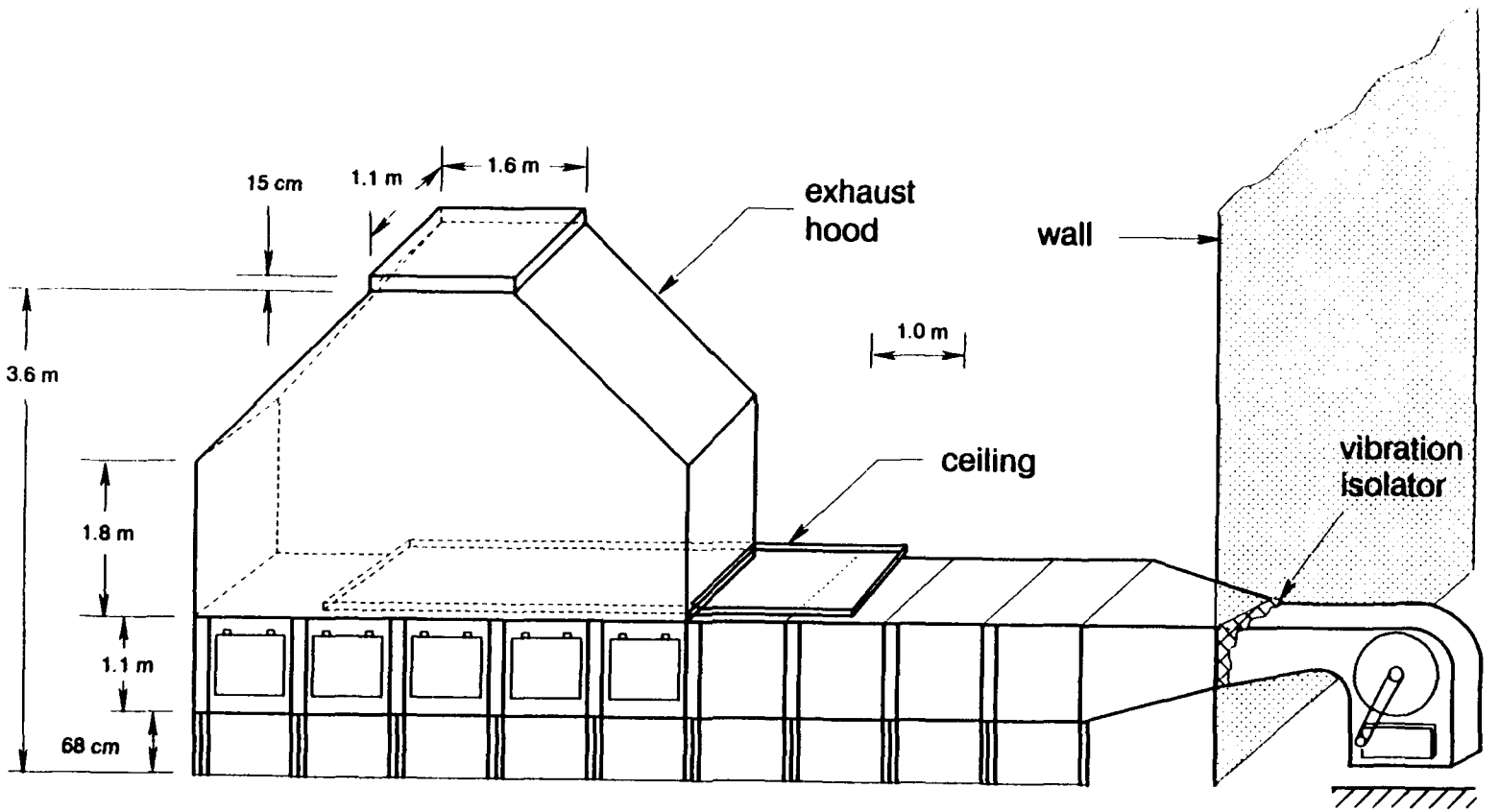

Figure 2. Fire-tunnel facility for wind-aided-spread experiments: external blower, flow preparation section, side-view windows and movable ceiling for the test section, and tall exhaust hood.

ceiling permits the buoyant firefront gas to rise with a minimum of obstruction, while also allowing an airflow of undiminished freestream speed to reach the propagating firefront, since the upwind cross-sectional area is maintained constant during the fire spread. (Of course, the thickness of the near-fuel-bed boundary layer does increase with downwind distance from the leading edge of the test section, but the dimensions of the test-section cross section, over 1.1 m x 1.1 m, assure that no appreciable acceleration of the freestreaming occurs.) Aiding winds in excess of 4 m/s are attainable in the tunnel.

The up-to-5-m-long fuel bed consists of ceramic trays with holes drilled at 1-cm intervals; i.e., the fuel bed may be envisioned as a checkerboard with a hole drilled at the center of each square, of 1-cm-edge dimension. The ceramic material (fiberfrax duraboard HD made by Carborundum Company, Niagra Falls, NY) was selected for its uniformity, thermal-insulation property, stability at high temperature, resistance to thermal shock and chemical attack, recovery after wetting by water, and ease of drilling and sawing. The discrete fuel elements utilized here are typified by thin white-pine toothpicks, oriented vertically, with 0-to-4 toothpicks per hole (Figure 3). The test-initiating ignition involves simultaneously lighting all the fuel elements in the upwindmost line (row), perpendicular to the airflow, by means of gaseous-diffusion-flame torch, that is then turned off. The flow exits without obstruction through an exhaust stack into the atmosphere.

The rate of firefront propagation is inferred via type-K thermocouples, spaced at 14-cm intervals along the streamwise centerline of the test bed, near the fuel-bed surface. The readings are recorded digitally by a Transera data-acquisition system and stored on an IBM PC. Since only the time of pyrolysis-temperature onset is used to indicate firefront transit, any delay in the relaxation to ambient temperature is of no concern for current purposes. [For the quasisteady propagation of a firefront (of finite streamwise extent) across a macroscopically uniform bed, tracking the downwind progression of any convenient isotherm (above ambient temperature) yields the rate of firespread.] The thermocouple voltages are converted by the acquisition system to temperatures and are

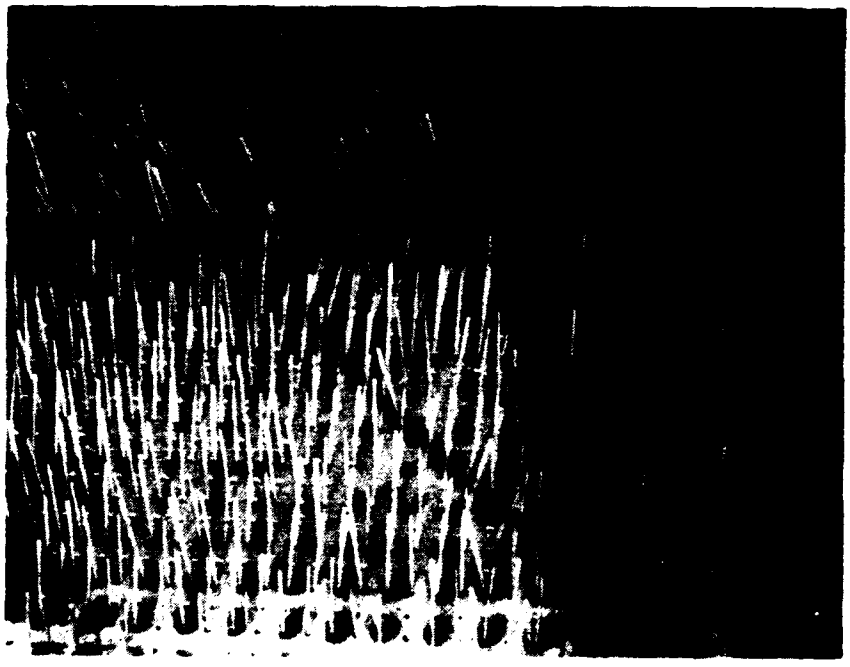

Figure 3. Ceramic trays, drilled with holes one centimeter apart, filled with a toothpick loading such that m = 0.02208 g/cm^2.

presented as functions of time. Also, a vertical array of thermocouples is positioned at the streamwise centerline of the fuel bed, at a distance of about 2 meters downwind from the leading edge of the fuel bed. The ten thermocouples present on the rake are spaced at 5-cm vertical intervals, with the lowest thermocouple positioned 8 cm above the surface of the substrate and the highest at 53 cm above the surface. For a steady rate of fire propagation, the time t can be scaled by the firefront-propagation speed v_f to yield the variation of the temperature T as a function of streamwise position. The spatial loci of isotherms can be inferred from the temperature profiles. From the isotherms, the tilt of the buoyant hot gases near the firefront can be inferred. In particular, the tilt angle A is measured from the ray pointed directly downwind, so that A = 0 describes buoyant hot gases blown flat to the downwind fuel-bed surface, while A = $\pi/2$ describes the hot gases as rising perpendicularly to the fuel-bed surface (without any downwind or upwind tilt). Typically one expects a downwind tilt such that $0 < A < \pi/2$. In addition, a side-view record of a test is obtained by manually moving a video camera mounted on a translatable platform outside the tunnel. An overhead view of a test is obtained by use of a video camera attached to the translating ceiling.

3.3.2 Test Conditions, Data Analysis, and Repeatability.

Attention was concentrated on ascertaining the dependence of flame-propagation rate on two parameters anticipated to be of particular importance: the wind speed (varied mostly from 0.0 m/s to 4.6 m/s) and the (planform-area-averaged) fuel loading (varied mostly from 0.011 g/cm^2 to 0.088 g/cm^2, with some tests ranging to about 0.3 g/cm^2). Other parameters varied were the fuel-bed width (varied from 30 cm to 100 cm), fuel-element height, fuel-element thickness, fuel-element composition, and inert-mass loading. While some mixed-element tests are described below, in the absence of an explicit statement to the contrary, every test is to be taken to involve regular arrangements of identical fuel elements. The fuel-bed inclination was held horizontal in all tests.

The individual white-pine toothpicks used as fuel elements in many tests were 6.1 cm in length, with about 4.6 cm exposed for burning above the drilled ceramic tray. The circumference of the lengthwise-varying-

rectangular-cross-section toothpicks was such that the average diameter for the equivalent-area circle was 0.13 cm, and the average mass per toothpick was about 0.052 g. Toothpicks, even in the tests with the widest loading distributions (100 cm), were more than 5 cm from the tunnel-test-section side walls. Table 1 presents some properties of the several other combustible and inert elements used in the experiments to be reported. A thermogravimetric analysis carried out on three types of the wood samples indicated that about 70% of the mass evolved as gas (during gradual heating in an inert atmosphere) over the range from about 575 K to 675 K (Figure 4). The densities of the three wood species utilized in the testing (white pine, birch, bamboo) are comparable. Also, after typical storage, baking 100 white-pine toothpicks at 573 K for 16 minutes removed 8.4% of the toothpick mass[1].

A typical thermocouple-output curve of temperature as a function of time describes a slow rise in temperature (interpreted as preheating), followed by a more rapid rise (interpreted as flame arrival), followed by a gradual decay (interpreted as forced-convective cooling of the thermocouple by the upwind air flow). A constant rate of flame propagation, i.e., steady spread, is indicated by the graph of isotherm progression vs. time approximating a straight line. [More explicitly, the graph is of the time (since ignition of the leading-edge row of fuel elements) at which each of the near-fuel-bed-surface thermocouples, distributed at known streamwise positions downwind from the leading edge of the fuel bed, first achieves a specified temperature above ambient.]

---

[1]Approximately 500 white-pine toothpicks at a time were subjected to the gross-heat-of-combustion technique specified in the National Fire Protection Association protocol 259 (Standard Test Method for Potential Heat of Building Materials); the tests were conducted in an isothermal jacketed oxygen bomb calorimeter. The test sample was stored in a conditioning room (held at 296 K $\pm$3 K, 50% $\pm$5% relative humidity) for about two months. Each sample was then ground via a rotary laboratory mill until it would pass through a 60-mesh screen, then returned to the conditioning room for a week before testing. The gross heat of combustion was about 17.7 kJ/g of fuel. Samples were also placed in an oven at 373 K for 48 hours prior to testing to remove free water (which proved to constitute 7% to 8% by mass of the sample). The gross heat of combustion then was about 19.0 kJ/g. The authors are very grateful to J. R. Lawson of the Center for Fire Research of the National Institute of Standards and Technology for these data.

Table 1. Properties of the fuel elements and inert elements used in experiments.

Element Type	Hydraulic Diameter (mm)	Exposed Height (cm)	Mass per Unit Length (g/cm)	Common Commercial Designation
White Pine I	1.3	4.6	0.009	Flat toothpicks
White Pine II	1.9	7.7	0.023	Sandwich picks
Bamboo I	2.3	3-22	0.030	9" bamboo skewers
Bamboo II	3.0	4.6-14	0.060	6" bamboo skewers
Birch I	3.3	2-14	0.061	1/8" dowels
Birch II	4.4	4.6	0.086	Sandwich skewers
Nails	3.8	3.8	0.350	Common 2" nails
Plastics	2.4*	4.6	0.022	Q-tip shafts

*Tube with hollow center

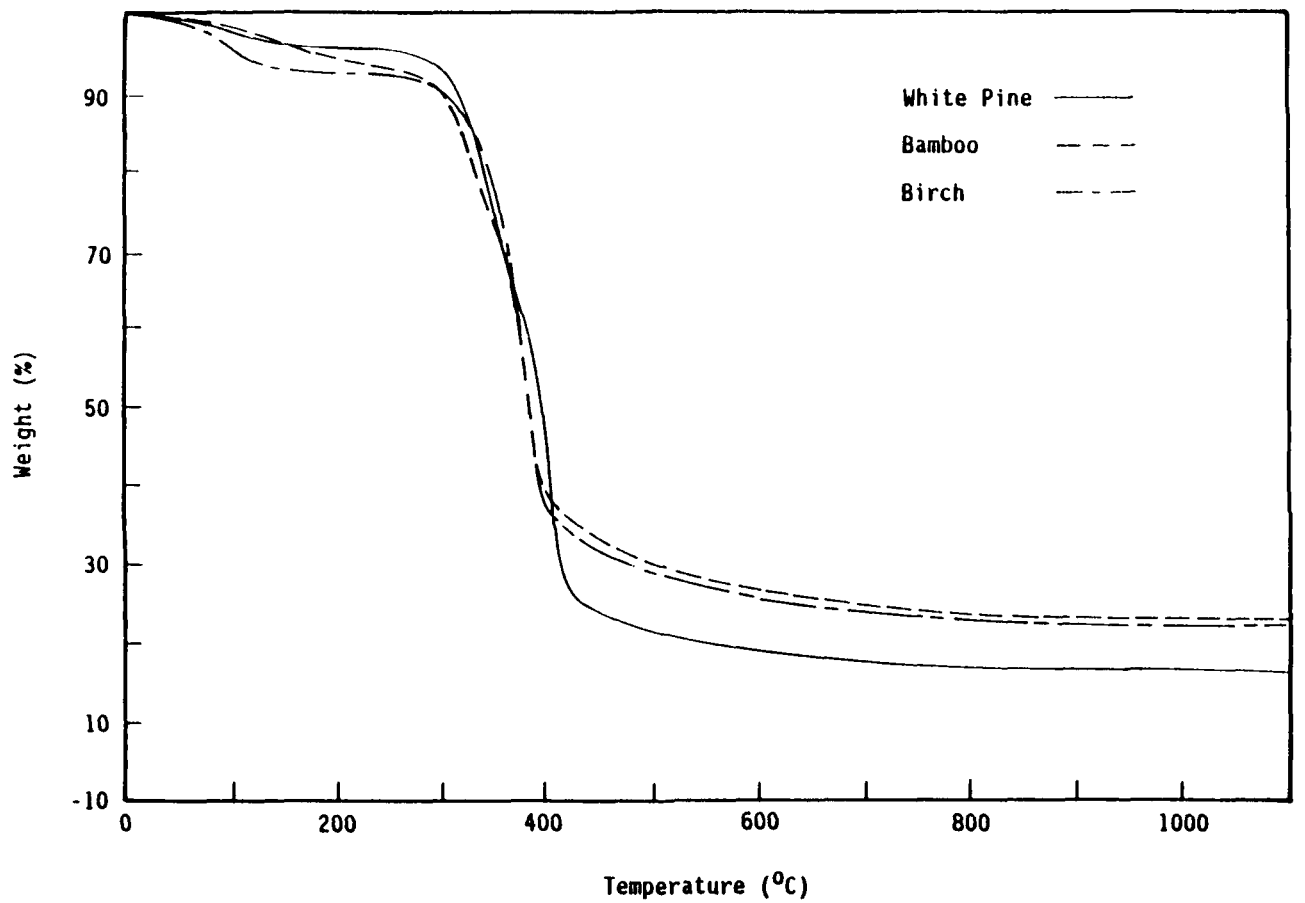

Figure 4. Percent of initial weight as a function of temperature from thermogravimetric analyses of three wood samples. Several milligrams of each sample were subjected to a temperature rise of 20 K/min, from room temperature to about 1400 K, with an argon purge of one liter/min, in a stainless steel line.

The ambient temperature varied from 287 K to 303 K, and the ambient relative humidity varied from 15% to 75%; however, the flame-propagation rate was judged to be insensitive to these variations. Several tests were conducted under the same controllable conditions on different days to investigate the repeatability of results: for a wind speed of 2 m/s, a fuel loading of 0.022 g/cm^2, and a test-bed width of 55 cm, tests were conducted on days when the humidity varied by 20% and the ambient temperature varied by 4 K, and the scatter owing to uncontrolled variables seemed to be minimal. However, other tests were conducted explicitly to examine fuel-moisture-content and/or substratum-moisture-content effects. In such tests, the fuel-element-loaded ceramic trays were placed in the test section, which was then sealed off from the exit duct and flow-preparation section and a humidifier was placed in the test section for three-to-four hours, until the relative humidity reached 100% and condensation occurred on the test-section walls. The test was executed expeditiously after the humidifier and test-section isolators were removed, but no attempt was made in any test to condition the ambient air blown into the test section. In other tests fine water droplets were sprayed onto the ceramic substratum while provision was taken to try to maintain the fuel elements at their ambient water content.

A nearly complete compilation of the conditions and results for all tests conducted appears in Tables 2-6.

3.3.3 The Effect of Microscale Variation ("Crystallinity") on the Rate of Firespread.

If effectively identical toothpick-like fuel elements of density ρ_s, (exposed) height H, and characteristic cross-sectional area d^2 are inserted upright into the regularly distributed, drilled holes, the fuel loading m is altered only by varying the porosity ϕ, more specifically, n, the number of fuel elements per unit planform area of the bed, since

$$m = \rho_s H(1-\phi) = \rho_s H n d^2. \qquad (3.1)$$

Table 2. Compilation of assigned parametric values for all tests, in chronological order.

Test #	Date	Bed Width (W) [cm]	Bed Length (L) [cm]	Temperature (in) (T) [C]	Temperature (out)	Pressure (P) [psia]	Humidity (in) [%]	Humidity (out)	Fan Speed [rpm]	Wind Speed (U) [m/s]	Elements (n) [#/cm^2]	Loading (wood) (m) [gm/cm^2]	Fuel Height (H) [cm]	Fuel Diam. (d) [mm]	Fuel H2O [%]	Bed H2O [%]	Bed Type	Fuel Type	Repeated Test #'s	Comments
1	07-25-85	100	1000		22				500	1.6	0.25	0.011	4.6	1.3	0%	0%	Ceram	W. Pine		
2	08-06-85	100	1000		22				500	1.6	0.25	0.011	4.6	1.3	0%	0%	Ceram	W. Pine		
3	09-17-85	100	1000		23				500	1.6	0.50	0.022	4.6	1.3	0%	0%	Ceram	W. Pine		
4	09-19-85	55	100			Video Data Only			500		1.00			1.3	0%	0%	Ceram	W. Pine		1/2 Tray Ignited
5	09-27-85	55	100						250	0.7	1.00	0.044	4.6	1.3	0%	0%	Ceram	W. Pine		
6	09-27-85	55	100						1000	3.4	1.00	0.044	4.6	1.3	0%	0%	Ceram	W. Pine		
7	10-02-85	55	100						0	0.0	1.00	0.044	4.6	1.3	0%	0%	Ceram	W. Pine		0 Wind Speed
8	10-02-85	55	100						0	0.0	1.00	0.044	4.6	1.3	0%	0%	Ceram	W. Pine		0 Wind Speed
9	10-02-85	55	100						190	0.4	1.00	0.044	4.6	1.3	0%	0%	Ceram	W. Pine	17-24	
10	10-04-85	4	20			Blow Out Attempt			----- Varied ----				4.6	1.3	0%	0%	Ceram	W. Pine		Blow Out Attempt
11	10-11-85	55	200			Uncertain Test Cond.			190	0.4	1.00	0.044	4.6	1.3	0%	0%	Ceram	W. Pine		?
12	10-08-85	55	100	19	22				190	0.4	2.00	0.088	4.6	1.3	0%	0%	Ceram	W. Pine	13,14 & 15	Crystallinity #1
13	10-08-85	55	100	21	23				190	0.4	2.00	0.088	4.6	1.3	0%	0%	Ceram	W. Pine	12,14 & 15	"
14	10-08-85	55	100	22	22				190	0.4	2.00	0.088	4.6	1.3	0%	0%	Ceram	W. Pine	13,12 & 15	"
15	10-08-85	55	100	21	22				190	0.4	2.00	0.088	4.6	1.3	0%	0%	Ceram	W. Pine	13,14 & 12	"
16	10-14-85	55	200	26	25				375	1.1	1.00	0.044	4.6	1.3	0%	0%	Ceram	W. Pine	98*	
17	10-14-85	55	100	31	26				190	0.4	1.00	0.044	4.6	1.3	0%	0%	Ceram	W. Pine	9 & 17-24	Crystallinity #2
18	10-14-85	55	100	29	25				190	0.4	1.00	0.044	4.6	1.3	0%	0%	Ceram	W. Pine	9 & 17-24	"
19	10-14-85	55	100	29	27				190	0.4	1.00	0.044	4.6	1.3	0%	0%	Ceram	W. Pine	9 & 17-24	"
20	10-14-85	55	100	29	26				190	0.4	1.00	0.044	4.6	1.3	0%	0%	Ceram	W. Pine	9 & 17-24	"
21	10-17-85	55	100	22	22	Computer Crash			190	0.4	1.00	0.044	4.6	1.3	0%	0%	Ceram	W. Pine	9 & 17-24	
22	10-17-85	55	100	22	22				190	0.4	1.00	0.044	4.6	1.3	0%	0%	Ceram	W. Pine	9 & 17-24	Repeatibility
23	10-17-85	55	100	-	21				190	0.4	1.00	0.044	4.6	1.3	0%	0%	Ceram	W. Pine	9 & 17-24	"
24	10-17-85	55	100	23	23				190	0.4	1.00	0.044	4.6	1.3	0%	0%	Ceram	W. Pine	9 & 17-24	"
25	11-01-85	55	200	19	22		70	55	250	0.7	0.50	0.044	4.6	1.3	0%	0%	Ceram	W. Pine		
26	11-01-85	55	200	24	23		58	55	357	1.0	0.73	0.032	4.6	1.3	0%	0%	Ceram	W. Pine		Fleeter Repeat
27	11-07-85	55	200	19	22		73	62	500	1.6	1.00	0.044	4.6	1.3	0%	0%	Ceram	W. Pine	99	
28	11-07-85	55	300	23	24		64	60	750	2.5	1.00	0.044	4.6	1.3	0%	0%	Ceram	W. Pine	56 & 82	
29	11-07-85	55	300	23	23		64	60	500	1.6	0.25	0.011	4.6	1.3	0%	0%	Ceram	W. Pine	76, 171, ++	
30	11-07-85	55	300	22	23		67	65	875	3.0	1.00	0.044	4.6	1.3	0%	0%	Ceram	W. Pine		
31	11-07-85	55	200	20	22		70	65	500	1.6	0.50	0.022	4.6	1.3	0%	0%	Ceram	W. Pine	38,50-52	

Table 2. Compilation of the assigned parametric values for all tests, in chronological order (continued).

Test #	Date	Bed Width (W) [cm]	Bed Length (L) [cm]	Temperature (in) (T) [C]	(out)	Pressure (P) [psia]	Humidity (in) [%]	(out)	Fan Speed [rpm]	Wind Speed (U) [m/s]	Elements (n) [#/cm^2]	Loading (wood) (m) [gm/cm^2]	Fuel Height (H) [cm]	Fuel Diam. (d) [mm]	Fuel H2O [%]	Bed H2O [%]	Bed Type	Fuel Type	Repeated Test #'s	Comments
32	11-14-85	55	100	21	21		29	30	190	0.4	0.50	0.022	4.6	1.3	0%	0%	Ceram	W. Pine		
33	11-14-85	55	200	20	22		35	32	500	1.6	2.00	0.088	4.6	1.3	0%	0%	Ceram	W. Pine		
34	11-14-85	55	300	22	23		32	34	1000	3.4	1.00	0.044	4.6	1.3	0%	0%	Ceram	W. Pine	57,58 & 62	
35	11-15-85	55	300	17	19		27	29	750	2.5	0.50	0.022	4.6	1.3	0%	0%	Ceram	W. Pine	90 & 91*	
36	11-15-85	55	100	20	21		23	26	190	0.4	0.25	0.011	4.6	1.3	0%	0%	Ceram	W. Pine		
37	11-21-85	100	400	20	22		54	48	500	1.6	0.50	0.022	4.6	1.3	0%	0%	Ceram	W. Pine		Width Variation
38	12-06-85	55	200	15	17		76	71	500	1.6	0.50	0.022	4.6	1.3	0%	0%	Ceram	W. Pine	50,51 & 52	
39	12-06-85	30	200	17	21		61	53	500	1.6	0.50	0.022	4.6	1.3	0%	0%	Ceram	W. Pine		Width Variation
40	12-06-85				Scattered Toothpicks				500	1.6	-	0.022	4.6	1.3	0%	0%	Ceram	W. Pine		Elements Scattered
41	12-06-85	55	300	21	22		55	50	750	2.5	2.00	0.088	4.6	1.3	0%	0%	Ceram	W. Pine		
42	12-19-85	55	300	17	19		25	25	1000	3.4	0.50	0.022	4.6	1.3	0%	0%	Ceram	W. Pine	66	
43	12-19-85	55	300	21	22		21	22	1000	3.4	0.25	0.011	4.6	1.3	0%	0%	Ceram	W. Pine	55,63 & 65	Roof Stop @TC#19
44	12-19-85	55	300						1000	3.4	0.13	0.006	4.6	1.3	0%	0%	Ceram	W. Pine		Loading too light
45	12-19-85	55	300						1000	3.4	0.13	0.006	4.6	1.3	0%	0%	Ceram	W. Pine		Loading too light
46	12-19-85	55	300						500	1.6	0.13	0.006	4.6	1.3	0%	0%	Ceram	W. Pine		Loading too light
47	01-15-86	55	300	17	21		65	53	750	2.5	0.25	0.011	4.6	1.3	0%	0%	Ceram	W. Pine	134, 165, ++	
48	01-15-86	30	200	19	22		64	55	500	1.6	0.25	0.011	4.6	1.3	0%	0%	Ceram	W. Pine		Width Variation
49	01-15-86	100	300	20	24		60	49	500	1.6	1.00	0.044	4.6	1.3	0%	0%	Ceram	W. Pine		Width Variation
50	01-28-86	55	200	16	20		36	34	500	1.6	0.50	0.022	4.6	1.3	0%	0%	Ceram	W. Pine	38,51 & 52	
51	01-28-86	55	200	18	19		32	33	500	1.6	0.50	0.022	4.6	1.3	0%	0%	Ceram	W. Pine	38,50 & 52	
52	01-28-86	55	200	22	23		24	28	500	1.6	0.50	0.022	4.6	1.3	0%	0%	Ceram	W. Pine	38,50 & 51	
53	01-28-86	55	200	24	24		20	25	500	1.6	0.50	0.022	4.6	1.3	0%	0%	Ceram	W. Pine		Ceiling at X=0cm
54	01-28-86	30	200	25	24		17	23	500	1.6	1.00	0.044	4.6	1.3	0%	0%	Ceram	W. Pine		
55	01-28-86	55	300	25	24		17	22	1000	3.4	0.25	0.011	4.6	1.3	0%	0%	Ceram	W. Pine	43,63 & 65	Repeat #43
56	06-26-87	55	300	22	21	14.69	56	59	(700)	2.5	1.00	0.044	4.6	1.3	0%	0%	Ceram	W. Pine	28 & 82	Repeat #28
57	07-13-87	55	300	24	23	14.68	57	60	(925)	3.4	1.00	0.044	4.6	1.3	0%	0%	Ceram	W. Pine		
58	07-20-87	55	300	21	21	14.66	62	59	(925)	3.4	1.00	0.044	4.6	1.3	0%	0%	Ceram	W. Pine		
59	07-20-87	55	300	23	22	14.66	58	56	(700)	2.5	0.25	0.110	12.1	2.3	0%	0%	Ceram	Bamboo I		Fuel Height Varied
60	07-30-87	55	300	22	21	14.64	61	59	(700)	2.5	0.50	0.110	6.2	2.3	0%	0%	Ceram	Bamboo I		Fuel Height Varied
61	07-30-87	55	300	24	22	14.64	63	58	(700)	2.5	1.00	0.116	3.0	2.3	0%	0%	Ceram	Bamboo I		Fuel Height Varied
62	08-06-87	55	300	24	22	14.63	65	62	(925)	3.4	1.00	0.044	4.6	1.3	0%	0%	Ceram	W. Pine	34,57 & 58	
63	08-06-87	55	300	24	22	14.62	65	56	(925)	3.4	0.25	0.011	4.6	1.3	0%	0%	Ceram	W. Pine	43,55 & 65	
64	08-20-87	55	300	25	23		57	42	(925)	3.4	2.00	0.088	4.6	1.3	0%	0%	Ceram	W. Pine		?Steady S. Region?

Table 2. Compilation of the assigned parametric values for all tests, in chronological order (continued).

Test #	Date	Bed Width (W) [cm]	Bed Length (L) [cm]	Temperature (in) (T) [C]	(out)	Pressure (P) [psia]	Humidity (in) [%]	(out)	Fan Speed [rpm]	Wind Speed (U) [m/s]	Elements (n) [#/cm^2]	Loading (wood) (m) [gm/cm^2]	Fuel Height (H) [cm]	Fuel Diam. (d) [mm]	Fuel H2O [%]	Bed H2O [%]	Bed Type	Fuel Type	Repeated Test #'s	Comments
65	08-20-87	55	300	24	23		57	50	(925)	3.4	0.25	0.011	4.6	1.3	0%	0%	Ceram	W. Pine	43,55 & 63	
66	09-08-87	55	300	23	22	14.6	56	59	(925)	3.4	0.50	0.022	4.6	1.3	0%	0%	Ceram	W. Pine	42	
67	09-08-87	55	300	27	24	14.6	51	56	(925)	3.4	1.00	0.044	4.6	1.3	0%	0%	Ceram	W. Pine	70,119,120	Ceiling @X=0.19m
68	09-08-87	55	300	28	24	14.6	51	51	(1200)	4.6	0.25	0.011	4.6	1.3	0%	0%	Ceram	W. Pine		
69	09-25-87	55	300	21	21	14.7	72	68	(300)	1.0	0.25	0.011	4.6	1.3	0%	0%	Ceram	W. Pine		
70	09-25-87	55	300	23	22	14.7	66	68	(925)	3.4	1.00	0.044	4.6	1.3	0%	0%	Ceram	W. Pine	67,119,120	Ceiling @X= 3.4m
71	09-25-87	55	300	25	22	14.7	59	63	(1200)	4.6	0.50	0.022	4.6	1.3	0%	0%	Ceram	W. Pine		
72	10-19-87	55	300	21	21	14.68	64	64	(1200)	4.6	1.00	0.044	4.6	1.3	0%	0%	Ceram	W. Pine		Shadowgraph
73	10-19-87	55	300	23	21	14.68	56	61	(925)	3.4	0.75	0.033	4.6	1.3	0%	0%	Ceram	W. Pine		Shadowgraph
74	11-03-87	55	300	21	21	14.69	45	47	(925)	3.4	2.00	0.088	4.6	1.3	0%	0%	Ceram	W. Pine		Shadowgraph
75	11-03-87	55	300	22	22	14.69	50	46	(300)	1.0	0.50	0.022	4.6	1.3	0%	0%	Ceram	W. Pine		Shadowgraph
76	11-17-87	55	300	19	20	14.72	51	50	(450)	1.6	0.25	0.011	4.6	1.3	0%	0%	Ceram	W. Pine	29, 171, ++	Repeat - TC Rake
77	11-17-87	55	400	20	19	14.71	55	54	(925)	3.4	1.00	0.180	4.6	2.3	0%	0%	Ceram	Bamboo I		4.6 cm Bamboo
78	12/03/87	55	300	17	16	14.77	59	59	(300)	1.0	0.75	0.033	4.6	1.3	0%	0%	Ceram	W. Pine		TC Rake Present
79	12/03/87	0-100	275	21	21	14.72	56	50	(700)	2.5	1.00	0.044	4.6	1.3	0%	0%	Ceram	W. Pine		Triangle Loading
80	12/22/87	55	300	14	18	14.74	47	40	(450)	1.6	0.50	0.022	4.6	1.3	0%	0%	Ceram	W. Pine		Nails in holes
81	12/22/87	55	300	19	19	14.69	55	54	0	0	1.00	0.044	4.6	1.3	0%	0%	Ceram	W. Pine		No Wind
82	12/22/87	55	300	20	20	14.69	52	52	(700)	2.5	1.00	0.044	4.6	1.3	0%	0%	Ceram	W. Pine	56 & 28	Repeat Test
83	1/21/88	55	300	14	20	14.91	25	26	(700)	2.5	0.75	0.066	4.6	1.3	0%	0%	Ceram	W. Pine		
84	1/21/88	55	300	18	20	14.95	35	31	(700)	2.5	0.25	0.045	4.6	2.3	0%	0%	Ceram	Bamboo I		
85	2/25/88	55	279	14	19	14.77	66	51	0	0	2.00	0.088	4.6	1.3	0%	0%	Ceram	W. Pine		0 Wind
86	2/25/88	55	300	18	20	14.78	58	50	(700)	2.5	0.50	0.089	4.6	2.3	0%	0%	Ceram	Bamboo I		4.6 cm Bamboo
87	3/02/88	55	329	15	19	14.68	56	44	(925)	3.4	0.50	0.022	4.6	1.3	0%	0%	Ceram	W. Pine		Nails in Tray #2
88	3/02/88	55	317	21	23	14.66	47	43	(1200)	4.6	0.25	0.045	4.6	2.3	0%	0%	Ceram	Bamboo I		4.6 cm Bamboo
89	3/10/88	65-107	330	18	19	14.72	15	19	(450)	1.6	1.00	0.044	4.6	1.3	0%	0%	Ceram	W. Pine		1:15 Tapered Loading
90	3/21/88	55	319	22	22	14.74	52	46	(700)	2.5	0.50	0.022	4.6	1.3	0%	0%	Ceram	W. Pine	35° & 91°	Crystalinity - #91
91	3/21/88	55	319	21	22	14.71	55	49	(700)	2.5	0.50	0.022	4.6	1.3	0%	0%	Ceram	W. Pine	35° & 90°	Crystalinity - #90
92	3/28/88	55	319	21	22	14.66	52	47	(300)	1.0	0.50	0.089	4.6	2.3	0%	0%	Ceram	Bamboo I		4.6 cm Bamboo
93	3/28/88	55	326	25	22	14.66	46	45	(700)	2.5	0.50	0.022	4.6	1.3	0%	0%	Ceram	W. Pine		Nails in Tray #2
94	4/06/88	33-108	385	23	22	14.72	56	55	(450)	1.6	1.00	0.044	4.6	1.3	0%	0%	Ceram	W. Pine		1:10 Tapered Loading
95	4/06/88	55	318	24	22	14.68	50	51	(450)	1.6	0.25	0.045	4.6	2.3	0%	0%	Ceram	Bamboo I		4.6 cm Bamboo
96	4/27/88	55	324	18	21	14.68	59	51	(700)	2.5	1.00	0.044	4.6	1.3	20-30%	~1%	Ceram	W. Pine	140	20-30% Moisture
97	5/03/88	100	274	18	20	14.72	45	38	(300)	1.0	1.00	0.044	4.6	1.3	0%	0%	Ceram	W. Pine		

Table 2. Compilation of the assigned parametric values for all tests, in chronological order (continued).

Test #	Date	Bed Width (W) [cm]	Bed Length (L) [cm]	Temperature (in) (T) [C]	(out)	Pressure (P) [psia]	Humidity (in) [%]	(out)	Fan Speed [rpm]	Wind Speed (U) [m/s]	Elements (n) [#/cm^2]	Loading (wood) (m) [gm/cm^2]	Fuel Height (H) [cm]	Fuel Diam. (d) [mm]	Fuel H2O [%]	Bed H2O [%]	Bed Type	Fuel Type	Repeated Test #'s	Comments
98	5/03/88	55	319	22	22	14.72	38	35	(300)	1.0	1.00	0.044	4.6	1.3	0%	0%	Ceram	W. Pine	16*	
99	5/03/88	55	300	24	22	14.72	38	41	(450)	1.6	1.00	0.044	4.6	1.3	0%	0%	Ceram	W. Pine	27	
100	7/07/88	55	322	24	21	14.67	59	56	(300)	1.0	1.00	0.044	4.6	1.3	24%	~1%	Ceram	W. Pine	141	24% Moisture
101	7/07/88	55	322	25	23	14.67	57	63	(700)	2.5	0.25	0.090	9.2	2.3	0%	0%	Ceram	Bamboo I		9.2cm Bamboo
102	7/07/88	100	331	25	22	14.65	58	58	(925)	3.4	1.00	0.044	4.6	1.3	0%	0%	Ceram	W. Pine		
103	7/19/88	100	276	21	21	–	60	62	(300)	1.0	2.00	0.088	4.6	1.3	0%	0%	Ceram	W. Pine		100 cm Test
104	7/19/88	55	320	24	21	–	60	54	(700)	2.5	0.50	0.022	4.6	1.3	0%	0%	Ceram	W. Pine		Nails in Tray #2
105	8/05/88	100	330	22	21	14.61	69	59	(925)	3.4	0.25	0.011	4.6	1.3	0%	0%	Ceram	W. Pine		
106	8/05/88	55	330	23	22	14.61	66	62	(200)	0.7	0.50	0.022	4.6	1.3	0%	0%	Ceram	W. Pine		Nails in Tray #2
107	8/05/88	100	324	23	21	14.63	65	60	(700)	2.5	1.00	0.044	4.6	1.3	0%	0%	Ceram	W. Pine		
108	8/23/88	55	324	23	21	14.61	69	64	(300)	1.0	1.00	0.044	4.6	1.3	8%	~1%	Ceram	W. Pine		
109	8/23/88	55	330	25	21	14.61	57	55	(700)	2.5	0.50	0.022	4.6	1.3	0%	0%	Ceram	W. Pine		Nail/4 holes-Tray #2
110	8/23/88	55	330	25	21	14.61	60	55	(700)	2.5	0.25	0.065	4.6	3.0	0%	0%	Ceram	Bamboo II		Bamboo #2
111	8/31/88	100	385	20	21	14.54	79	69	(1200)	4.6	0.25	0.011	4.6	1.3	0%	0%	Ceram	W. Pine		Very fast test
112	8/31/88	55	324	23	22	14.54	69	65	(700)	2.5	0.50	0.022	4.6	1.3	0%	0%	Ceram	W. Pine		Nail/4 holes-Tray #2
113	9/06/88	55	330	23	20	14.56	71	69	(700)	2.5	1.00	0.044	4.6	1.3	4-13%	~1%	Ceram	W. Pine		Moisture Test
114	9/06/88	55	330	23	22	14.56	70	60	(700)	2.5	0.25	0.078	4.6	3.3	0%	0%	Ceram	Birch I		1st Birch test
115	9/06/88	55	325	26	22	14.58	60	58	(700)	2.5	0.50	0.022	4.6	1.3	0%	0%	Ceram	W. Pine		Nail/8 holes-Tray #2
116	10/10/88	100	330	19	20	14.59	56	50	(200)	0.7	0.50	0.022	4.6	1.3	0%	0%	Ceram	W. Pine		
117	10/10/88	55	330	24	22	14.59	35	43	(450)	1.6	0.25	0.060	6.2	2.3	0%	0%	Ceram	Bamboo I		6.2 cm Height Test
118	10/10/88	55	330	30	24	14.59	42	49	(450)	1.6	0.25	0.102	6.2	3.3	0%	0%	Ceram	Birch I		6.2 cm Height Test
119	10/19/88	55	330	21	20	14.65	68	58	(925)	3.4	1.00	0.044	4.6	1.3	0%	0%	Ceram	W. Pine	Many(eg.57)	Wind Deflection-Pitot
120	10/19/88	55	300	22	21	14.63	66	63	(925)	3.4	1.00	0.044	4.6	1.3	0%	0%	Ceram	W. Pine	Many(eg.57)	Wind Deflection-Pitot
121	10/21/88	55	330	20	21	14.67	71	61	(200)	0.7	1.00	0.237	14.0	3.3	0%	0%	Ceram	Birch I		Tall Elements
122	10/27/88	100	330	16	18	14.59	54	51	(200)	0.7	0.25	0.011	4.6	1.3	0%	0%	Ceram	W. Pine		
123	10/27/88	55	330	15	16	14.61	50	45	(925)	3.4	0.25	0.050	3.0	3.3	0%	0%	Ceram	Birch I		
124	10/27/88	55	310	20	20	14.61	53	51	(925)	3.4	1.00	0.044	4.6	1.3	0%	0%	Ceram	W. Pine		Open Ceiling x=0.2m
125	10/27/88	100	303	21	21	14.59	53	53	(1200)	4.6	0.50	0.022	4.6	1.3	0%	0%	Ceram	W. Pine		
126	11/11/88	55	330	19	20	14.67	64	59	(1200)	4.6	0.25	0.060	6.2	2.3	0%	0%	Ceram	Bamboo I		
127	11/11/88	55	325	21	19	14.67	65	59	(1200)	4.6	0.25	0.093	6.2	3.3	0%	0%	Ceram	Birch I		
128	11/11/88	55	320	21	21	14.67	57	56	(1200)	4.6	0.25	0.209	21.6	2.3	0%	0%	Ceram	Bamboo I		
129	11/11/88	55	320	21	21	14.67	61	62	(1200)	4.6	0.50	0.110	6.2	2.3	0%	0%	Ceram	Bamboo I		
130	11/15/88	55	310	18	21	14.73	50	40	(1200)	4.6	2.00	0.088	4.6	1.3	0%	0%	Ceram	W. Pine		Demo George Ulrich?

Table 2. Compilation of the assigned parametric values for all tests, in chronological order (continued).

Test #	Date	Bed Width (W) [cm]	Bed Length (L) [cm]	Temperature (in) (T) [C]	(out)	Pressure (P) [psia]	Humidity (in) [%]	(out)	Fan Speed [rpm]	Wind Speed (U) [m/s]	Elements (n) [#/cm^2]	Loading (wood) (m) [gm/cm^2]	Fuel Height (H) [cm]	Fuel Diam. (d) [mm]	Fuel H2O [%]	Bed H2O [%]	Bed Type	Fuel Type	Repeated Test #'s	Comments
131	12/02/88	55	300	19	21	14.74	17	21	(700)	2.5	0.25	0.071	Mix	2.3	0%	0%	Ceram	Bamboo I		9.0 & 5.4 cm Heights
132	12/02/88	55	330	22	21	14.74	14	21	(200)	0.7	0.50	0.114	3.0	3.3	0%	0%	Ceram	Birch I		
133	12/02/88	55	320	23	23	14.74	14	21	(200)	0.7	0.50	0.377	14.0	3.0	0%	0%	Ceram	Bamboo II		Very High Flames
134	1/04/89	55	330	19	21	14.67	29	27	(700)	2.5	0.25	0.011	4.6	1.3	0%	0%	Ceram	W. Pine	47, 165, ++	Demo Maj R. Hartley
135	1/12/89	55	330	17	19	14.85	17	16	(1200)	4.6	0.50	0.134	4.6	3.0	0%	0%	Ceram	Bamboo II		2 Pitot Tubes
136	1/18/89	55	330	18	20	14.75	24	25	(925)	3.4	0.75	0.359	Mix	3.3	0%	0%	Ceram	Birch I		Mixed Heights
137	1/30/89	55	330	18	20	14.73	37	36	(925)	3.4	0.25	0.253	14.0	3.3	0%	0%	Ceram	Birch I		Tall Birch
138	1/30/89	55	330	22	21	14.73	26	34	(925)	3.4	0.50	0.106	3.0	3.3	0%	0%	Ceram	Birch I		Short Birch
139	2/02/89	55	360	19	21	14.73	38	38	(1200)	4.6	0.25	0.188	14.0	3.0	0%	0%	Ceram	Bamboo II		
140	2/03/89	55	330	17	19	14.73	-	42	(700)	2.5	1.00	0.044	4.6	1.3	9-15%	~1%	Ceram	W. Pine	96	Moisture
141	2/15/89	55	330	21	19	14.73	-	35	(300)	1.0	1.00	0.044	4.6	1.3	20-24%	~1%	Ceram	W. Pine	100	Moisture
142	2/15/89	55	330	21	20	14.73	37	35	(200)	0.7	1.00	0.212	3.0	3.3	0%	0%	Ceram	Birch I		
143	2/15/89	55	350	22	22	14.73	36	37	(200)	0.7	0.17	0.168	14.0	3.3	0%	0%	Ceram	Birch I		
144	2/21/89	55	330	20	18	14.77	-	46	(300)	1.0	1.00	0.044	4.6	1.3	5-10%	~1%	Ceram	W. Pine		Moisture
145	2/24/89	55	330	21	20	14.69	45	47	(300)	1.0	0.50	0.022	4.6	1.3	5-7%	~1%	Ceram	W. Pine		Moisture
146	2/24/89	55	330	22	21	14.71	47	46	(700)	2.5	0.50	0.089	4.6	Mix	0%	0%	Ceram	Pine-Br.I	see 151*	3.3mm & 1.3mm Diam
147	3/07/89	55	330	19	20	14.61	66	63	(450)	1.6	0.25	0.011	4.6	1.3	~0%	0%	Clay	W. Pine	169, ++	Clay Bed (unfired)
148	3/07/89	55	330	21	21	14.61	58	57	(700)	2.5	1.00	0.199	7.7	1.9	0%	0%	Ceram	W. Pine II		Swandwich Picks
149	3/07/89	55	330	21	20	14.61	55	52	(700)	2.5	0.50	0.377	14.0	3.0	0%	0%	Ceram	Bamboo II		Tall Bamboo II
150	3/23/89	55	330	19	20	14.63	50	46	(700)	2.5	1.00	0.044	4.6	1.3	0%	10%	Ceram	W. Pine		Wet Bed
151	3/23/89	55	330	19	20	14.63	50	46	(700)	2.5	-	0.083	4.6	Mix	0%	0%	Ceram	Pine-Br.I	see 146*	3.3mm & 1.3mm Diam
152	3/29/89	55	330	20	20	14.71	57	53	(925)	3.4	1.00	0.312	4.6	3.3	0%	0%	Ceram	Birch		
153	4/06/89	55	330	20	27	14.67	16	37	(700)	2.5	0.38	0.041	4.6	Mix	0%	0%	Ceram	Pine-Br.II		4.4mm & 1.3mm Diam
154	4/06/89	55	330	33	21	14.67	13	31	(300)	1.0	0.50	0.022	4.6	1.3	~1-3%	10%	Ceram	W. Pine	181	Wet Bed
155	4/11/89	55	110	-	-	-	-	-	- Varied -		-	-	4.6	1.3	0%	0%	Ceram	W. Pine		Go, No-Go Tests
156	4/18/89	55	110	20	20	14.67	56	56	0	0	1.50	0.066	4.6	1.3	0%	0%	Ceram	W. Pine		No Wind: 1.5 per hole
157	5/05/89	55	330	21	20	14.63	63	56	(925)	3.4	0.25	0.011	4.6	1.3	0%	0%	Clay	W. Pine		Clay Bed (#2 of 6)
158	5/05/89	55	110	21	21	14.63	58	58	0	0	4.00	0.176	4.6	1.3	0%	0%	Ceram	W. Pine		No Wind - 4 per hole
159	5/05/89	55	330	22	21	14.63	62	56	(925)	3.4	1.00	0.163	2.0	3.3	0%	0%	Ceram	Birch I		Short Birch
160	5/10/89	55	330	20	20	14.67	43	46	(925)	3.4	0.50	0.083	2.0	3.3	0%	0%	Ceram	Birch I		Short Birch
161	5/17/89	55	330	19	19	-	58	49	(700)	2.5	0.25	0.011	4.6	1.3	0%	0%	Clay	W. Pine	166, ++	Clay Bed (#3 of 6)
162	5/17/89	55	330	19	21	-	58	53	(700)	2.5	0.25	0.011	4.6	1.3	0%	0%	Ceram	W. Pine		Nails Present
163	5/17/89	55	330	19	21	-	58	54	(450)	1.6	0.17	0.007	4.6	1.3	0%	0%	Ceram	W. Pine		Sparce Loading

Table 2. Compilation of the assigned parametric values for all tests, in chronological order (continued).

Test #	Date	Bed Width (W) [cm]	Bed Length (L) [cm]	Temperature (in) (T) [C]	Temperature (out)	Pressure (P) [psia]	Humidity (in) [%]	Humidity (out)	Fan Speed [rpm]	Wind Speed (U) [m/s]	Elements (n) [#/cm^2]	Loading (wood) (m) [gm/cm^2]	Fuel Height (H) [cm]	Fuel Diam. (d) [mm]	Fuel H2O [%]	Bed H2O [%]	Bed Type	Fuel Type	Repeated Test #'s	Comments
164	5/30/89	55	330	20	19	-	52	54	(700)	2.5	0.17	0.007	4.6	1.3	0%	0%	Ceram	W. Pine		Sparse Loading
165	5/30/89	55	330	20	19	-	51	49	(700)	2.5	0.25	0.011	4.6	1.3	0%	0%	Ceram	W. Pine	47, 134, ++	Repeat
166	5/30/89	55	330	21	20	-	53	50	(700)	2.5	0.25	0.011	4.6	1.3	0%	0%	Clay	W. Pine	161, ++	Clay Bed (#4 of 6)
167	6/07/89	75	330	18	20	14.63	64	50	(450)	1.6	0.50	0.022	4.6	1.3	0%	0%	Ceram	W. Pine		75cm Width
168	6/07/89	75	330	18	20	14.63	65	52	(450)	1.6	0.25	0.011	4.6	1.3	0%	0%	Ceram	W. Pine		75cm Width
169	6/07/89	55	330	20	20	14.63	60	59	(450)	1.6	0.25	0.011	4.6	1.3	0%	0%	Clay	W. Pine	147, ++	Clay Bed (#5 of 6)
170	6/07/89	55	330	19	20	14.63	62	56	(450)	1.6	0.50	0.022	4.6	1.3	0%	0%	Ceram	W. Pine	38,50-52...	Repeat
171	6/07/89	55	330	20	20	14.63	60	52	(450)	1.6	0.25	0.011	4.6	1.3	0%	0%	Ceram	W. Pine	29, 76, ++	Repeat
172	6/07/89	55	330	19	21	14.63	64	55	(450)	1.6	0.06	0.030	4.6	4.4	0%	0%	Ceram	Birch II		No Burn
173	6/22/89	55	330	20	20	14.56	70	59	(700)	2.5	0.13*	0.033	4.6	Mix	0%	0%	Ceram	Pine-Br II		No Propagation
174	6/22/89	55	330	21	20	14.56	68	55	(700)	2.5	0.17	0.007	4.6	1.3	0%	0%	Ceram	W. Pine	164	No Thermocouple Rake
175	6/22/89	55	330	21	19	14.56	66	55	(700)	2.5	0.13	0.061	4.6	4.4	0%	0%	Ceram	Birch II		!! Propagation !!
176	6/22/89	55	330	22	20	14.56	65	54	(700)	2.5	0.19*	0.036	4.6	Mix	0%	0%	Ceram	Pine-Br II		No Propagation
177	6/22/89	55	330	23	21	14.56	59	57	(1200)	4.6	0.19*	0.036	4.6	Mix	0%	0%	Ceram	Pine-Br II		No Propagation
178	6/28/89	55	330	19	20	14.65	63	54	(700)	2.5	0.25	0.011	4.6	1.3	0%	0%	Clay	Pine/Plast.		0.008gm/cm^2 Plastics
179	6/28/89	55	330	21	21	14.65	61	55	(1200)	4.6	0.31	0.041	4.6	Mix	0%	0%	Ceram	Pine-Br II		Thin Gone/Thick Not
180	7/25/89	75	330	20	21	14.59	67	62	(450)	1.6	1.00	0.044	4.6	1.3	0%	0%	Ceram	W. Pine		75cm Wide test
181	7/25/89	55	330	21	21	14.59	66	59	(300)	1.0	0.50	0.011	4.6	1.3	~8%	~10%	Ceram	W. Pine	154	Wet Bed 1 of 3
182	7/25/89	55	330	23	21	14.59	65	57	(300)	1.0	0.50	0.011	4.6	1.3	~5%	~20%	Ceram	W. Pine		Wet Bed 2 of 3
183	7/25/89	55	330	23	21	14.59	62	55	(300)	1.0	0.50	0.011	4.6	1.3	~13%	~30%	Ceram	W. Pine		Wet Bed 3 of 3
184	9/26/89	55	330	20	20	14.63	74	58	(1200)	4.6	0.31*	0.041	4.6	Mix	0%	0%	Ceram	Pine-Br II	179*	Thin gone/thick not
185	9/26/89	55	330	21	20	14.61	70	58	(700)	2.5	0.31*	0.041	4.6	Mix	0%	0%	Ceram	Pine-Br II		No TC Rake Used
186	9/26/89	15	330	25	20	14.61	60	57	(450)	1.6	1.00	0.044	4.6	1.3	0%	0%	Ceram	W. Pine		15cm wide test
187	10/09/89	15	330	20	21	14.71	65	57	(450)	1.6	0.50	0.022	4.6	1.3	0%	0%	Ceram	W. Pine		15cm wide test
188	10/09/89	30	330	21	21	14.71	63	61	(450)	1.6	2.00	0.088	4.6	1.3	0%	0%	Ceram	W. Pine		30cm wide test
189	10/09/89	55	330	22	21	14.71	60	54	(925)	3.4	1.00	0.044*	4.6	1.3	0%	0%	Ceram	W.Pine-Tar		Roof Cement Coating
190	10/13/89	55	278	20	21	14.67	67	61	(700)	2.5	1.00	0.494	4.6	4.4	0%	0%	Ceram	Birch II		
191a	10/13/89	55	330	21	21	14.67	66	60	(700)	2.5	0.50	0.505	14.0	3.3	0%	0%	Ceram	Birch I		'm' based on #137
191b	-	-	-	-	-	-	-	-	0	0	-	-	-	-	-	-	-	-		Wind turned off!

Table 2. Compilation of the assigned parametric values for all tests, in chronological order (continued).

Test #	Date	Bed Width (W) [cm]	Bed Length (L) [cm]	Temperature (in) (T) [C]	(out)	Pressure (P) [psia]	Humidity (in) [%]	(out)	Fan Speed [rpm]	Wind Speed (U) [m/s]	Elements (n) [#/cm^2]	Loading (wood) (m) [gm/cm^2]	Fuel Height (H) [cm]	Fuel Diam. (d) [mm]	Fuel H2O [%]	Bed H2O [%]	Bed Type	Fuel Type	Repeated Test #'s	Comments
192	11/01/89	55	13 rows	23	21	14.67	16	22	(300)	1.0	10x10 cm	0.031	2.8	-	0%	0%	Ceram	Boxes		2.8 x2.4 x3.8cm Box
193	11/03/89	55	15 rows	20	20	14.65	18	26	(450)	1.6	8x 8 cm	0.048	2.8	-	0%	0%	Ceram	Boxes		2.8 x2.4 x3.8cm Box
194	11/06/89	55	12 rows	20	21	14.71	48	69	(450)	1.6	6x 6 cm	0.086	2.8	-	0%	0%	Ceram	Boxes		2.8 x2.4 x3.8cm Box

Note: Fan speeds in parentheses ( ) are tests after 1st refurbishment

* Note: Variation or restrictions apply

++ Note: Tests performed with both clay and ceramic beds

Table 3. Compilation of the firespread-rate results from all tests, in chronological order.

Test #	Flame Speed (vf) [cm/s]	Error in speed [cm/s]	Error (upper) [cm/s]	Error (lower) [cm/s]	TCs Used in vf fit	Wind Speed (U) [m/s]	Loading (m) gm/cm^2	Bed Width (W) [cm]	Fuel Diam. (d) [mm]	Fuel Height (H) [cm]	Fuel Type	(UH/md) ^.5 Sqrt[m^3 (s-kg)]	(U/m) ^.5 (m^3/s-kg)^.5	Repeated Test #'s	Comments
1	6.7	1.19	7.89	5.51	1-16	1.6	0.011	100	1.3	4.6	White Pine	22.5	3.8		100 cm Width
2	6.8	0.86	7.70	5.98	1-17	1.6	0.011	100	1.3	4.6	White Pine	22.5	3.8		100 cm Width
3	8.8	0.99	9.76	7.78	1-18	1.6	0.022	100	1.3	4.6	White Pine	15.9	2.7		100 cm Width
4	Data not recorded				-	1.6	0.022	55	1.3	4.6	White Pine	16.0	2.7		1/2 Tray Ignited
5	Uncertain Conditions				-	0.7	0.044	55	1.3	4.6	White Pine	7.2	1.2		55 cm Test Width
6	Steady State not Achieved				-	3.4	0.044	55	1.3	4.6	White Pine	16.6	2.8		55 cm Test Width
7	0	0	0	0	-	0	0.044	55	1.3	4.6	White Pine	0	0.0		0 Wind Speed
8	0	0	0	0	-	0	0.044	55	1.3	4.6	White Pine	0	0.0		0 Wind Speed
9	1.1	0.02	1.14	1.10	1-8	0.4	0.044	55	1.3	4.6	White Pine	5.9	1.0	17-24	
10	Data not recorded				-	Varied	Varied	4	1.3	4.6	White Pine	-			Blow Out Attempt
11	Uncertain Conditions				-	0.4	0.044	55	1.3	4.6	White Pine	5.9	1.0		?
12	0.82	0.05	0.87	0.77	1-8	0.4	0.088	55	1.3	4.6	White Pine	4.1	0.7	13,14 & 15	Crystallinity I
13	0.80	0.05	0.85	0.75	1-8	0.4	0.088	55	1.3	4.6	White Pine	4.1	0.7	12,14 & 15	Crystallinity I
14	0.77	0.03	0.80	0.74	1-8	0.4	0.088	55	1.3	4.6	White Pine	4.1	0.7	13,12 & 15	Crystallinity I
15	0.92	0.07	0.99	0.85	1-8	0.4	0.088	55	1.3	4.6	White Pine	4.1	0.7	13,14 & 12	Crystallinity I
16	2.2	0.20	2.38	1.98	6-16	1.1	0.044	55	1.3	4.6	White Pine	9.4	1.6	98*	
17	1.0	0.09	1.08	0.90	1-8	0.4	0.044	55	1.3	4.6	White Pine	5.9	1.0	9 & 17-24	Crystallinity
18	1.1	0.05	1.19	1.09	1-8	0.4	0.044	55	1.3	4.6	White Pine	5.9	1.0	9 & 17-24	Crystallinity
19	1.2	0.15	1.31	1.01	1-8	0.4	0.044	55	1.3	4.6	White Pine	5.9	1.0	9 & 17-24	Crystallinity
20	1.2	0.13	1.37	1.11	1-8	0.4	0.044	55	1.3	4.6	White Pine	5.9	1.0	9 & 17-24	Crystallinity
21	Computer Crash				-	0.4	0.044	55	1.3	4.6	White Pine	5.9	1.0	9 & 17-24	No Data
22	1.3	0.07	1.34	1.20	1-8	0.4	0.044	55	1.3	4.6	White Pine	5.9	1.0	9 & 17-24	Repeatibility
23	1.4	0.10	1.51	1.31	1-8	0.4	0.044	55	1.3	4.6	White Pine	5.9	1.0	9 & 17-24	Repeatibility
24	1.2	0.09	1.30	1.12	1-8	0.4	0.044	55	1.3	4.6	White Pine	5.9	1.0	9 & 17-24	Repeatibility
25	1.7	0.19	1.85	1.47	2-16	0.7	0.044	55	1.3	4.6	White Pine	7.2	1.2		Extend Data Set
26	3.0	0.23	3.25	2.79	1-16	1.0	0.032	55	1.3	4.6	White Pine	10.8	1.8		Fleeter Repeat
27	1.9	0.26	2.14	1.62	4-14	1.6	0.044	55	1.3	4.6	White Pine	11.2	1.9	99	Extend Data Set
28	2.3	0.28	2.56	2.00	10-19	2.5	0.044	55	1.3	4.6	White Pine	14.2	2.4	56 & 82	Extend Data Set
29	4.2	0.37	4.57	3.83	1-23	1.6	0.011	55	1.3	4.6	White Pine	22.5	3.8	76 & 171	Extend Data Set
30	2.7	0.54	3.27	2.19	6-23	3.0	0.044	55	1.3	4.6	White Pine	15.4	2.6		Extend Data Set
31	3.8	0.46	4.28	3.36	4-15	1.6	0.022	55	1.3	4.6	White Pine	15.9	2.7		Extend Data Set

Table 3. Compilation of the firespread-rate results from all tests, in chronological order (continued).

Test #	Flame Speed (vf) [cm/s]	Error in speed [cm/s]	Error (upper) [cm/s]	Error (lower) [cm/s]	TCs Used in vf fit	Wind Speed (U) [m/s]	Loading (m) gm/cm^2	Bed Width (W) [cm]	Fuel Diam. (d) [mm]	Fuel Height (H) [cm]	Fuel Type	(UH/md)^.5 Sqrt[m^3/(s-kg)]	(U/m)^.5 (m^3/s-kg)^.5	Repeated Test #'s	Comments
32	1.7	0.17	1.85	1.51	1-8	0.4	0.022	55	1.3	4.6	White Pine	8.3	1.4		Extend Data Set
33	1.4	0.37	1.76	1.02	6-16	1.6	0.088	55	1.3	4.6	White Pine	7.9	1.3		Extend Data Set
34	2.6	0.71	3.33	1.91	15-23	3.4	0.044	55	1.3	4.6	White Pine	16.6	2.8	57,58 & 62	Extend Data Set
35	4.6	0.61	5.20	3.98	12-21	2.5	0.022	55	1.3	4.6	White Pine	20.0	3.4	90 & 91*	Extend Data Set
36	1.9	0.17	2.07	1.73	2-8	0.4	0.011	55	1.3	4.6	White Pine	11.7	2.0		Extend Data Set
37	6.6	0.63	7.24	5.98	3-14	1.6	0.022	100	1.3	4.6	White Pine	15.9	2.7		100 cm Width
38	3.6	0.39	4.02	3.24	1-15	1.6	0.022	55	1.3	4.6	White Pine	15.9	2.7	50,51 & 52	Extend Data Set
39	2.8	0.37	3.21	2.47	3-16	1.6	0.022	30	1.3	4.6	White Pine	15.9	2.7		30 cm Width
40			0.00	0.00	-	1.6	0.022	55	1.3	4.6	White Pine	15.9	2.7		Elements Scattered
41	1.3	0.21	1.46	1.04	13-22	2.5	0.088	55	1.3	4.6	White Pine	10.0	1.7		Extend Data Set
42	5.5	1.05	6.51	4.41	2-23	3.4	0.022	55	1.3	4.6	White Pine	23.4	3.9	66	Extend Data Set
43	6.3	1.05	7.30	5.20	7-17	3.4	0.011	55	1.3	4.6	White Pine	33.1	5.6	55,63 & 65	Roof Stop @TC#19
44	0	0	0	0	-	3.4	0.006	55	1.3	4.6	White Pine	46.9			No propagation
45	0	0	0	0	-	3.4	0.006	55	1.3	4.6	White Pine	46.0			No propagation
46	0	0	0	0	-	1.6	0.006	55	1.3	4.6	White Pine	31.2			No propagation
47	4.9	0.78	5.69	4.13	5-21	2.5	0.011	55	1.3	4.6	White Pine	28.4	4.8	134	
48	4.1	0.46	4.52	3.60	1-12	1.6	0.011	30	1.3	4.6	White Pine	22.5	3.8		30 cm Width
49	5.4	0.47	5.90	4.96	2-12	1.6	0.044	100	1.3	4.6	White Pine	11.2	1.9		100 cm Width
50	4.3	0.47	4.76	3.82	4-15	1.6	0.022	55	1.3	4.6	White Pine	15.9	2.7	38,51 & 52	
51	4.3	0.43	4.77	3.91	3-15	1.6	0.022	55	1.3	4.6	White Pine	15.9	2.7	38,50 & 52	
52	4.4	0.30	4.74	4.14	3-16	1.6	0.022	55	1.3	4.6	White Pine	15.9	2.7	38,50 & 51	
53	3.8	0.47	4.31	3.37	5-14	1.6	0.022	55	1.3	4.6	White Pine	15.9	2.7		Ceiling at X=0cm
54	1.8	0.15	1.90	1.60	4-15	1.6	0.044	30	1.3	4.6	White Pine	11.2	1.9		30 cm Width
55	5.8	1.40	7.16	4.36	12-23	3.4	0.011	55	1.3	4.6	White Pine	33.1	5.6	43,63 & 65	Repeat #43
56	2.8	0.67	3.51	2.17	9-21	2.5	0.044	55	1.3	4.6	White Pine	14.2	2.4	28 & 82	Repeat #28
57	2.9	0.93	3.82	1.96	11-22*	3.4	0.044	55	1.3	4.6	White Pine	16.5	2.8	34,58 & 62	
58	3.1	0.79	3.87	2.29	9-23	3.4	0.044	55	1.3	4.6	White Pine	16.5	2.8	34,57 & 62	
59	2.1	0.48	2.55	1.59	10-23	2.5	0.110	55	2.3	12.1	Bamboo I	10.9	1.5		Fuel Height Varied
60	1.1	0.20	1.32	0.92	9-22	2.5	0.110	55	2.3	6.2	Bamboo I	7.8	1.5		Fuel Height Varied
61	0.69	0.18	0.87	0.51	8-18	2.5	0.116	55	2.3	3.0	Bamboo I	5.3	1.5		Fuel Height Varied
62	2.7	0.26	2.92	2.40	7-23	3.4	0.044	55	1.3	4.6	White Pine	16.5	2.8	34,57 & 58	
63	6.3	1.26	7.52	5.00	6-21	3.4	0.011	55	1.3	4.6	White Pine	33.0	5.6	43,55 & 65	
64	2.6	0.46	3.09	2.17	5-21	3.4	0.088	55	1.3	4.6	White Pine	11.7	2.0		?Steady S. Region?

Table 3. Compilation of the firespread-rate results from all tests, in chronological order (continued).

Test #	Flame Speed (vf) [cm/s]	Error in speed [cm/s]	Error (upper) [cm/s]	Error (lower) [cm/s]	TCs Used in vf fit	Wind Speed (U) [m/s]	Loading (m) gm/cm^2	Bed Width (W) [cm]	Fuel Diam. (d) [mm]	Fuel Height (H) [cm]	Fuel Type	(UH/md)^.5 Sqrt[m^3/(s-kg)]	(U/m)^.5 (m^3/s-kg)^.5	Repeated Test #'s	Comments
65	6.6	1.24	7.87	5.39	5-21	3.4	0.011	55	1.3	4.6	White Pine	33.0	5.6	43,55 & 63	
66	4.6	1.04	5.63	3.55	5-19	3.4	0.022	55	1.3	4.6	White Pine	23.3	3.9	42	
67	Computer Crash					3.4	0.044	55	1.3	4.6	White Pine	16.5	2.8	Many(e.g. 57)	Ceiling @X=0.19 m
68	6.9	2.25	9.18	4.68	1-22	4.6	0.011	55	1.3	4.6	White Pine	38.4	6.5		
69	2.3	0.32	2.58	1.94	10-23	1.0	0.011	55	1.3	4.6	White Pine	17.9	3.0		
70	4.3	1.81	6.07	2.45	4-22*	3.4	0.044	55	1.3	4.6	White Pine	16.5	2.8	58*, 70, 124	Ceiling @X=3.4 m
71	5.5	1.02	6.49	4.45	4-22	4.6	0.022	55	1.3	4.6	White Pine	27.2	4.6		
72	3.3	0.70	4.01	2.61	10-21	4.6	0.044	55	1.3	4.6	White Pine	19.2	3.2		Shadowgraph
73	3.8	0.82	4.62	2.98	7-23	3.4	0.033	55	1.3	4.6	White Pine	19.1	3.2		Shadowgraph
74	2.1	0.52	2.61	1.57	6-22	3.4	0.088	55	1.3	4.6	White Pine	11.7	2.0		Shadowgraph
75	2.5	0.14	2.62	2.34	1-23	1.0	0.022	55	1.3	4.6	White Pine	12.7	2.1		Shadowgraph
76	4.2	0.56	4.74	3.62	1-23	1.6	0.011	55	1.3	4.6	White Pine	22.7	3.8	29 & 171	Repeat - TC Rake
77	1.1	0.28	1.33	0.77	4-30	3.4	0.180	55	2.3	4.6	Bamboo I	6.1	1.4		
78	2.3	0.26	2.51	1.99	1-23	1.0	0.033	55	1.3	4.6	White Pine	10.4	1.7		TC Rake Present
79	7.3	2.84	10.16	4.48	2-16*	2.5	0.044	0-100	1.3	4.6	White Pine	14.2	2.4		Tapered Loading
80	No propagation					1.6	0.022	55	1.3	4.6	Pine & Nails	16.0	2.7		Nails in all Trays
81	0	0	0	0	-	0	0.044	55	1.3	4.6	White Pine	0	0.0		No Wind
82	2.7	0.41	3.09	2.27	6-19	2.5	0.044	55	1.3	4.6	White Pine	14.2	2.4	56 & 28	Repeat Test
83	3.5	0.59	4.09	2.91	4-23	2.5	0.033	55	1.3	4.6	White Pine	16.4	2.8		
84	2.1	0.28	2.36	1.80	5-23	2.5	0.045	55	2.3	4.6	Bamboo I	10.5	2.4		
85	0.29	0.03	0.32	0.26	1-21	0	0.088	55	1.3	4.6	White Pine	0	0.0		No Wind (0 m/s)
86	1.6	0.31	1.90	1.28	4-23	2.5	0.090	55	2.3	4.6	Bamboo I	7.5	1.7		
87	Computer Crash					3.4	0.022	55	1.3	4.6	Pine & Nails	23.4	3.9		Nails in Tray #2
88	3.1	0.71	3.79	2.37	12-22	4.6	0.045	55	2.3	4.6	Bamboo I	14.3	3.2		
89	7.6	1.09	8.71	6.53	5-22	1.6	0.044	5-107	1.3	4.6	White Pine	11.3	1.9		Tapered Loading
90	4.3	0.78	5.05	3.49	11-23	2.5	0.022	55	1.3	4.6	White Pine	20.1	3.4	35* & 91*	Perpend. Loading
91	4.6	0.42	4.99	4.15	5-19	2.5	0.022	55	1.3	4.6	White Pine	20.1	3.4	35 & 90*	Parallel Loading
92	1.0	0.16	1.17	0.85	1-18	1.0	0.090	55	2.3	4.6	Bamboo I	4.7	1.1		
93	1.3	0.16	1.42	1.10	9-17*	2.5	0.022	55	1.3	4.6	Pine & Nails	20.1	3.4		Nails in Tray #2
94	6.2	0.96	7.11	5.19	3-17	1.6	0.044	3-106	1.3	4.6	White Pine	11.3	1.9		Tapered Loading
95	1.3	0.26	1.58	1.06	4-23	1.6	0.045	55	2.3	4.6	Bamboo I	8.4	1.9		
96	2.0	0.48	2.47	1.51	1-23	2.5	0.044	55	1.3	4.6	White Pine	14.2	2.4		20-30% Moisture
97	4.2	0.88	5.03	3.27	2-12	1.0	0.044	100	1.3	4.6	White Pine	9.0	1.5		100 cm Width

Table 3. Compilation of the firespread-rate results from all tests, in chronological order (continued).

Test #	Flame Speed (vf) [cm/s]	Error in speed [cm/s]	Error (upper) [cm/s]	Error (lower) [cm/s]	TCs Used in vf fit	Wind Speed (U) [m/s]	Loading (m) gm/cm^2	Bed Width (W) [cm]	Fuel Diam. (d) [mm]	Fuel Height (H) [cm]	Fuel Type	(UH/md)^.5 Sqrt[m^3/(s-kg)]	(U/m)^.5 (m^3/s-kg)^.5	Repeated Test #'s	Comments
98	1.9	0.37	2.29	1.55	1-23	1.0	0.044	55	1.3	4.6	White Pine	9.0	1.5	16*	
99	2.5	0.52	3.02	1.98	4-24	1.6	0.044	55	1.3	4.6	White Pine	11.3	1.9	27	
100	1.0	0.14	1.15	0.87	1-16	1.0	0.044	55	1.3	4.6	White Pine	9.0	1.5		24% Moisture
101	1.7	0.33	2.06	1.40	11-23	2.5	0.090	55	2.3	9.2	Bamboo I	10.5	1.7		Fuel Height Varied
102	9.2	2.56	11.72	6.60	7-23	3.4	0.044	100	1.3	4.6	White Pine	16.5	2.8		100 cm Width
103	2.7	0.46	3.14	2.22	3-22	1.0	0.088	100	1.3	4.6	White Pine	6.3	1.1		100 cm Width
104	0.71	0.24	0.95	0.47	9-17*	2.5	0.022	55	1.3	4.6	Pine & Nails	20.1	3.4		Nails in Tray #2*
105	6.0	1.28	7.23	4.67	2-20	3.4	0.011	100	1.3	4.6	White Pine	33.0	5.6		100 cm Width
106	0.83	0.08	0.91	0.75	9-17*	2.5	0.022	55	1.3	4.6	Pine & Nails	20.1	3.4		Nails in Tray #2*
107	3.3	0.63	3.88	2.62	10-23	0.7	0.044	100	1.3	4.6	White Pine	7.5	1.3		100 cm Width
108	1.0	0.14	1.15	0.87	1-19	1.0	0.044	55	1.3	4.6	White Pine	9.0	1.5		8% Moisture
109	2.5	0.24	2.75	2.27	9-17*	2.5	0.022	55	1.3	4.6	Pine & Nails	20.1	3.4		1/2 Nails Tray #2*
110	1.7	0.45	2.15	1.25	4-23	2.5	0.065	55	3.0	4.6	Bamboo II	7.7	2.0		
111	7.5	2.97	10.43	4.49	1-22	4.6	0.011	100	1.3	4.6	White Pine	38.4	6.5		100 cm Width
112	2.3	0.44	2.76	1.88	9-17*	2.5	0.022	55	1.3	4.6	Pine & Nails	20.1	3.4		1/2 Nails Tray #2*
113	2.1	0.51	2.57	1.55	1-23	2.5	0.044	55	1.3	4.6	White Pine	14.2	2.4		4-13% Moisture
114	1.5	0.36	1.85	1.13	9-23	2.5	0.078	55	3.3	4.6	Birch	6.7	1.8		
115	3.5	0.64	4.14	2.86	9-17*	2.5	0.022	55	1.3	4.6	Pine & Nails	20.1	3.4		1/4 Nails Tray #2*
116	3.3	0.59	3.84	2.66	6-23	0.7	0.022	100	1.3	4.6	White Pine	10.6	1.8		100 cm Width
117	1.6	0.33	1.92	1.26	6-23	1.6	0.060	55	2.3	6.2	Bamboo I	8.5	1.6		Fuel Height Varied
118	1.5	0.20	1.66	1.26	1-23	1.6	0.102	55	3.3	6.2	Birch	5.4	1.3		Fuel Height Varied
119	3.0	0.54	3.56	2.48	5-23	3.4	0.044	55	1.3	4.6	White Pine	16.6	2.8	Many(e.g 57)	See 34,57,58,62,70
120	3.0	1.49	4.49	1.51	5-23	3.4	0.044	55	1.3	4.6	White Pine	16.6	2.8	Many(e.g 57)	See 34,57,58,62,70
121	0.84	0.07	0.91	0.77	1-14	0.7	0.23	55	3.3	14.0	Birch	3.6	0.6		Fuel Height Varied
122	4.0	0.87	4.85	3.11	4-23	0.7	0.011	100	1.3	4.6	White Pine	15.0	2.5		100 cm Width
123	2.0	0.40	2.42	1.62	1-22	3.4	0.050	55	3.3	3.0	Birch	7.9	2.6		Fuel Height Varied
124	1.6	0.35	1.95	1.25	12-23*	3.4	0.044	55	1.3	4.6	White Pine	16.5	2.8		Ceiling @X=0.20 m
125	9.1	2.29	11.42	6.84	5-22	4.6	0.022	100	1.3	4.6	White Pine	27.2	4.6		100 cm Width
126	2.8	0.61	3.43	2.21	1-22	4.6	0.060	55	2.3	6.2	Bamboo I	14.4	2.8		Fuel Height Varied
127	2.5	0.43	2.92	2.06	6-23	4.6	0.093	55	3.3	6.2	Birch	9.6	2.2		Fuel Height Varied
128	4.7	-	-	-	1-23	4.6	0.209	55	2.3	21.6	Bamboo I	14.4	1.5		Still Unsteady
129	1.8	0.42	2.19	1.35	13-23	4.6	0.120	55	2.3	6.2	Bamboo I	10.2	2.0		Fuel Height Varied
130	2.9	0.61	3.46	2.24	6-23	4.6	0.088	55	1.3	4.6	White Pine	13.6	2.3		

Table 3. Compilation of the firespread-rate results from all tests, in chronological order (continued).

Test #	Flame Speed (vf) [cm/s]	Error in speed [cm/s]	Error (upper) [cm/s]	Error (lower) [cm/s]	TCs Used in vf fit	Wind Speed (U) [m/s]	Loading (m) gm/cm^2	Bed Width (W) [cm]	Fuel Diam. (d) [mm]	Fuel Height (H) [cm]	Fuel Type	(U-H/md) ^.5 Sqrt[m^3 (s-kg)]	(U/m) ^.5 (m^3/s-kg)^.5	Repeated Test #'s	Comments
131	2.4	0.56	3.00	1.88	6-23	2.5	0.071	55	2.3	Mix	Bamboo I	-	1.9		5.4 & 9.0cm Height
132	0.49	0.09	0.58	0.40	1-17	0.7	0.114	55	3.3	3.0	Birch	2.4	0.8		Fuel Height Varied
133	0.49	0.15	0.64	0.34	1-17	0.7	0.377	55	3.0	14.0	Bamboo II	2.9	0.4		
134	6.6	1.31	7.93	5.31	4-23	2.5	0.011	55	1.3	4.6	White Pine	28.4	4.8	47, 165, +	Vf Inconsistent
135	1.6	0.38	2.02	1.26	14-23	4.6	0.134	55	3.0	4.6	Bamboo II	7.3	1.9		
136	Thermocouple Height Varied				-	3.4	0.359	55	3.3	Mix	Birch	-	1.0		Mixed Diameters
137	2.7	-	-	-	-	3.4	0.253	55	3.3	14.0	Birch	7.6	1.2		Almost Steady
138	1.2	0.28	1.46	0.90	3-22	3.4	0.106	55	3.3	3.0	Birch	5.4	1.8		Fuel Height Varied
139	2.3	0.63	2.93	1.67	17-26	4.6	0.189	55	3.0	14.0	Bamboo II	10.7	1.6		Steady Established
140	1.9	0.53	2.44	1.38	1-23	2.5	0.044	55	1.3	4.6	White Pine	14.2	2.4		9-15% Moisture
141	1.2	0.18	1.39	1.03	1-23	1.0	0.044	55	1.3	4.6	White Pine	9.0	1.5		20-24% Moisture
142	0.31	0.06	0.37	0.25	1-11	0.7	0.212	55	3.3	3.0	Birch	1.7	0.6		Fuel Height Varied
143	1.5	0.11	1.59	1.37	4-24	0.7	0.168	55	3.3	14.0	Birch	4.2	0.6		Fuel Height Varied
144	1.2	0.17	1.39	1.05	1-23	1.0	0.044	55	1.3	4.6	White Pine	9.0	1.5		5-10% Moisture
145	1.3	0.12	1.38	1.14	1-23	1.0	0.022	55	1.3	4.6	White Pine	12.7	2.1		5- 7% Moisture
146	1.4	0.38	1.80	1.04	8-23	2.5	0.089	55	Mix	4.6	Pine/Br.I	-	1.7		Thickness Mixture
147	3.0	0.32	3.35	2.71	1-23	1.6	0.011	55	1.3	4.6	White Pine	22.7	3.8	169, +	? wet ? Clay bed
148	1.23	0.26	1.49	0.97	6-23	2.5	0.199	55	1.9	7.7	W. Pine II	7.1	1.1		Sandwich Picks
149	Steady State not Achieved				-	2.5	0.377	55	3.0	14.0	Bamboo II	5.6	0.8		
150	2.4	0.61	2.96	1.74	1-13	2.5	0.044	55	1.3	4.6	White Pine	14.2	2.4		10% Wet Bed
151	1.91	0.36	2.27	1.55	1-23	2.5	0.083	55	Mix	4.6	Pine/Br.I	-	1.7		Mixed Diameters
152	0.78	0.15	0.93	0.63	4-23	3.4	0.312	55	3.3	4.6	Birch	3.9	1.0		
153	1.65	0.33	1.98	1.32	4-23	2.5	0.041	55	Mix	4.6	Pine/Br.I	-	2.5	see 162	Mixed Diameters
154	0.97	0.06	1.03	0.91	1-23	1.0	0.022	55	1.3	4.6	White Pine	12.7	2.1		10% Wet Bed
155	Data not recorded				-	Varied	Varied	55	1.3	4.6	White Pine	-	-		Go, No-Go Tests
156	0.21	0.01	0.22	0.20	4-7	0	0.066	55	1.3	4.6	White Pine	0	0		No Wind (0 m/s)
157	6.5	1.26	7.75	5.23	1-23	3.4	0.011	55	1.3	4.6	White Pine	33.1	5.6	++	Dry Clay Bed
158	0.23	0.01	0.24	0.22	1-7	0.0	0.176	55	1.3	4.6	White Pine	0	0		4 toothpicks/hole
159	0.74	0.13	0.87	0.61	5-23	3.4	0.163	55	3.3	2.0	Birch	3.6	1.4		Fuel Height Varied
160	1.29	0.40	1.69	0.89	6-23	3.4	0.082	55	3.3	2.0	Birch	5.0	2.0		Fuel Height Varied
161	4.9	1.13	6.04	3.78	1-23	2.5	0.011	55	1.3	4.6	White Pine	28.4	4.8	166, ++	
162	3.2	0.56	3.79	2.67	7-23	2.5	0.011	55	1.3	4.6	Pine & Nails	28.4	4.8	see 153	1 Nail / 16 holes
163	0+	0	0	0	-	1.6	0.007	55	1.3	4.6	White Pine	28.4	4.8		Spread ceased

Table 3. Compilation of the firespread-rate results from all tests, in chronological order (continued).

Test #	Flame Speed (vf) [cm/s]	Error in speed [cm/s]	Error (upper) [cm/s]	Error (lower) [cm/s]	TCs Used in vf fit	Wind Speed (U) [m/s]	Loading (m) gm/cm^2	Bed Width (W) [cm]	Fuel Diam. (d) [mm]	Fuel Height (H) [cm]	Fuel Type	(UH/md) ^.5 Sqrt[m^3 (s-kg)]	(U/m) ^.5 (m^3/s-kg)^.5	Repeated Test #'s	Comments
184	0+	0	0	0	-	2.5	0.[illegible]7	55	1.3	4.6	White Pine	35.5	6.0		Spread ceased
185	5.2	0.90	6.05	4.25	1-23	2.5	0.011	55	1.3	4.6	White Pine	28.4	4.8	47, 134, ++	
186	5.2	0.87	6.08	4.34	5-23	2.5	0.011	55	1.3	4.6	White Pine	28.4	4.8	161, ++	Dry Clay Bed
187	5.2	0.86	6.01	4.29	1-23	1.6	0.022	75	1.3	4.6	White Pine	16.0	2.7		75 cm Width
188	5.5	0.54	6.05	4.97	1-23	1.6	0.011	75	1.3	4.6	White Pine	22.7	3.8		75 cm Width
189	4.2	0.51	4.68	3.66	1-23	1.6	0.011	55	1.3	4.6	White Pine	22.7	3.8	147, ++	Dry Clay Bed
170	3.5	0.62	4.12	2.88	1-23	1.6	0.022	55	1.3	4.6	White Pine	15.9	2.7		
171	3.9	0.55	4.44	3.34	2-23	1.6	0.011	55	1.3	4.6	White Pine	22.7	3.8	29 & 76	Repeat - TC Rake
172	0	0	0	0	-	2.5	0.030	55	4.4	4.6	Birch II	9.3	2.9		No propagation
173	0	0	0	0	-	2.5	0.033	55	Mix	4.6	Pine I/Br.II	-	2.8		No propagation
174#	4.3	-	-	-	8-23	2.5	0.007	55	1.3	4.6	W. Pine I	35.5	6.0		Spread slowing
175	1.2	0.19	1.38	0.98	7-23	2.5	0.601	55	4.4	4.6	Birch II	2.1	0.6		Thick Fuel
176	0	0	0	0	-	2.5	0.030	55	Mix	4.6	Pine I/Br.II	-	2.9		No propagation
177	0	0	0	0	-	4.6	0.030	55	Mix	4.6	Pine I/Br.II	-	3.9		Blew Out
178	4.2	0.54	4.69	3.61	5-23	2.5	0.011	55	1.3	4.6	Pine/Plastic	-	-		Plastics Present
179	?2.2?	0.56	-	-	10-15	4.6	0.041	55	Mix	4.6	Pine I/Br.II	-	3.3		? Steady ?
180	3.0	0.53	3.50	2.44	1-23	1.6	0.044	75	1.3	4.6	W. Pine I	11.3	1.9		75 cm Width
181	1.71	0.12	1.83	1.59	1-23	1.0	0.022	55	1.3	4.6	W. Pine I	12.7	2.1	154	~0.5l H20 per tray
182	1.76	0.14	1.90	1.62	1-23	1.0	0.022	55	1.3	4.6	W. Pine I	12.7	2.1		~1.0l H20 per tray
183	1.57	0.15	1.72	1.42	1-23	1.0	0.022	55	1.3	4.6	W. Pine I	12.7	2.1		~1.5l H20 per tray
184	?2.4?	0.14	-	-	10-15	4.6	0.041	55	Mix	4.6	Pine I/Br.II	-	3.3	see 179	? Steady ?
185	1.5	0.16	1.61	1.29	3-23	2.5	0.041	55	Mix	4.6	Pine I/Br.II	-	2.5		Mixed Diameters
186	1.1	0.09	1.22	1.04	2-21	1.6	0.044	15	1.3	4.6	W. Pine I	11.3	1.9		15 cm Width
187	1.6	0.19	1.79	1.41	3-23	1.6	0.022	15	1.3	4.6	W. Pine I	16.0	2.7		"
188	0.81	0.12	0.93	0.69	3-23	1.6	0.088	30	1.3	4.6	W. Pine I	8.0	1.3		30 cm Width
189	4.0	0.84	4.87	3.19	6-23	3.4	0.011	55	1.3	4.6	Pine / Tar	-	-		Roof Cement Coated
190	0.36	0.08	0.44	0.28	4-20	2.5	0.494	55	4.4	4.6	Birch II	2.3	0.7		Thick Fuel
191a	2.2	0.30	2.50	1.90	7-17*	2.5	0.505	55	3.3	14.0	Birch I	4.6	0.7		12cm High TCs Used
191b	0.19	0.05	0.24	0.14	17-23*	0	0.505	55	3.3	14.0	Birch I	0	0		Fuel Height Varied

Table 3. Compilation of the firespread-rate results from all tests, in chronological order (continued).

Test #	Flame Speed (vf) [cm/s]	Error in speed [cm/s]	Error (upper) [cm/s]	Error (lower) [cm/s]	TCs Used in vf fit	Wind Speed (U) [m/s]	Loading (m) gm/cm^2	Bed Width (W) [cm]	Fuel Diam. (d) [mm]	Fuel Height (H) [cm]	Fuel Type	(UH/md) ^.5 Sqrt[m^3 (e-kg)]	(U/m) ^.5 (m^3/s-kg)^.5	Repeated Test #'s	Comments
192	No sustained propagation					1.0	0.031	55	-	2.8	Boxes	-	1.8		10cm x 10cm grid
193	No sustained propagation					1.6	0.048	55	-	2.8	Boxes	-	1.8		8cm x 8cm grid
194	0.8	-	-	-	-	1.6	0.086	55	-	2.8	Boxes	-	1.4		6cm x 6cm grid

* Restrictions or conditions apply

++ Repeated tests done in both clay and ceramic substrates

Spread un-steady

Table 4. Compilation of the firespread-rate results for all tests, in convenient groupings.

Test #	Flame Speed (vf) [cm/s]	Error in speed [cm/s]	Error (upper) [cm/s]	Error (lower) [cm/s]	TCs Used in Vf ht	Wind Speed (U) [m/s]	Loading (wood) (m) [gm/cm^2	Bed Width (W) [cm]	Fuel Diam. (d) [mm]	Fuel Height (H) [cm]	Fuel Type(s)	(UH/md) ^.5 Sqrt[m^3/ (s-kg)]	(U/m) ^.5 (m^3/s-kg)^.5	Repeated Test #'s	Comments
44	0	0	0	0	-	3.4	0.006	55	1.3	4.6	W. Pine I	46.9	7.9		No propagation
45	0	0	0	0	-	3.4	0.006	55	1.3	4.6	W. Pine I	46.0	7.7		No propagation
46	0	0	0	0	-	1.6	0.006	55	1.3	4.6	W. Pine I	31.2	5.2		No propagation
163	0+	0	0	0	-	1.6	0.007	55	1.3	4.6	W. Pine I	28.4	4.8		Spread ceased
164	0+	0	0	0	-	2.5	0.007	55	1.3	4.6	W. Pine I	35.5	6.0		Spread ceased
174#	4.3	-	-	-	8-23	2.5	0.007	55	1.3	4.6	W. Pine I	35.5	6.0		Spread slowing
36	1.9	0.17	2.07	1.73	2-8	0.4	0.011	55	1.3	4.6	W. Pine I	11.7	2.0		Extend Data Set
69	2.3	0.32	2.58	1.94	10-23	1.0	0.011	55	1.3	4.6	W. Pine I	17.9	3.0		
29	4.2	0.37	4.57	3.83	1-23	1.6	0.011	55	1.3	4.6	W. Pine I	22.5	3.8	76 & 171	Extend Data Set
76	4.2	0.56	4.74	3.62	1-23	1.6	0.011	55	1.3	4.6	W. Pine I	22.7	3.8	29 & 171	Repeat - TC Rake
171	3.9	0.55	4.44	3.34	2-23	1.6	0.011	55	1.3	4.6	W. Pine I	22.7	3.8	29 & 76	Repeat - TC Rake
47	4.9	0.78	5.69	4.13	5-21	2.5	0.011	55	1.3	4.6	W. Pine I	28.4	4.8	134	
165	5.2	0.90	6.05	4.25	1-23	2.5	0.011	55	1.3	4.6	W. Pine I	28.4	4.8	47, 134, ++	
63	6.3	1.26	7.52	5.00	6-21	3.4	0.011	55	1.3	4.6	W. Pine I	33.0	5.6	43,55 & 65	
65	6.6	1.24	7.87	5.39	5-21	3.4	0.011	55	1.3	4.6	W. Pine I	33.0	5.6	43,55 & 63	
43	6.3	1.05	7.30	5.20	7-17	3.4	0.011	55	1.3	4.6	W. Pine I	33.1	5.6	55,63 & 65	Roof Stop @TC#19
55	5.8	1.40	7.16	4.36	12-23	3.4	0.011	55	1.3	4.6	W. Pine I	33.1	5.6	43,63 & 65	Repeat #43
68	6.9	2.25	9.18	4.68	1-22	4.6	0.011	55	1.3	4.6	W. Pine I	38.4	6.5		
32	1.7	0.17	1.85	1.51	1-8	0.4	0.022	55	1.3	4.6	W. Pine I	8.3	1.4		Extend Data Set
75	2.5	0.14	2.62	2.34	1-23	1.0	0.022	55	1.3	4.6	W. Pine I	12.7	2.1		Shadowgraph
31	3.8	0.46	4.28	3.36	4-15	1.6	0.022	55	1.3	4.6	W. Pine I	15.9	2.7		Extend Data Set
38	3.6	0.39	4.02	3.24	1-15	1.6	0.022	55	1.3	4.6	W. Pine I	15.9	2.7	50,51 & 52	Extend Data Set
50	4.3	0.47	4.76	3.82	4-15	1.6	0.022	55	1.3	4.6	W. Pine I	15.9	2.7	38,51 & 52	
51	4.3	0.43	4.77	3.91	3-15	1.6	0.022	55	1.3	4.6	W. Pine I	15.9	2.7	38,50 & 52	
52	4.4	0.30	4.74	4.14	3-16	1.6	0.022	55	1.3	4.6	W. Pine I	15.9	2.7	38,50 & 51	
53	3.8	0.47	4.31	3.37	5-14	1.6	0.022	55	1.3	4.6	W. Pine I	15.9	2.7		Ceiling at X=0cm
170	3.5	0.62	4.12	2.88	1-23	1.6	0.022	55	1.3	4.6	W. Pine I	15.9	2.7		
35	4.6	0.61	5.20	3.98	12-21	2.5	0.022	55	1.3	4.6	W. Pine I	20.0	3.4	90 & 91°	Extend Data Set
91	4.6	0.42	4.99	4.15	5-19	2.5	0.022	55	1.3	4.6	W. Pine I	20.1	3.4	35 & 90°	Parallel Loading
90	4.3	0.78	5.05	3.49	11-23	2.5	0.022	55	1.3	4.6	W. Pine I	20.1	3.4	35° & 91°	Perpend. Loading
66	4.6	1.04	5.63	3.55	5-19	3.4	0.022	55	1.3	4.6	W. Pine I	23.3	3.9	42	
42	5.5	1.05	6.51	4.41	2-23	3.4	0.022	55	1.3	4.6	W. Pine I	23.4	3.9	66	Extend Data Set
71	5.5	1.02	6.49	4.45	4-22	4.6	0.022	55	1.3	4.6	W. Pine I	27.2	4.6		
78	2.3	0.26	2.51	1.99	1-23	1.0	0.033	55	1.3	4.6	W. Pine I	10.4	1.7		TC Rake Present

Table 4. Compilation of the firespread-rate results from all tests, in convenient groupings (continued).

Test #	Flame Speed (vf) [cm/s]	Error In speed [cm/s]	Error (upper) [cm/s]	Error (lower) [cm/s]	TCs Used in Vf fit	Wind Speed (U) [m/s]	Loading (wood) (m) [gm/cm^2	Bed Width (W) [cm]	Fuel Diam. (d) [mm]	Fuel Height (H) [cm]	Fuel Type(s)	(UH/md) ^.5 Sqrt[m^3/ (s-kg)]	(U/m) ^.5 (m^3/s-kg)^.5	Repeated Test #'s	Comments
26	3 0	0 23	3 25	2 79	1-16	1 0	0 032	55	1 3	4 6	W Pine I	10 8	1 8		Fleeter Repeat
83	3 5	0 59	4 09	2 91	4-23	2 5	0 033	55	1 3	4 6	W Pine I	16 4	2 8		
73	3 8	0 82	4 62	2 98	7-23	3 4	0 033	55	1 3	4 6	W Pine I	19 1	3 2		Shadowgraph
7	0	0	0	0	-	0	0 044	55	1 3	4 6	W Pine I	0	0		0 Wind Speed
8	0	0	0	0	-	0	0 044	55	1 3	4 6	W Pine I	0	0		0 Wind Speed
81	0	0	0	0	-	0	0 044	55	1 3	4 6	W Pine I	0	0		No Wind
9	1 1	0 02	1 14	1 10	1-8	0 4	0 044	55	1 3	4 6	W Pine I	5 9	1 0	17-24	
17	1 0	0 09	1 08	0 90	1-8	0 4	0 044	55	1 3	4 6	W Pine I	5 9	1 0	9 & 17-24	Crystallinity II
18	1 1	0 05	1 19	1 09	1-8	0 4	0 044	55	1 3	4 6	W Pine I	5 9	1 0	9 & 17-24	"
19	1 2	0 15	1 31	1 01	1-8	0 4	0 044	55	1 3	4 6	W Pine I	5 9	1 0	9 & 17-24	"
20	1 2	0 13	1 37	1 11	1-8	0 4	0 044	55	1 3	4 6	W Pine I	5 9	1 0	9 & 17-24	"
22	1 3	0 07	1 34	1 20	1-8	0 4	0 044	55	1 3	4 6	W Pine I	5 9	1 0	9 & 17-24	Repeatibility
23	1 4	0 10	1 51	1 31	1-8	0 4	0 044	55	1 3	4 6	W Pine I	5 9	1 0	9 & 17-24	"
24	1 2	0 09	1 30	1 12	1-8	0 4	0 044	55	1 3	4 6	W Pine I	5 9	1 0	9 & 17-24	"
25	1 7	0 19	1 85	1 47	2-16	0 7	0 044	55	1 3	4 6	W Pine I	7 2	1 2		Extend Data Set
98	1 9	0 37	2 29	1 55	1-23	1 0	0 044	55	1 3	4 6	W Pine I	9 0	1 5	16*	
16	2 2	0 20	2 38	1 98	6-16	1 1	0 044	55	1 3	4 6	W Pine I	9 4	1 6	98*	
99	2 5	0 52	3 02	1 98	4-24	1 6	0 044	55	1 3	4 6	W Pine I	11 3	1 9	27	
27	1 9	0 26	2 14	1 62	4-14	1 6	0 044	55	1 3	4 6	W Pine I	11 2	1 9	99	Extend Data Set
56	2 8	0 67	3 51	2 17	9-21	2 5	0 044	55	1 3	4 6	W Pine I	14 2	2 4	28 & 82	Repeat #28
82	2 7	0 41	3 09	2 27	6-19	2 5	0 044	55	1 3	4 6	W Pine I	14 2	2 4	56 & 28	Repeat Test
28	2 3	0 28	2 56	2 00	10-19	2 5	0 044	55	1 3	4 6	W Pine I	14 2	2 4	56 & 82	Extend Data Set
30	2 7	0 54	3 27	2 19	6-23	3 0	0 044	55	1 3	4 6	W Pine I	15 4	2 6		Extend Data Set
57	2 9	0 93	3 82	1 96	11-22*	3 4	0 044	55	1 3	4 6	W Pine I	16 5	2 8	34,58 & 62	
58	3 1	0 79	3 87	2 29	9-23	3 4	0 044	55	1 3	4 6	W Pine I	16 5	2 8	34,57 & 62	
62	2 7	0 26	2 92	2 40	7-23	3 4	0 044	55	1 3	4 6	W Pine I	16 5	2 8	34,57 & 58	
34	2 6	0 71	3 33	1 91	15-23	3 4	0 044	55	1 3	4 6	W Pine I	16 6	2 8	57,58 & 62	Extend Data Set
119	3 0	0 54	3 56	2 48	5-23	3 4	0 044	55	1 3	4 6	W Pine I	16 6	2 8	Many(e g 57)	See 34,57,58,62,70
120	3 0	1 49	4 49	1 51	5-23	3 4	0 044	55	1 3	4 6	W Pine I	16 6	2 8	Many(e g 57)	See 34,57,58,62,70
72	3 3	0 70	4 01	2 61	10-21	4 6	0 044	55	1 3	4 6	W Pine I	19 2	3 2		Shadowgraph
156	0 21	0 01	0 22	0 20	4-7	0	0 066	55	1 3	4 6	W Pine I	0	0		No Wind (0 m/s)
85	0 29	0 03	0 32	0 26	1-21	0	0 088	55	1 3	4 6	W Pine I	0	0		No Wind (0 m/s)
12	0 82	0 05	0 87	0 77	1-8	0 4	0 088	55	1 3	4 6	W Pine I	4 1	0 7	13,14 & 15	Crystallinity I
13	0 80	0 05	0 85	0 75	1-8	0 4	0 088	55	1 3	4 6	W Pine I	4 1	0 7	12,14 & 15	"
14	0 77	0 03	0 80	0 74	1-8	0 4	0 088	55	1 3	4 6	W Pine I	4 1	0 7	13,12 & 15	"
15	0 92	0 07	0 99	0 85	1-8	0 4	0 088	55	1 3	4 6	W Pine I	4 1	0 7	13,14 & 12	"
33	1 4	0 37	1 76	1 02	6-16	1 6	0 088	55	1 3	4 6	W Pine I	7 9	1 3		Extend Data Set
41	1 3	0 21	1 46	1 04	13-22	2 5	0 088	55	1 3	4 6	W Pine I	10 0	1 7		Extend Data Set
84	2 6	0 46	3 09	2 17	5-21	3 4	0 088	55	1 3	4 6	W Pine I	11 7	2 0		?Steady S Region?
74	2 1	0 52	2 61	1 57	6-22	3 4	0 088	55	1 3	4 6	W Pine I	11 7	2 0		Shadowgraph
130	2 9	0 61	3 46	2 24	6 23	4 6	0 088	55	1 3	4 6	W Pine I	13 6	2 3		

Table 4. Compilation of the firespread-rate results for all tests, in convenient groupings (continued).

Test #	Flame Speed (vf) (cm/s)	Error in speed (cm/s)	Error (upper) (cm/s)	Error (lower) (cm/s)	TCs Used in Vf ht	Wind Speed (U) (m/s)	Loading (wood) (m) (gm/cm^2	Bed Width (W) (cm)	Fuel Diam (d) (mm)	Fuel Height (H) (cm)	Fuel Type(s)	(UH/md) ^.5 Sqrt[m^3/ (s-kg)]	(U/m) ^.5 (m^3/s-kg)^.5	Repeated Test #'s	Comments
158	0.23	0.01	0.24	0.22	1-7	0	0.176	55	1.3	4.6	W. Pine I	0	0		4 toothpicks/hole
186	1.1	0.09	1.22	1.04	2-21	1.6	0.044	15	1.3	4.6	W. Pine I	11.3	1.9		15 cm Width
187	1.6	0.19	1.79	1.41	3-23	1.6	0.022	15	1.3	4.6	W. Pine I	16.0	2.7		"
48	4.1	0.46	4.52	3.60	1-12	1.6	0.011	30	1.3	4.6	W. Pine I	22.5	3.8		30 cm Width
39	2.8	0.37	3.21	2.47	3-16	1.6	0.022	30	1.3	4.6	W. Pine I	15.9	2.7		"
54	1.8	0.15	1.90	1.60	4-15	1.6	0.044	30	1.3	4.6	W. Pine I	11.2	1.9		"
188	0.81	0.12	0.93	0.69	3-23	1.6	0.088	30	1.3	4.6	W. Pine I	8.0	1.3		"
167	5.2	0.86	6.01	4.29	1-23	1.6	0.022	75	1.3	4.6	W. Pine I	16.0	2.7		75 cm Width
168	5.5	0.54	6.05	4.97	1-23	1.6	0.011	75	1.3	4.6	W. Pine I	22.7	3.8		"
180	3.0	0.53	3.50	2.44	1-23	1.6	0.044	75	1.3	4.6	W. Pine I	11.3	1.9		"
122	4.0	0.87	4.85	3.11	4-23	0.7	0.011	100	1.3	4.6	W. Pine I	15.0	2.5		100 cm Width
1	6.7	1.19	7.89	5.51	1-16	1.6	0.011	100	1.3	4.6	W. Pine I	22.5	3.8		"
2	6.8	0.86	7.70	5.98	1-17	1.6	0.011	100	1.3	4.6	W. Pine I	22.5	3.8		"
105	6.0	1.28	7.23	4.67	2-20	3.4	0.011	100	1.3	4.6	W. Pine I	33.0	5.6		"
111	7.5	2.97	10.43	4.49	1-22	4.6	0.011	100	1.3	4.6	W. Pine I	38.4	6.5		"
116	3.3	0.59	3.84	2.66	6-23	0.7	0.022	100	1.3	4.6	W. Pine I	10.6	1.8		"
3	8.8	0.99	9.76	7.78	1-18	1.6	0.022	100	1.3	4.6	W. Pine I	15.9	2.7		"
37	6.6	0.63	7.24	5.98	3-14	1.6	0.022	100	1.3	4.6	W. Pine I	15.9	2.7		"
125	9.1	2.29	11.42	6.84	5-22	4.6	0.022	100	1.3	4.6	W. Pine I	27.2	4.6		"
107	3.3	0.63	3.88	2.62	10-23	0.7	0.044	100	1.3	4.6	W. Pine I	7.5	1.3		"
97	4.2	0.88	5.03	3.27	2-12	1.0	0.044	100	1.3	4.6	W. Pine I	9.0	1.5		"
49	5.4	0.47	5.90	4.96	2-12	1.6	0.044	100	1.3	4.6	W. Pine I	11.2	1.9		"
102	9.2	2.56	11.72	6.60	7-23	3.4	0.044	100	1.3	4.6	W. Pine I	16.5	2.8		"
103	2.7	0.46	3.14	2.22	3-22	1.0	0.088	100	1.3	4.6	W. Pine I	6.3	1.1		"
148	1.23	0.26	1.49	0.97	6-23	2.5	0.199	55	1.9	7.7	W. Pine II	7.1	1.1		Sandwich Picks
88	3.1	0.71	3.79	2.37	12-22	4.6	0.045	55	2.3	4.6	Bamboo I	14.3	3.2		
84	2.1	0.28	2.38	1.80	5-23	2.5	0.045	55	2.3	4.6	Bamboo I	10.5	2.4		
95	1.3	0.26	1.58	1.06	4-23	1.6	0.045	55	2.3	4.6	Bamboo I	8.4	1.9		
86	1.6	0.31	1.90	1.28	4-23	2.5	0.090	55	2.3	4.6	Bamboo I	7.5	1.7		
92	1.0	0.16	1.17	0.85	1-18	1.0	0.090	55	2.3	4.6	Bamboo I	4.7	1.1		
77	1.1	0.28	1.33	0.77	4-30	3.4	0.180	55	2.3	4.6	Bamboo I	6.1	1.4		
159	0.74	0.13	0.87	0.61	5-23	3.4	0.163	55	3.3	2.0	Birch I	3.6	1.4		Fuel Height Varied
160	1.29	0.40	1.69	0.89	6-23	3.4	0.082	55	3.3	2.0	Birch I	5.0	2.0		"
81	0.69	0.18	0.87	0.51	8-18	2.5	0.116	55	2.3	3.0	Bamboo I	5.3	1.5		"
132	0.49	0.09	0.58	0.40	1-17	0.7	0.114	55	3.3	3.0	Birch I	2.4	0.8		"
123	2.0	0.40	2.42	1.62	1-22	3.4	0.050	55	3.3	3.0	Birch I	7.9	2.6		"

Table 4. Compilation of the firespread-rate results for all tests, in convenient groupings (continued).

Test #	Flame Speed (vf) [cm/s]	Error in speed [cm/s]	Error (upper) [cm/s]	Error (lower) [cm/s]	TCs Used in Vf ft*	Wind Speed (U) [m/s]	Loading (wood) (m) [gm/cm^2	Bed Width (W) [cm]	Fuel Diam. (d) [mm]	Fuel Height (H) [cm]	Fuel Type(s)	(UH/md) ^.5 Sqrt[m^3/ (s-kg)]	(U/m) ^.5 (m^3/s-kg)^.5	Repeated Test #'s	Comments
138	1.2	0.28	1.46	0.90	3-22	3.4	0.106	55	3.3	3.0	Birch I	5.4	1.8		Fuel Height Varied
142	0.31	0.06	0.37	0.25	1-11	0.7	0.212	55	3.3	3.0	Birch I	1.7	0.6		"
60	1.1	0.20	1.32	0.92	9-22	2.5	0.110	55	2.3	6.2	Bamboo I	7.8	1.5		"
129	1.8	0.42	2.19	1.35	13-23	4.6	0.120	55	2.3	6.2	Bamboo I	10.2	2.0		"
117	1.6	0.33	1.92	1.26	6-23	1.6	0.060	55	2.3	6.2	Bamboo I	8.5	1.6		"
126	2.8	0.61	3.43	2.21	1-22	1.6	0.060	55	2.3	6.2	Bamboo I	14.4	2.8		"
118	1.5	0.20	1.68	1.26	1-23	1.6	0.102	55	3.3	6.2	Birch I	5.4	1.3		"
127	2.5	0.43	2.92	2.06	6-23	4.6	0.093	55	3.3	6.2	Birch I	9.6	2.2		"
101	1.7	0.33	2.06	1.40	11 23	2.5	0.090	55	2.3	9.2	Bamboo I	10.5	1.7		"
59	2.1	0.48	2.55	1.59	10-23	2.5	0.110	55	2.3	12.1	Bamboo I	10.9	1.5		"
191b	0.19	0.05	0.24	0.14	17-23*	0	0.505	55	3.3	14.0	Birch I	0	0		"
121	0.84	0.07	0.91	0.77	1-14	0.7	0.230	55	3.3	14.0	Birch I	3.6	0.6		"
143	1.5	0.11	1.59	1.37	4-24	0.7	0.168	55	3.3	14.0	Birch I	4.2	0.6		"
191a	2.2	0.30	2.50	1.90	7-17*	2.5	0.505	55	3.3	14.0	Birch I	4.6	0.7		12cm High TCs Used
137	2.7	-	-	-	-	3.4	0.253	55	3.3	14.0	Birch I	7.6	1.2		Almost Steady
133	0.49	0.15	0.64	0.34	1-17	0.7	0.377	55	3.0	14.0	Bamboo II	2.9	0.4		
139	2.3	0.63	2.93	1.67	17-26	4.6	0.189	55	3.0	14.0	Bamboo II	10.7	1.6		Steady Established
128	4.7	-	-	-	1-23	4.6	0.209	55	2.3	21.6	Bamboo I	14.4	1.5		Still Unsteady
131	2.4	0.56	3.00	1.88	6-23	2.5	0.071	55	2.3	Mix	Bamboo I	-	1.9		5.4 & 9.0cm Height
110	1.7	0.45	2.15	1.25	4-23	2.5	0.065	55	3.0	4.6	Bamboo II	7.7	2.0		
135	1.6	0.38	2.02	1.26	14-23	4.6	0.134	55	3.0	4.6	Bamboo II	7.3	1.9		
175	1.2	0.19	1.36	0.98	7-23	2.5	0.601	55	4.4	4.6	Birch II	2.1	0.6		Thick Fuel
190	0.36	0.08	0.44	0.28	4-20	2.5	0.494	55	4.4	4.6	Birch II	2.3	0.7		"
114	1.5	0.36	1.85	1.13	9-23	2.5	0.078	55	3.3	4.6	Birch I	6.7	1.8		
152	0.78	0.15	0.93	0.63	4-23	3.4	0.312	55	3.3	4.6	Birch I	3.9	1.0		
146	1.4	0.38	1.80	1.04	8-23	2.5	0.089	55	Mix	4.6	Pine I/Br I	-	1.7		Mixed Diameters
151	1.9	0.36	2.27	1.55	1-23	2.5	0.083	55	Mix	4.6	Pine I/Br.I	-	1.7		Mixed Diameters
153	1.7	0.33	1.98	1.32	4-23	2.5	0.041	55	Mix	4.6	Pine I/Br II	-	2.5	see 162	Mixed Diameters
179	?2.2?	0.56	-	-	10-15	4.6	0.041	55	Mix	4.6	Pine I/Br.II	-	3.3	see 184	? Steady ?
184	?2.4?	0.14	-	-	10-15	4.6	0.041	55	Mix	4.6	Pine I/Br II	-	3.3	see 179	? Steady ?
185	1.5	0.16	1.61	1.29	3-23	2.5	0.041	55	Mix	4.6	Pine I/Br II	-	2.5		Mixed Diameters
136	Thermocouple Height Varied				-	3.4	0.359	55	3.3	Mix	Birch I	-	1.0		Mixed Height
147	3.0	0.32	3.35	2.71	1-23	1.6	0.011	55	1.3	4.6	W. Pine I	22.7	3.8	169, ++	? wet ? Clay bed
169	4.2	0.51	4.68	3.66	1-23	1.6	0.011	55	1.3	4.6	W. Pine I	22.7	3.8	147, ++	Dry Clay Bed
161	4.9	1.13	6.04	3.78	1-23	2.5	0.011	55	1.3	4.6	W. Pine I	28.4	4.8	166, ++	
166	5.2	0.87	6.08	4.34	5-23	2.5	0.011	55	1.3	4.6	W Pine I	28.4	4.8	161, ++	Dry Clay Bed
157	6.5	1.26	7.75	5.23	1-23	3.4	0.011	55	1.3	4.6	W Pine I	33.1	5.6	++	"
79	7.3	2.84	10.16	4.48	2-16*	2.5	0.044	0-100	1.3	4.6	W Pine I	14.2	2.4		Tapered Loading
89	7.6	1.09	8.71	6.53	5-22	1.6	0.044	5-107	1.3	4.6	W Pine I	11.3	1.9		"

Table 4. Compilation of the firespread-rate results for all tests, in convenient groupings (continued).

Test #	Flame Speed (vf) [cm/s]	Error in speed [cm/s]	Error (upper) [cm/s]	Error (lower) [cm/s]	TCs Used in Vf fit	Wind Speed (U) [m/s]	Loading (wood) (m) [gm/cm^2	Bed Width (W) [cm]	Fuel Diam. (d) [mm]	Fuel Height (H) [cm]	Fuel Type(s)	(UH/md) ^.5 Sqrt[m^3/ (s-kg)]	(U/m) ^.5 (m^3/s-kg)^.5	Repeated Test #'s	Comments
94	6.2	0.96	7.11	5.19	3-17	1.6	0.044	3-106	1.3	4.6	W. Pine I	11.3	1.9		Tapered Loading
96	2.0	0.48	2.47	1.51	1-23	2.5	0.044	55	1.3	4.6	W. Pine I	14.2	2.4		20-30% Moisture
113	2.1	0.51	2.57	1.55	1-23	2.5	0.044	55	1.3	4.6	W. Pine I	14.2	2.4		4-13% Moisture
140	1.9	0.53	2.44	1.38	1-23	2.5	0.044	55	1.3	4.6	W. Pine I	14.2	2.4		9-15% Moisture
100	1.0	0.14	1.15	0.87	1-16	1.0	0.044	55	1.3	4.6	W. Pine I	9.0	1.5		24% Moisture
108	1.0	0.14	1.15	0.87	1-19	1.0	0.044	55	1.3	4.6	W. Pine I	9.0	1.5		8% Moisture
141	1.2	0.18	1.39	1.03	1-23	1.0	0.044	55	1.3	4.6	W. Pine I	9.0	1.5		20-24% Moisture
144	1.2	0.17	1.39	1.05	1-23	1.0	0.044	55	1.3	4.6	W. Pine I	9.0	1.5		5-10% Moisture
145	1.3	0.12	1.38	1.14	1-23	1.0	0.022	55	1.3	4.6	W. Pine I	12.7	2.1		5-7% Moisture
150	2.4	0.61	2.98	1.74	1-13	2.5	0.044	55	1.3	4.6	W. Pine I	14.2	2.4		10% Wet Bed
154	0.97	0.06	1.03	0.91	1-23	1.0	0.022	55	1.3	4.6	W. Pine I	12.7	2.1	181	10% Wet Bed
181	1.71	0.12	1.83	1.59	1-23	1.0	0.022	55	1.3	4.6	W. Pine I	12.7	2.1	154	~0.5l H20 per tray
182	1.76	0.14	1.90	1.62	1-23	1.0	0.022	55	1.3	4.6	W. Pine I	12.7	2.1		~1.0l H20 per tray
183	1.57	0.15	1.72	1.42	1-23	1.0	0.022	55	1.3	4.6	W. Pine I	12.7	2.1		~1.5l H20 per tray
80	No propagation				-	1.6	0.022	55	1.3	4.6	Pine I-Nails	16.0	2.7		Nails in all Trays
87	Computer Crash				-	3.4	0.022	55	1.3	4.6	Pine I-Nails	23.4	3.9		Nails in Tray #2
93	1.3	0.16	1.42	1.10	9-17*	2.5	0.022	55	1.3	4.6	Pine I-Nails	20.1	3.4		Nails in Tray #2
104	0.71	0.24	0.95	0.47	9-17*	2.5	0.022	55	1.3	4.6	Pine I-Nails	20.1	3.4		Nails in Tray #2*
106	0.83	0.08	0.91	0.75	9-17*	2.5	0.022	55	1.3	4.6	Pine I-Nails	20.1	3.4		Nails in Tray #2*
109	2.5	0.24	2.75	2.27	9-17*	2.5	0.022	55	1.3	4.6	Pine I-Nails	20.1	3.4		1/2 Nails Tray #2*
112	2.3	0.44	2.76	1.88	9-17*	2.5	0.022	55	1.3	4.6	Pine I-Nails	20.1	3.4		1/2 Nails Tray #2*
115	3.5	0.64	4.14	2.86	9-17*	2.5	0.022	55	1.3	4.6	Pine I-Nails	20.1	3.4		1/4 Nails Tray #2*
162	3.2	0.58	3.79	2.67	7-23	2.5	0.011	55	1.3	4.6	Pine I-Nails	28.4	4.8	see 153	1 Nail / 16 holes
178	4.2	0.54	4.69	3.61	5-23	2.5	0.011	55	1.3	4.6	Pine/Plastic	-	-		Plastics Present
189	4.0	0.84	4.87	3.19	6-23	3.4	0.011	55	1.3	4.6	Pine / Tar	-	-		Roof Cement Coated
4	Data not recorded				-	1.6	0.022	55	1.3	4.6	W. Pine I	16.0	2.7		1/2 Tray Ignited
40	0	0	0	0	-	1.6	0.022	55	1.3	4.6	W. Pine I	15.9	2.7		Elements Scattered
10	Data not recorded				-	Varied	Varied	4	1.3	4.6	W. Pine I	-	-		Blow Out Attempt
155	Data not recorded				-	Varied	Varied	55	1.3	4.6	W. Pine I	-	-		Go, No-Go Tests
67	Computer Crash				-	3.4	0.044	55	1.3	4.6	W. Pine I	16.5	2.8	34, 62, 57	Ceiling @X=0.19 m
70	4.3	1.81	6.07	2.45	4-22*	3.4	0.044	55	1.3	4.6	W. Pine I	16.5	2.8	58*, 70, 124	Ceiling @X=3.4 m
124	1.6	0.35	1.95	1.25	12-23*	3.4	0.044	55	1.3	4.6	W. Pine I	16.5	2.8	above	Ceiling @X=0.20 m
192	No sustained propagation					1.0	0.031	55	-	2.8	Boxes	-	1.8		10cm x 10cm grid
193	No sustained propagation					1.6	0.048	55	-	2.8	Boxes	-	1.8		8cm x 8cm grid
194	0.8	-	-	-	-	1.6	0.086	55	-	2.8	Boxes	-	1.4		6cm x 6cm grid
5	Uncertain Conditions				-	0.7	0.044	55	1.3	4.6	W. Pine I	7.2	1.2		55 cm Test Width

Table 4. Compilation of the firespread-rate results for all tests, in convenient groupings (continued).

Test #	Flame Speed (vf) [cm/s]	Error in speed [cm/s]	Error (upper) [cm/s]	Error (lower) [cm/s]	TCs Used in Vf fit	Wind Speed (U) [m/s]	Loading (wood) (m) [gm/cm^2	Bed Width (W) [cm]	Fuel Diam. (d) [mm]	Fuel Height (H) [cm]	Fuel Type(s)	(UH/md) ^.5 Sqrt[m^3/ (s-kg)]	(U/m) ^.5 (m^3/s-kg)^.5	Repeated Test #'s	Comments
6	Steady State not Achieved				-	3.4	0.044	55	1.3	4.6	W. Pine I	16.6	2.8		55 cm Test Width
149	Steady State not Achieved				-	2.5	0.377	55	3.0	14.0	Bamboo II	5.6	0.8		
11	Uncertain Conditions				-	0.4	0.044	55	1.3	4.6	W. Pine I	5.9	1.0		?
21	Computer Crash				-	0.4	0.044	55	1.3	4.6	W. Pine I	5.9	1.0	9 & 17-24	No Data
134	6.6	1.31	7.93	5.31	4-23	2.5	0.011	55	1.3	4.6	W. Pine I	28.4	4.8	47, 165, ++	Vf Inconsistent
172	0	0	0	0	-	2.5	0.030	55	4.4	4.6	Birch II	9.3	2.9		No propagation
173	0	0	0	0	-	2.5	0.033	55	Mix	4.6	Pine I/Br II	-	2.8		No propagation
176	0	0	0	0	-	2.5	0.030	55	Mix	4.6	Pine I/Br II	-	2.9		No propagation
177	0	0	0	0	-	4.6	0.030	55	Mix	4.6	Pine I/Br II	-	3.9		Blew Out

* Restrictions or conditions apply

++ Repeated tests done in both clay and ceramic substrates

Spread un-steady

Table 5. Compilation of the tilt angle of the buoyant gases, in convenient groupings (based on a vertical, centerline array of thermocouples and assuming steady-state propagation).

Test #	Fuel Type(s)	Test Width [cm]	Wind Speed (U) [m/s]	Loading (m) [kg/m^2]	Elements per hole (n) [#/cm^2]	Diameter (d) [mm]	Height (H) [cm]	Flame Speed (vf) [cm/s]	Flame Speed (vf) [m/s]	(m/U) [kg-s/m^3]	(ndH/U) [#ms/hole]	Angle <55cm (deg)	Angle Up Err (deg)	Angle own Err (deg)
76	W.Pine I	55	1.6	0.11	0.25	1.3	4.6	4.1	0.041	0.069	9.34E-06	28	31	26
78	W.Pine I	55	1.0	0.33	0.75	1.3	4.6	2.2	0.022	0.330	4.48E-05	35	38	32
82	W.Pine I	55	2.5	0.44	1.00	1.3	4.6	2.7	0.027	0.176	2.39E-05	46	52	38
83	W.Pine I	55	2.5	0.33	0.75	1.3	4.6	3.6	0.036	0.132	1.79E-05	31	33	29
90	W.Pine I	55	2.5	0.22	0.50	1.3	4.6	4.3	0.043	0.088	1.20E-05	24	26	22
91	W.Pine I	55	2.5	0.22	0.50	1.3	4.6	4.6	0.046	0.088	1.20E-05	27	29	24
98	W.Pine I	55	1.0	0.44	1.00	1.3	4.6	1.9	0.019	0.440	5.98E-05	45	48	41
99	W.Pine I	55	1.6	0.44	1.00	1.3	4.6	2.5	0.025	0.275	3.74E-05	28	31	25
119	W.Pine I	55	3.4	0.44	1.00	1.3	4.6	3.0	0.030	0.129	1.76E-05	30	32	27
120	W.Pine I	55	3.4	0.44	1.00	1.3	4.6	3.0	0.030	0.129	1.76E-05	29	32	27
124	W.Pine I	55	3.4	0.44	1.00	1.3	4.6	1.6	0.016	0.129	1.76E-05	32	35	29
125	W.Pine I	55	4.6	0.22	0.50	1.3	4.6	9.1	0.091	0.048	6.50E-06	21	22	19
130	W.Pine I	55	4.6	0.88	2.00	1.3	4.6	2.9	0.029	0.191	2.60E-05	23	25	21
134	W.Pine I	55	2.5	0.11	0.25	1.3	4.6	6.6	0.066	0.044	5.98E-06			
77	Bamboo I	55	3.4	1.80	1.00	2.3	4.6	0.80	0.008	0.529	3.11E-05	22	29	14
84	Bamboo I	55	2.5	0.45	0.25	2.3	4.6	2.0	0.020	0.180	1.06E-05	19	22	17
86	Bamboo I	55	2.5	0.90	0.50	2.3	4.6	1.6	0.016	0.360	2.12E-05	26	28	24
88	Bamboo I	55	4.6	0.45	0.25	2.3	4.6	3.6	0.036	0.098	5.75E-06	10	12	9
92	Bamboo I	55	1.0	0.90	0.50	2.3	4.6	1.0	0.010	0.900	5.29E-05	41	44	37
95	Bamboo I	55	1.6	0.45	0.25	2.3	4.6	1.3	0.013	0.281	1.65E-05	26	28	24
110	Bamboo I	55	2.5	0.65	0.25	3.0	4.6	1.7	0.017	0.260	1.38E-05	31	34	28
135	Bamboo I	55	4.6	1.34	0.50	3.0	4.6	1.6	0.016	0.291	1.50E-05	25	23	28
114	Birch I	55	2.5	0.78	0.25	3.3	4.6	1.5	0.015	0.312	1.52E-05	23	25	21
152	Birch I	55	3.4	3.12	1.00	3.3	4.6	0.78	0.008	0.918	4.46E-05	30	33	27
97	W.Pine I	100	1.0	0.44	1.00	1.3	4.6	4.2	0.042	0.440	5.98E-05	38	41	34
102	W.Pine I	100	3.4	0.44	1.00	1.3	4.6	9.2	0.092	0.129	1.76E-05			
103	W.Pine I	100	1.0	0.88	2.00	1.3	4.6	2.7	0.027	0.880	1.20E-04	54	56	51
105	W Pine I	100	3.4	0.11	0.25	1.3	4.6	6.0	0.060	0.032	4.40E-06	23	26	21
107	W Pine I	100	0.7	0.44	1.00	1.3	4.6	3.3	0.033	0.629	8.54E-05	53	55	50
111	W Pine I	100	4.6	0.11	0.25	1.3	4.6	7.5	0.075	0.024	3.25E-06	21	23	20
116	W Pine I	100	0.7	0.22	0.50	1.3	4.6	3.3	0.033	0.314	4.27E-05	44	48	40
122	W Pine I	100	0.7	0.11	0.25	1.3	4.6	4.0	0.040	0.157	2.14E-05	46	49	42

Table 5. Compilation of the tilt angle of the buoyant gases, in convenient groupings (based on a vertical, centerline array of thermocouples and assuming steady-state propagation) (continued).

Test #	Fuel Type(s)	Test Width [cm]	Wind Speed (U) [m/s]	Loading (m) [kg/m^2]	Elements per hole (n) [#/cm^2]	Diameter (d) [mm]	Height (H) [cm]	Flame Speed (vf) [cm/s]	Flame Speed (vf) [m/s]	(m/U) [kg-s/m^3]	(ndH/U) [#ms/hole]	Angle <55cm (deg)	Angle Up Err (deg)	Angle own Err (deg)
101	Bamboo I	55	2.5	0.90	0.25	2.3	9.2	1.7	0.017	0.360	2.12E-05	28	31	25
117	Bamboo I	55	1.6	0.60	0.25	2.3	6.2	1.6	0.016	0.375	2.23E-05	35	38	32
118	Birch I	55	1.6	1.02	0.25	3.3	6.2	1.5	0.015	0.638	3.20E-05	29	31	26
123	Birch I	55	3.4	0.50	0.25	3.3	3.0	2.0	0.020	0.147	7.28E-06	14	16	13
126	Bamboo I	55	4.6	0.60	0.25	2.3	6.2	2.8	0.028	0.130	7.75E-06	19	21	17
127	Birch I	55	4.6	0.93	0.25	3.3	6.2	2.5	0.025	0.202	1.11E-05	21	23	19
129	Bamboo I	55	4.6	1.10	1.50	2.3	6.2	1.8	0.018	0.239	4.65E-05	17	18	16
131	Bamboo I	55	2.5	0.71	2.00	2.3	Mix	2.4	0.024	0.284	--	27	29	25
132	Birch I	55	0.7	1.14	1.50	3.3	3.0	0.49	0.005	1.629	2.12E-04	40	43	36
133	Bamboo I	55	0.7	3.77	0.50	3.0	14	0.49	0.005	5.386	3.00E-04	50	53	46
138	Birch I	55	3.4	1.06	0.50	3.3	3.0	1.2	0.012	0.312	1.46E-05	21	23	20
139	Bamboo I	55	4.6	1.88	0.25	3.3	14.0	2.3	0.023	0.409	2.51E-05	27	30	25
143	Birch I	55	0.7	1.68	0.17	3.3	14.0	1.5	0.015	2.400	1.12E-04	43	46	40
148	W Pine II	55	2.5	1.99	1.00	1.9	7.7	1.2	0.012	0.796	5.85E-05	39	42	35
159	Birch I	55	3.4	1.63	1.00	3.3	2.0	0.74	0.007	0.479	1.94E-05	27	29	25
160	Birch I	55	3.4	0.82	0.50	3.3	2.0	1.3	0.013	0.240	9.71E-06			
Moisture Tests														
140	W.Pine I	55	2.5	0.44	1.00	1.3	4.6	1.9	0.019	0.176	2.39E-05	26	29	24
141	W.Pine I	55	1.0	0.44	1.00	1.3	4.6	1.2	0.012	0.440	5.98E-05	32	37	26
144	W.Pine I	55	1.0	0.44	1.00	1.3	4.6	1.2	0.012	0.440	5.98E-05	35	38	32
145	W.Pine I	55	1.0	0.22	0.50	1.3	4.6	1.3	0.013	0.220	2.99E-05			
Wet Bed														
150	W.Pine I	55	2.5	0.44	1.00	1.3	4.6	2.4	0.024	0.176	2.39E-05	Tray 3 Dry-Mixed Conditi		
154	W.Pine I	55	1.0	0.22	0.50	1.3	4.6	0.97	0.010	0.220	2.99E-05	62	65	58
Open Ceiling														
124	W.Pine I	55	3.4	0.44	1.00	1.3	4.6	1.6	0.016	0.129	1.76E-05	32	35	29
Clay Bed														
147	W.Pine I	55	1.6	0.11	0.25	1.3	4.6	3.0	0.030	0.069	9.34E-06	40	43	37
157	W.Pine I	55	3.4	0.11	0.25	1.3	4.6	6.5	0.065	0.032	4.40E-06	27	29	25
Mixed Bed														
146	Pi II/Br I	55	2.5	0.89	0.50	Mix	4.6	1.4	0.014	0.356	--	32	35	29
151	Pi II/Br I	55	2.5	0.83	---	Mix	4.6	1.9	0.019	0.332	--	31	34	28
153	Pi II/Br II	55	2.5	0.41	0.38	Mix	4.6	1.7	0.017	0.165	--	17	19	16

Table 5. Compilation of the tilt angle of the buoyant gases, in convenient groupings (based on a vertical, centerline array of thermocouples and assuming steady-state propagation) (continued).

Test #	Fuel Type(s)	Test Width [cm]	Wind Speed (U) [m/s]	Loading (m) [kg/m^2]	Elements per hole (n) [#/cm^2]	Diameter (d) [mm]	Height (H) [cm]	Flame Speed (vf) [cm/s]	Flame Speed (vf) [m/s]	(m/U) [kg-s/m^3]	(ndH/U) [#ms/hole]	Angle <55cm (deg)	Angle Up Err (deg)	Angle own Err (deg)
Un-usuable Tests														
128	Birch I	55	4.6	2.09	0.25	3.3	21.6	NS		Non-Steady				
136	Birch I	55	3.4	3.59	0.75	3.3	Mix	?		Flame Speed Indeterminate				
137	Birch I	55	3.4	2.53	0.25	3.3	14.0	NS		Non-Steady				
142	Birch I	55	0.7	2.12	1.00	3.3	3.0	0.31	0.003	3.029	1.41E-04	Insufficient Data		
149	Bamboo I	55	2.5	3.77	0.50	3.0	14.0	NS		Non-Steady				

Note: Uncertain Rake Thermocouple Traces in Test #102

Table 6. Compilation for many tests, in convenient groupings, of the time interval for firefront passage (based on the duration above 573 K of a centerline near-surface 130-μm thermocouple).

Test #	Fuel Type	Test Width (W) [cm]	Wind Speed (U) [m/s]	Loading (m) [kg/m^2]	Elements per cm^2 (n) [#/cm^2]	Diameter (d) [mm]	Height (H) [cm]	Flame Speed (vf) [cm/s]	Temp used (T) [C]	T Rise 5 mil (T1) [sec]	T Fall 5 mil (T2) [sec]	del t (T2-T1) [sec]	Comments
77	Bamboo I	55	3.4	1.80	1.00	2.3	4.6	0.85	200	133.50	276.50	143.00	H=4.6cm, Not Pin
84	Bamboo I	55	2.5	0.45	0.25	2.3	4.6	2.0	200	78.00	102.25	24.25	"
86	Bamboo I	55	2.5	0.90	0.50	2.3	4.6	1.6	200	106.25	153.25	47.00	"
88	Bamboo I	55	4.6	0.45	0.25	2.3	4.6	3.7	200	59.00	87.75	28.75	"
92	Bamboo I	55	1.0	0.89	0.50	2.3	4.6	1.0	200	193.50	248.25	54.75	"
95	Bamboo I	55	1.6	0.45	0.25	2.3	4.6	1.3	200	127.00	152.25	25.25	"
126	Bamboo I	55	4.6	0.60	0.25	2.3	4.6	2.8	200	86.00	134.75	48.75	"
110	Bamboo II	55	2.5	0.65	0.25	3.0	4.6	1.7	200	119.00	189.75	70.75	"
135	Bamboo II	55	4.6	1.34	0.50	3.0	4.6	1.6	200	103.75	193.00	89.25	"
114	Birch I	55	2.5	0.78	0.25	3.3	4.6	1.5	200	119.50	181.00	61.50	"
152	Birch I	55	3.4	3.12	1.00	3.3	4.6	0.78	200	258.0	500.0	242.00	"
76	W. Pine I	55	1.6	0.11	0.25	1.3	4.6	4.1	200	50.75	60.75	10.00	Pine, H=4.6cm
78	W. Pine I	55	1.0	0.33	0.75	1.3	4.6	2.3	200	102.75	116.50	13.75	"
82	W. Pine I	55	2.5	0.44	1.00	1.3	4.6	2.7	200	65.75	81.50	15.75	"
83	W. Pine I	55	2.5	0.33	0.75	1.3	4.6	3.6	200	54.00	71.25	17.25	"
85	W. Pine I	55	0.0	0.88	2.00	1.3	4.6	0.29	200	795.00	834.00	39.00	"
90	W. Pine I	55	2.5	0.22	0.50	1.3	4.6	4.3	200	50.25	70.75	20.50	"
91	W. Pine I	55	2.5	0.22	0.50	1.3	4.6	4.6	200	43.50	58.25	14.75	"
98	W. Pine I	55	1.0	0.44	1.00	1.3	4.6	1.9	200	112.25	131.50	19.25	"
99	W. Pine I	55	1.6	0.44	1.00	1.3	4.6	2.5	200	82.00	109.00	27.00	"
119	W. Pine I	55	1.0	0.44	1.00	1.3	4.6	3.0	200	55.00	85.25	30.25	"
120	W. Pine I	55	1.0	0.44	1.00	1.3	4.6	3.0	200	49.50	87.50	38.00	"
124	W. Pine I	55	3.4	0.44	1.00	1.3	4.6	1.6	200	74.25	101.50	27.25	"
130	W. Pine I	55	4.6	0.88	2.00	1.3	4.6	2.9	200	83.00	147.75	64.75	"
134	W. Pine I	55	2.5	0.11	0.25	1.3	4.6	6.6	200	Not Connected			"
158	W. Pine I	55	0	1.76	4.00	1.3	4.6	0.23	200	486	590	104.00	"
165	W. Pine I	55	2.5	0.11	0.25	1.3	4.6	5.2	200	48.250	59.375	11.125	"
170	W. Pine I	55	1.6	0.22	0.50	1.3	4.6	3.5	200	57.75	74.75	17.00	"
171	W. Pine I	55	1.6	0.11	0.25	1.3	4.6	3.9	200	52.00	61.50	9.50	"
167	W. Pine I	75	1.6	0.22	0.50	1.3	4.6	5.2	200	46.75	65.25	18.50	W= 75cm, Pine
168	W. Pine I	75	1.6	0.11	0.25	1.3	4.6	5.5	200	42.75	53.25	10.50	"
97	W. Pine I	100	1.0	0.44	1.00	1.3	4.6	4.2	200	Not Connected			W=100cm, Pine
102	W. Pine I	100	3.4	0.44	1.00	1.3	4.6	9.2	200	38.25	76.00	37.75	"
103	W. Pine I	100	1.0	0.88	2.00	1.3	4.6	2.7	200	109.00	185.50	76.50	"
105	W. Pine I	100	3.4	0.11	0.25	1.3	4.6	6.0	200	40.000	56.625	16.625	"
107	W. Pine I	100	2.5	0.44	1.00	1.3	4.6	3.3	200	125.00	141.00	16.00	"

Table 6. Compilation for many tests, in convenient groupings, of the time interval for firefront passage (based on the duration above 573 K of a centerline near-surface 130-μm thermocouple) (continued).

Test #	Fuel Type	Test Width (W) [cm]	Wind Speed (U) [m/s]	Loading (m) [kg/m^2]	Elements per cm^2 (n) [#/cm^2]	Diameter (d) [mm]	Height (H) [cm]	Flame Speed (vf) [cm/s]	Temp used (T) [C]	T Rise 5 mil (T1) [sec]	T Fall 5 mil (T2) [sec]	del t (T2-T1) [sec]	Comments
111	W. Pine I	100	4.6	0.11	0.25	1.3	4.6	7.5	200	28.13	42.75	14.63	W=100cm, Pine
116	W. Pine I	100	1.6	0.22	0.50	1.3	4.6	3.3	200	109.25	122.25	13.00	"
122	W. Pine I	100	0.7	0.11	0.25	1.3	4.6	4.0	200	83.000	97.125	14.13	"
125	W. Pine I	100	4.6	0.22	0.50	1.3	4.6	9.1	200	Broken Probe			"
101	Bamboo I	55	2.5	0.90	0.25	2.3	9.2	1.7	200	88.25	126.00	37.75	Non 4.6cm Height
117	Bamboo I	55	1.6	0.60	0.25	2.3	6.2	1.6	200	110.25	148.00	37.75	"
129	Bamboo I	55	4.6	1.10	1.50	2.3	6.2	1.8	200	79.00	203.75	124.75	"
131	Bamboo I	55	2.5	0.71	2.00	2.3	Mix	2.4	200	80.00	130.00	50.00	"
139	Bamboo II	55	4.6	1.88	0.25	3.0	14.0	2.3	200	63.75	152.25	88.50	"
118	Birch I	55	1.6	1.02	0.25	3.3	6.2	1.5	200	Uncertain			"
123	Birch I	55	3.4	0.50	0.25	3.3	3.0	2.0	200	108.5	156.5	48.00	"
127	Birch I	55	4.6	0.93	0.25	3.3	6.2	2.5	200	82.00	170.25	88.25	"
132	Birch I	55	0.7	1.14	1.50	3.3	3.0	0.49	200	Insufficient Time			"
138	Birch I	55	3.4	1.06	0.50	3.3	3.0	1.2	200	170.5	267.0	96.50	"
143	Birch I	55	0.7	1.68	0.17	3.3	14.0	1.5	200	Not Connected			"
159	Birch I	55	3.4	1.63	1.00	3.3	2.0	0.74	200	223.5	392.5	169.00	"
160	Birch I	55	3.4	0.82	0.50	3.3	2.0	1.3	200	141.0	199.5	58.50	"
175	Birch II	55	2.5	0.60	0.13	4.4	4.6	1.2	200	155.0	203.5	48.5	"
148	W. Pine II	55	2.5	1.99	1.00	1.9	7.7	1.2	200	164	342	178.00	"
93	Pine & Nails	55	2.5	0.22	0.50	1.3	4.6	1.3	200	102.25	125.25	23.00	Iron Nails Used
106	Pine & Nails	55	2.5	0.22	0.50	1.3	4.6	0.8	200	143.75	163.00	19.25	"
104	Pine & Nails	55	2.5	0.22	0.50	1.3	4.6	0.7	200	171.25	196.00	24.75	"
109	Pine & Nails	55	2.5	0.22	0.50	1.3	4.6	2.5	200	76.50	99.00	22.50	"
112	Pine & Nails	55	2.5	0.22	0.50	1.3	4.6	2.3	200	70.50	92.50	22.00	"
115	Pine & Nails	55	2.5	0.22	0.50	1.3	4.6	3.5	200	51.50	76.25	24.75	"
162	Pine & Nails	55	2.5	0.11	0.25	1.3	4.6	3.2	200	Broken Probe			"
96	W. Pine I	55	2.5	0.44	1.00	1.3	4.6	2.0	200	126.50	162.00	35.50	Humidifier Used
100	W. Pine I	55	1.0	0.44	1.00	1.3	4.6	1.0	200	225.75	244.50	18.75	"
108	W. Pine I	55	1.0	0.44	1.00	1.3	4.6	1.0	200	196.75	214.25	17.50	"
113	W. Pine I	55	2.5	0.44	1.00	1.3	4.6	2.1	200	101.25	120.25	19.00	"
140	W. Pine I	55	2.5	0.44	1.00	1.3	4.6	1.9	200	114.50	150.50	36.00	"
141	W. Pine I	55	1.0	0.44	1.00	1.3	4.6	1.2	200	185.0	207.5	22.50	"
144	W. Pine I	55	1.0	0.44	1.00	1.3	4.6	1.2	200	170.0	197.5	27.50	"
145	W. Pine I	55	1.0	0.22	0.50	1.3	4.6	1.3	200	166.5	183.0	16.50	"
150	W. Pine I	55	2.5	0.44	1.00	1.3	4.6	2.4	200	96.50	129.75	33.25	Wet Substrate
154	W. Pine I	55	1.0	0.22	0.50	1.3	4.6	0.97	-TBD-				"
147	W. Pine I	55	1.6	0.11	0.25	1.3	4.6	3.0	200	77	87.5	10.50	Clay Bed
157	W. Pine I	55	3.4	0.11	0.25	1.3	4.6	6.5	200	40.625	50.625	10.00	"

Table 6. Compilation for many tests, in convenient groupings, of the time interval for firefront passage (based on the duration above 573 K of a centerline near-surface 130-μm thermocouple) (continued).

Test #	Fuel Type	Test Width (W) [cm]	Wind Speed (U) [m/s]	Loading (m) [kg/m^2]	Elements per cm^2 (n) [#/cm^2]	Diameter (d) [mm]	Height (H) [cm]	Flame Speed (vf) [cm/s]	Temp. used (T) [C]	T Rise 5 mil (T1) [sec]	T Fall 5 mil (T2) [sec]	delt (T2-T1) [sec]	Comments
161	W. Pine I	55	3.4	0.11	0.25	1.3	4.6	4.9	200	Broken Probe			Clay Bed
166	W. Pine I	55	2.5	0.11	0.25	1.3	4.6	5.2	200	46.125	56.125	10.000	"
169	W. Pine I	55	1.6	0.11	0.25	1.3	4.6	4.2	200	51.50	62.25	10.75	"
146	Pine I-Br I	55	2.5	0.89	0.50	Mix	4.6	1.4	200	133.75	194.75	61.00	Mixed Diameters
151	Pine I-Br.I	55	2.5	0.83	---	Mix	4.6	1.9	200	112.5	190.5	78.00	"
153	Pine I-Br.II	55	2.5	0.41	0.31	Mix	4.6	2.4	200	116.5	137.5	21.00	"
128	Birch I	55	4.6	2.09	0.25	2.3	21.6	NS	200	---	---	NS	Nonsteady
137	Birch I	55	3.4	2.53	0.25	3.3	14.0	NS	200	57.5	160.0	NS	"
149	Bamboo II	55	2.5	3.77	0.50	3.0	14.0	NS	200	120.0	384.5	NS	"
163	W. Pine I	55	1.6	0.07	0.17	1.3	4.6	NS	200	Broken Probe			"
164	W. Pine I	55	2.5	0.07	0.17	1.3	4.6	NS	200	46.00	55.00	NS	"
174	W. Pine I	55	2.5	0.07	0.17	1.3	4.6	NS	200	---	---	NS	"
133	Bamboo II	55	0.7	3.77	0.50	3.0	14	0.49	Insufficient Time				No Data
136	Birch I	55	3.4	3.59	0.75	3.3	Mix	?	Insufficient Time				"
142	Birch I	55	0.7	2.12	1.00	3.3	3.0	0.31	Insufficient Time				"
155	W. Pine I	55	- - - Varied - - -			1.3	4.6	---	Not Instrumented				"
156	W. Pine I	55	0	0.66	2.00	1.3	4.6	0.21	Not Instrumented				"

Note: NS - Non Steady Propagation

*Note: Temperature measurement made with 20 mil thermocouple rather than a 5 mil thermocouple.

The (averaged) initial mass of fuel per unit planform area of the bed is conceptually distinguishable from the mass per area consumed during firefront passage; however, for virtually all the thin-fuel-element testing to be reported here, the fuel loading is entirely burned during firefront passage, so that the two quantities are equivalent. [In the absence of any explicit statement, no inert loading is present; whenever present, the discrete inert upright elements will also be characterized by an areal average. For beds with elements of multiple heights, thicknesses, and composition, (3.1) requires generalization, usually in the form of additive terms on the right-hand side].

Implicit in the adoption of the characterization of the fuel bed by the overall parameter m is the intention to seek firespread-rate results, to the fullest extent reasonably consistent with experimental observation, without concern for details concerning the fuel distribution (other than for provision that the elements are "thin," are not "prone" to the substratum, and are composed of common wood species with "typical" chemical exothermicity per unit of ovendry mass). It seems worth noting that, in the absence of special provision for meticulous and tedious inventorying, little is often known concerning discrete-element fuel distributions of practical interest other than an estimate of the initial total fuel loading m and an estimate of the total fuel loading after all burning (not immediately after firefront passage).

Nevertheless, experiments are conducted with regular arrangements, for the purpose of achieving a well-defined, nominally reproducible bed, to permit repetition of test conditions. For experiments limited to variation of m by variation of n only, one may alter either the number N of the fuel elements per unit planform area s^2 of the bed, where s is the spacing between the above-described "checkerboard-distributed", equal-diameter, equal-depth holes, or the between-nearest-holes spacing s; in the present experiments, only the number N is altered. If, in addition, n itself is held fixed, only small-scale variability within a fuel bed uniform on a grosser scale is permitted. This microscale indefiniteness within macroscopic uniformity here is termed crystallinity, a concept familiar (for example) in the continuum treatment of (say) elastic solids. In

particular, the allotment of toothpicks to the smallest four-hole square delineated by drilled holes constitutes for this section the basic "building block"; this element (conveniently taken with one side parallel to the leading edge) is meticulously repeated to comprise the entire array for the tests discussed immediately below. Thus, one can obtain an average of one toothpick in each hole by placing a single toothpick in every hole or by placing two toothpicks in every other hole.[2] (For more complicated arrays, with mixed elements, a larger basic "building block" is adopted.)

One concern is that the firefront might propagate appreciably faster for those arrangements [with fixed wind speed, fixed fuel-loading parameters (ρ_s, H, n, d^2), and fixed bed width] for which a downwind element is closer to an upwind element, with both oblique and in-line considerations of consequence. If such details of small-scale nonuniformity are of appreciable import for firespread rate, a description of the fuel bed in terms of the single macroscopic property m would be frustrated from the outset. While there is some variability of firespread rate, probably ascribable to the just-described proximity considerations, especially for lighter loadings, it is concluded that the macroscopic description m suffices. For example, Figure 5 indicates the sensitivity of firespread rate to details of fuel-element-distributions in which there is the equivalent of two white-pine toothpicks in each hole; Figure 6 indicates the sensitivity for variations on the equivalent of one toothpick per hole.

---

[2]For a square grid of holes, each of which can accommodate up to and including four toothpicks, for a four-hole-square basis there are four ways to achieve the equivalent of one-half a toothpick per hole, eight ways to achieve the equivalent of one toothpick per hole, and sixteen ways to achieve two per hole--if one precludes subdividing toothpicks and disregards effectively equivalent arrangements. The presence of more than one toothpick per hole augments the possibility of the shading of one fuel element from some radiation owing to the presence of others. Incidentally, since virtually all synthetic polymers readily available in toothpick-type configuration are thermoplastic and melt upon heating, a small pool of (not necessarily equal) mass of viscous, largely unburned fluid at the site of each plastic element results from their use in a bed of mixed polymers, and (except for one test) attention is limited to tests with natural polymers only.

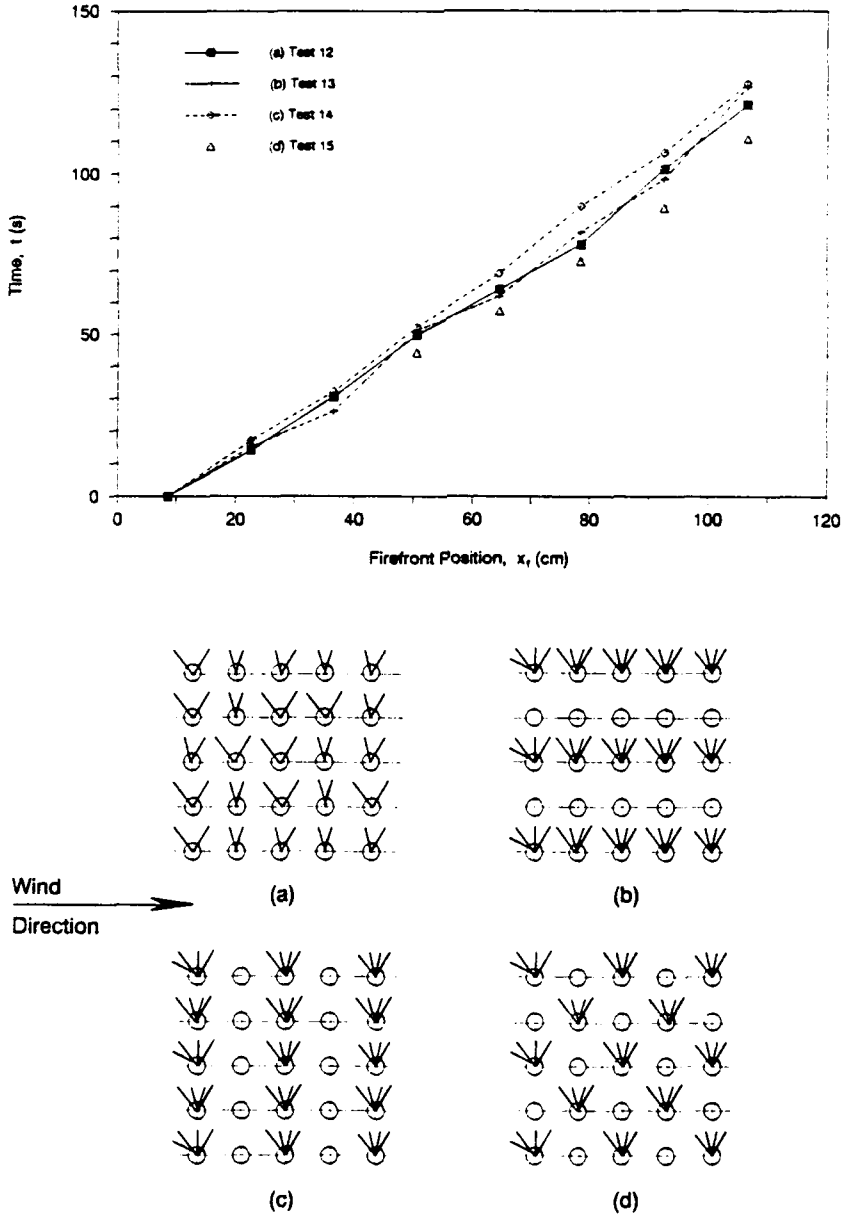

Figure 5. Effect of the fuel-loading pattern on the rate of firefront propagation for fuel loading m = 0.08830 g/cm^2, bed width W = 55 cm, and wind speed U = 70 cm/s. The quantity x_f is the streamwise-centerline position of the firefront (downwind from the leading edge of the fuel bed) and t is time since ignition.

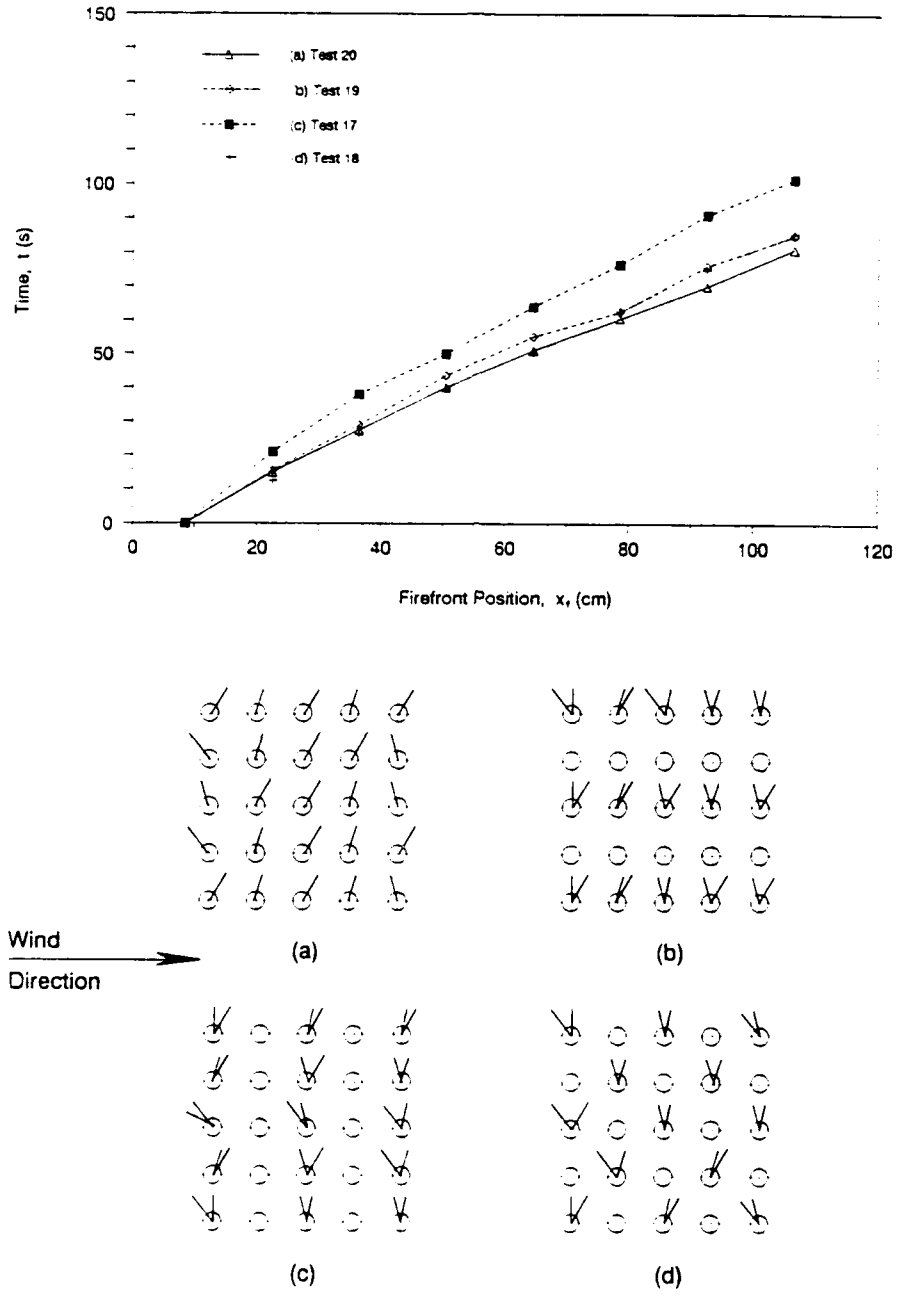

Figure 6. Effect of the fuel-loading pattern on the rate of firefront propagation for fuel loading m = 0.04415 g/cm^2, bed width W = 55 cm, and wind speed U = 70 cm/s. The quantity x_f is the streamwise-centerline position of the firefront (downwind from the leading edge of the fuel bed) and t is time since ignition.

SECTION 4

ANALYSIS

4.1 A MODEL OF THE PHENOMENOLOGY.

We shall formulate and solve a convenient, tractable model of the phenomenology encompassed by Figure 1, by adopting many approximations. In particular, we seek from the simple model an expression for the rate of firefront propagation, v_f, taken to be quasisteady, as a function entirely of parameters known prior to test execution. At several turns in the analysis, alternative approximations might be adopted; consideration of these alternatives is taken up later in the main text, and more broadly in the appendix, in which a semi-empirical treatment of the phenomenology is developed. The semi-empirical treatment is relegated to the appendix because we regard it as an inferior approach to the present problem; the only reason for including the appendix at all is to develop the implications of some alternative approximations, in order to demonstrate succinctly that the resulting predictions are much at variance with the experimental observations.

In the frame of reference of a steadily propagating two-dimensional (line-type) firefront, with the origin of coordinates at the downwindmost site at which the fuel surface is at the (known) pyrolysis temperature T_{pyr}, we let the streamwise coordinate be denoted by x (positive downwind) and the transverse coordinate be denoted by y (positive into the gas phase, negative into the fuel bed) (Figure 7). In such a frame of reference, the fuel bed is translating upwind (i.e., in the negative x direction) at constant speed v_f, the key unknown. The wind is flowing in the positive x direction at constant known speed $(U - v_f)$, but, since we are interested in cases in which $U \gg v_f$, the wind speed is taken to be U. We also anticipate tentatively that the fuel loading can be characterized adequately for present purposes by the overall quantity m, the mass of combustible matter [per unit (planform) area of the bed] consumed with firefront passage. We anticipate that v_f may be primarily a function of U and m because the other parameters may not vary much from case to case

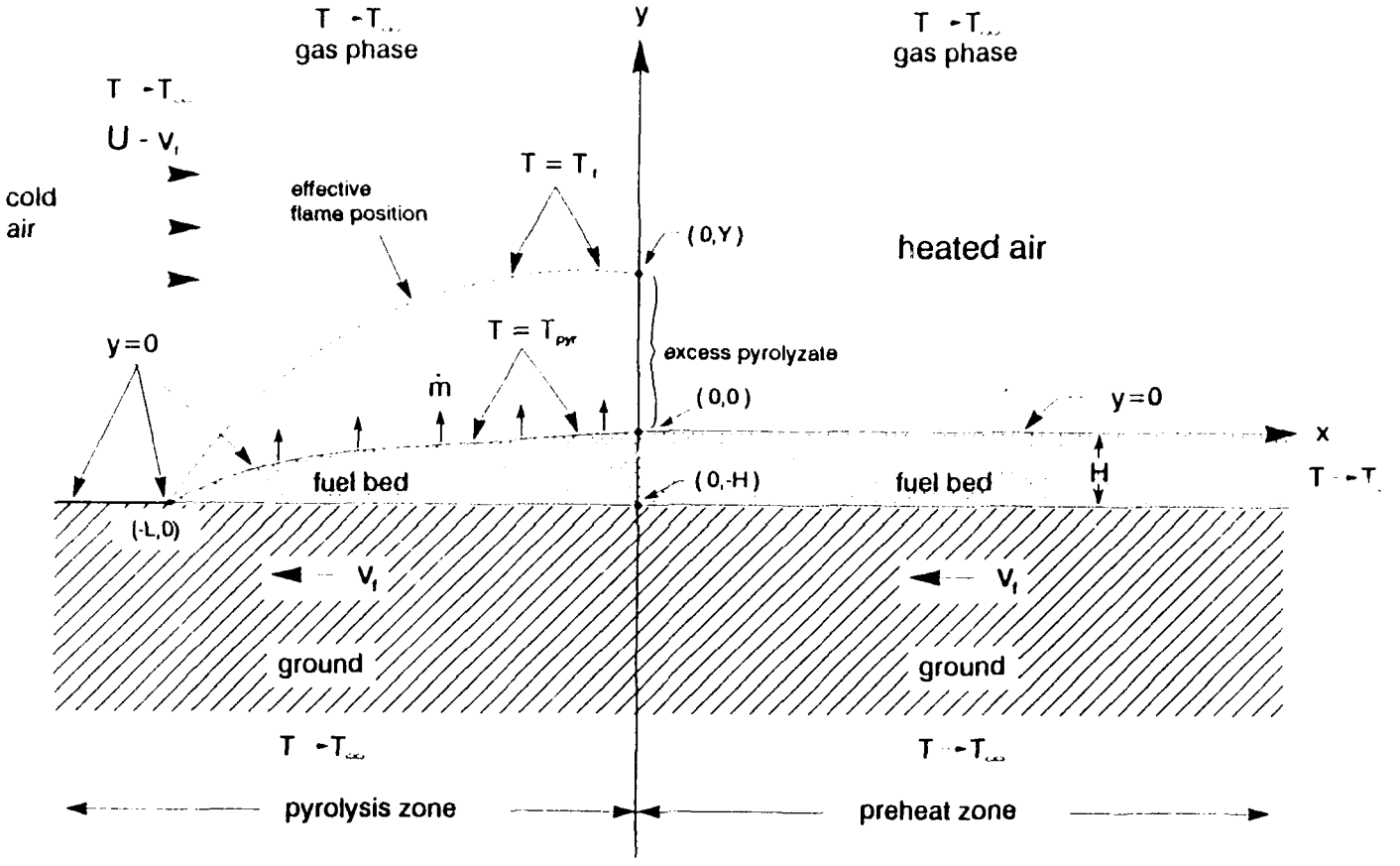

Figure 7. A simplistic idealization of wind-aided firespread across a bed of discrete fuel elements, for the purpose of modeling a quasisteady spread at the rate v_f, typically much slower than the speed $(U - v_f)$ of the cold oncoming air stream, in the frame of reference of the firefront. At the origin of coordinates, the surface of the fuel bed, of initial depth H, achieves the pyrolysis temperature T_{pyr} after preheating; the evolved pyrolyzate burns with ambient air in a gas-phase turbulent diffusion flame, to create a hot layer of characteristic thickness Y at the onset-of-pyrolysis front position x = 0.

of interest[3]. Among the other parameters are Q, the heat released per unit mass of fuel burned [adjusted to account for a modest amount of moisture present in the fuel (Luke and McArthur 1977)[4], and for the amount of sensible heat required to raise even the dry fuel from the ambient temperature to its pyrolysis temperature]; κ is the thermal diffusivity of the gas phase, where c_p is the typical specific heat capacity of the gas at constant pressure, ρ_o is the density of the gas near the flame, and k is the thermal conductivity of the gas near the gas-solid interface near the origin of coordinates; κ_b is the effective (bulk) thermal diffusivity of the fuel bed, where k_b is the effective thermal conductivity of the fuel bed, c_b is the effective specific heat of the bed, and ρ_b is the mass of the bed per unit volume of the bed.

From dimensional analysis, we might expect that the normalized rate of firespread depends on the following groups:

$$\frac{v_f}{U} = F\left[\frac{k}{k_b}, \frac{\rho_o}{\rho_b}, \frac{c_p}{c_b}, \frac{T_f}{T_{pyr}}, \frac{q}{c_p T_f}, \frac{(m/\rho_o)U}{\kappa}\right], \qquad (4.1)$$

where the flame temperature T_f can be rephrased in terms of more fundamental thermodynamic (and thermochemical) properties, such as the stoichiometrically adjusted ambient oxygen mass fraction and the ambient temperature (Fendell 1965), but such detail does not serve our objectives because vigorous-flame temperatures do not vary much for present purposes. Clearly several further approximations are being adopted by so limiting the

---

[3]Holding the mean wind U constant, and arranging for the properties of the ambient fuel bed to spatially uniform (macroscopically), are prerequisites for achieving a quasisteady rate of spread. Of course, such experiments are designed to yield the dependence of the rate of spread on these parameters, and cannot yield the dependence (believed to be generally less important) on the rates of change of these parameters. In applications, the firespread rate implicitly is taken to depend primarily on the local and instantaneous values of pertinent parameters themselves, presumably because these parameters generally vary slowly.

[4]Among the other consequences on firespread of fuel-moisture content may be the role of additional water vapor (1) in interfering with collisions of oxygen and pyrolyzate molecules, and (2) in modifying the radiative transport of heat. However, the latent-heat requirement to evaporate the water is taken to be the principal effect.

number of dimensionless groups on the right-hand side of (4.1); e.g., the molecular diffusion coefficients for the gas phase are being taken as comparable, radiative transfer and gravitational effects are being neglected, any latent heat for pyrolyzation of the wooden fuel is being ignored, heat loss to inert content in the bed is being omitted, (for the vigorous burning of interest) the rate of reaction is being taken as indefinitely rapid relative to the transport rates, and residual unpyrolyzed fuel does not occur for the thin-fuel loading. In fact, the only generalization of (4.1) that we shall discuss below concerns the possible presence of additional groups on the right-hand side of (4.1) for cases in which the characterization of the bed by the gross parameter m does not suffice. In such cases, the additional groups that we select for inclusion may be written (for the case of identical fuel elements)

$$\frac{HU}{\kappa}, \frac{dU}{\kappa}, \frac{WU}{\kappa}, \frac{\theta U}{\kappa}, \tag{4.2}$$

where H is the length of the fuel elements, d characterizes the thickness of fuel elements (recall that d^2 characterizes the cross-section area of the elements), W is the width of the fuel bed, and θ is the width of the test section. The last parameter θ is distinct from the others, and is the only example that we choose to include of a property of the particular experimental facility. Were there to arise evidence of the need to include the parameter θ, it would imply that in practice the firespread phenomenon may be nontrivially altered by the facility used; for the mathematical idealization of a line-type spread, θ is infinite. For a fuel bed composed of identical upright matchstick-type elements, the height of the bed H is also the height of the elements, as adopted in (4.2); more generally, the two heights are not the same, and the first group in (4.2) is not redundant.

We envision the fuel as being preheated from ambient temperature to pyrolysis-onset temperature T_{pyr} by the heat released by the gas-phase-diffusion-flame burning over the pyrolyzing portion of the fuel bed. We take all the heat derivable by combustion of the pyrolyzate with ambient oxygen to have been released over the pyrolyzing surface; i.e., we ignore the fact that some of the combustible vapor evolved from the polymeric

loading either is not burned or is burned downwind of the pyrolysis-front position (which is recalled to lie at $x = 0$, by choice). If the amount of fuel not burned is relatively negligible, then it may be noted that we are altering the streamwise distribution of the heat derived from the burning of "excess pyrolyzate" in $x > 0$, but we are <u>not</u> altering the total exothermic heat obtainable from the burning of the available fuel loading m.

A statement of the conservation of the energy per time per unit depth (perpendicular to the plane of Figure 7) is given by

$$v_f \, Q \, m = \rho_o c_p \, T_f \, UY, \tag{4.3}$$

where Y characterizes the stand-off distance (at the pyrolysis-front position $x = 0$) from the two-phase interface ($y = 0$) of the peak gas-phase temperature, taken to be the adiabatic flame temperature T_f of a pyrolyzate/air diffusion flame (Figure 8). In fact, the value Y fluctuates on the integral scale of the turbulence, so Y is an average value. We are ignoring any heating of the oncoming air stream (by a warmed substratum) upwind of the fuel-bed burn-out site, just as we are ignoring any gas-phase velocity-boundary-layer formation upwind of that burn-out site, in our idealized formulation. The statement (4.3) equates (1) the heat content per depth per time entering the gas phase across the interphase with the pyrolyzing portion of the fuel bed and (2) the heat content (above ambient) per depth per time of the gas stream crossing the pyrolysis-front plane $x = 0$. The datum for temperature adopted throughout this analysis is the ambient temperature, taken to be the same for the air and the bed for convenience.

The downward heat flux (in energy per area per time) from the gas phase to the fuel bed over the preheating zone $\infty > x > 0$ is expressed by

$$q = \frac{kT_f}{Y} \, f\left(\frac{x}{Y}\right), \tag{4.4a}$$

where the dimensionless function $f(x/Y)$ decreases to zero as its argument increases. Equation (4.4a) implies that a convective-diffusive mechanism

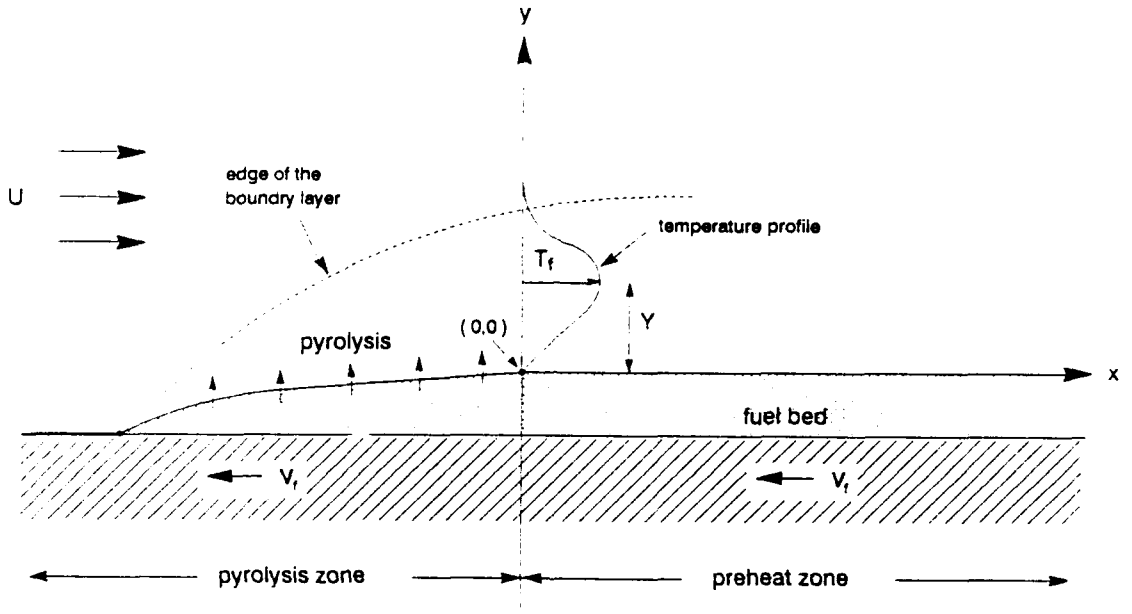

Figure 8. A schematic (supplementary to Figure 7) in which it is emphasized that the diffusion-flame burning of pyrolyzate with ambient air occurs within the forced-convective boundary layer in the adopted model. The characteristic stand-off distance Y of the maximum temperature T_f at the onset-of-pyrolysis front $x = 0$ is noted, along with a rough conjecture of the entire gas-phase temperature profile at that streamwise position.

effects the preheating of fresh fuel from ambient temperature to the pyrolysis temperature T_{pyr}. For later reference, were radiation the mechanism for preheating of fresh downwind fuel, if ϵ is the absorption coefficient of the hot gas and σ is the Stefan-Boltzmann constant, then, with Y characterizing the depth of the hot layer,

$$q = Y\epsilon\sigma\, T_f^4\, g\left(\frac{x}{Y}\right), \tag{4.4b}$$

where the dimensionless function g(x/Y) also decreases to zero as its argument increases.

For the heat balance within the fuel bed for the preheat zone, it is convenient (for this paragraph only) to reverse the sense of the coordinate axes, such that x is positive upwind and y is positive downward into the fuel bed. Then, if subscripts y and ξ denote partial derivatives,

$$\kappa_b\, T_{yy} - \frac{v_f}{Y}\, T_\xi = 0,\ \xi = x/Y. \tag{4.5}$$

Any flow-associated transport of heat within the fuel bed is ignored (unless we take the phenomenon to be parameterized by the effective transport property κ_b). The Laplace-transform pair is recalled to be

$$\bar{h}(s) = \int_0^\infty [\exp(-s\xi)]\, h(\xi)\, d\xi,\ h(\xi) = \frac{1}{2\pi i}\int_{-i\infty+\beta}^{i\infty+\beta} [\exp(s\xi)]\, \bar{h}(s)\, ds, \tag{4.6}$$

where β is chosen so that all singularities lie to the left of Re(s) = β in the complex s plane. Applying the transform (4.6) to (4.5), and then solving under the condition of boundedness (for a fuel bed approximated for this manipulation only as of semi-infinite depth, for simplicity of expression), yields, if A(s) is a function of integration to be identified,

$$\bar{T}(y,s) = A(s)\, \exp\left[-\left(\frac{v_f s}{\kappa_b Y}\right)^{1/2} y\right]. \tag{4.7}$$

Application of the boundary condition (4.4a) gives, under the Laplace transform,

$$\bar{q}(s) = \frac{kT_f}{\gamma}\,\bar{f}(s) = -k_b\bar{T}_y(0,s) = k_b\left[\frac{v_f s}{\kappa_b \gamma}\right]^{1/2} A(s). \qquad (4.8)$$

Therefore, by (4.7) and (4.8),

$$\bar{T}(0,s) = A(s) = \frac{k}{k_b}\,T_f\left[\frac{k_b}{v_f \gamma}\right]^{1/2} s^{1/2}\,\bar{f}(s). \qquad (4.9)$$

But $T(y = 0,\ \xi = 0) = T_{pyr}$, so

$$T_{pyr} = \frac{k}{k_b}\,T_f\left[\frac{\kappa_b}{v_f \gamma}\right]^{1/2} N, \text{ where } N \equiv \frac{1}{2\pi i}\int_{-i\infty+\beta}^{i\infty+\beta} s^{1/2}\,\bar{f}(s)\,ds; \qquad (4.10)$$

that is, N is just a positive real number whose value depends on details (of the heat-transfer profile) that we do not specify. If (4.3) is solved for Y and substituted in (4.10), there results

$$\frac{v_f}{U} = N\left[\frac{k\rho_o c_p}{k_b \rho_b c_b}\right]^{1/2}\left[\frac{T_f}{\bar{T}_{pyr}}\right]\left[\frac{kT_f}{\overline{Qm}U}\right]^{1/2}. \qquad (4.11)$$

The dependence on the square root of the ratio of the so-called conductance for the gas phase to that for the solid phase is conventional in such phenomena (Carslaw and Jaeger 1959, pp. 87-88). We regard $k_b\rho_b c_b$ as a composite property of the bed, and do not regard it as appropriate to attempt an approximate evaluation of any one factor in terms of other quantities that have been introduced.

Accordingly, by (4.11), $v_f \sim (U/m)^{1/2}$, a dependence indicated below to be in agreement with experimental observations obtained for thin-fuel-element-firespread tests in the TRW firetunnel facility. The expression

(4.11) is nondimensional, but in practice none of the factors other than m and U can be easily varied, so that, superficially, the (incidental) dimensionless presentation adds little further insight. In fact, more can be learned from (4.11), as will be discussed below.

First, it should be emphasized that the relation $v_f \sim (U/m)^{1/2}$ can hold over only a limited range of parametric values, since we expect that other processes may permit finite (albeit slow) rates of spread against the wind or in the absence of wind; that sufficiently high wind could result in forced-convective extinction; that a continuum model of the bed may better serve for very dense loading; and that nonpropagation may ensue for sufficiently sparse loading. Also, repeating the derivation with (4.4b) in place of (4.4a) results in the expression

$$\frac{v_f}{U} = \left[\frac{\rho_o c_p T_f}{mQ}\right]^{3/2} \left[\frac{T_{pyr}}{T_f}\right] \frac{\left(k_b \rho_b c_b U\right)^{1/2}}{M\epsilon\sigma T_f^{\,4}}, \qquad (4.12)$$

where the definition of the positive real constant M is that given in (4.10), if $\bar{f} \to \bar{g}$, where g is defined in (4.4b). Equation (4.12) gives $v_f \sim (U/m)^{3/2}$, at variance with observations reported below. In the appendix this topic, and the implications of a model in which the bed is modeled as well-mixed (i.e., approximately isothermal because k_b is indefinitely large), are developed further.

Since, according to observations with thin-fuel-element distributions, (4.11) captures the entire dependence of the rate of firespread v_f on the parameters U and m quite well, one infers that any (probably modest) dependence of v_f on the groups (4.2) is of the form (H/d), (W/d), and/or (W/θ); we rely on experiment to shed light on such dependence, if any. Incidentally, from inspection of (3.1), we identify still another length scale $n^{-1/2}$; however, H, d, and n are related to m via (3.1), so $n^{-1/2}$ is not an independent length scale.

4.2 FURTHER NOTES ON THE ROLE OF RADIATIVE PREHEATING IN WIND-AIDED FIRESPREAD ACROSS BEDS OF DISCRETE FUEL ELEMENTS.

A first-principles argument is undertaken to indicate the conditions under which radiative heat transfer is competitive with convective/conductive heat transfer for preheating in wind-aided firespread across an array of discrete fuel elements.

The radiation from the products of burning wood, including (as they sometimes do) glowing soot, is incident, in part, on the cool fuel which the fire is approaching. The total (time-integrated) heat $\tilde{Q}$ (in ergs/g of fuel) incident on that fuel during its entire heating history is given by

$$\tilde{Q} = \sigma T^4 \epsilon Y(V_1 f)\left[\tilde{L}/v_f\right](1/m), \qquad (4.13)$$

where $\epsilon\sigma T^4$ is the radiative output per unit volume of the hot gas, $(\tilde{L}/v_f)$ is the preheating time, and Y is the "thickness" of that slab of hot gas. Explicitly,

σ = 5.67 x 10^{-5} erg/(s cm^2 K^4);

T = temperature of the hot gas (K);

ϵ = absorption coefficient of the hot gas (cm^{-1});

Y = vertical thickness of the hot-gas region (cm);

V_1 = fuel-geometry and orientation portion of the view factor (dimensionless);

f = fraction of the horizontal area occupied by fuel (dimensionless);

$\tilde{L}$ = effective streamwise (horizontal) distance over which radiative heating is received (cm);

v_f = rate of firespread (cm/s); and

m = mass of thin fuel per unit planform area of the bed (g/cm^2).

We adopt m = 0.1 g/cm^2 and v_f = 5 cm/s, values appropriate for a windspeed of 2-3 m/s, according to observations reported below. The highest temperature in the luminous zone is about 2000 K (from decades of investigation of vigorous hydrocarbon/air diffusion flames). The length $\tilde{L}$,

here the length that glowing gas overhangs the preheating zone, is observed to be not more than 30 cm. (The value of $\tilde{L}$ appropriate to radiatively preheated burning will be addressed below.) The absorption coefficient $\epsilon \simeq 10^{-2}$ cm^{-1}, on the basis of experiments carefully executed at Factory Mutual Corporation in Norwood, MA (J. deRis, private communication). The height Y of the glowing region is observed to be about 5 cm. The quantity V, equal to the product $V_1 f$, can be estimated by noting that the upward radiation is as large as the downward, the downstream radiation is as large as the radiation directed upstream, and much radiation is lost laterally. Only the forward and downward radiation can serve to preheat fuel, but much of that impinges on the facility walls. That portion of the forward, downward radiation that is incident on the fuel bed is divided between that which encounters the discrete fuel elements and that which encounters the floor (i.e., the substrate). The fuel elements are sparsely distributed in current experiments, so V is less than 0.005; for more extensive fuel covering, V might be as large as 0.05. This value implies that the radiation is received by fuel and substrate over 0.25 rad (of the possible 4π rad), and 0.2 of that radiation is incident on the fuel, not on the substrate. If we adopt V = 0.01, then, with the values given in this paragraph for the other parameters, we obtain the crude estimate from (4.13) that $\tilde{Q}$ = 2.9 J/g. This value falls far short of the preheating necessary to pyrolyze wood, a value close to 250 J/g. Thus, it is convective-diffusive heat transfer which enables firespread to occur in the TRW experiments described above.

Let the reference fuel loading of 0.1 g/cm^2 henceforth be denoted m_0. For a value of m that is n times m_0, for a fire propagating at the flame speed of the convective-diffusive model (4.11), v_f is multiplied by a factor $n^{-1/2}$. The simple energy balance (4.3) gives

$$m\, v_f \sim Y\, U. \tag{4.14}$$

Hence, Y is multiplied by a factor $n^{1/2}$. The parameter V_1 is unchanged, but the factor f is multiplied by a factor n, just as is the quantity m itself. It is argued below that the downwind-thermal-decay length of a

stream that is losing its heat by radiation does not change with m, but the distance downwind to which the radiation reaches scales with Y just because of the geometry; i.e., $\tilde{L}$ is multiplied by a factor $n^{1/2}$. By combining these factors, we find from (4.13) that the effect of increasing the fuel loading by a factor n results in an increase in the radiative preheating $\tilde{Q}$ by a factor $n^{3/2}$. Since a fuel loading m_o = 0.1 g/cm^2 yields $\tilde{Q}$ = 2.9 J/g, and since a value of $\tilde{Q}$ about 85 times greater is required to achieve pyrolysis, a fuel loading roughly sufficient to achieve pyrolysis by radiation is estimated by setting $n^{3/2} = 85$. Hence, a sufficient loading, nm_o, is about 1.7 g/cm^2. This is <u>not</u> a universal result; radiative preheating does <u>not</u> always become either comparable or dominant at m = 1.7 g/cm^2. However, the result does suggest the level of loading near which the transition from the domination of preheating by convective-diffusive heat transfer might be expected in a firespread facility.

Incidentally, since every parameter (including $\tilde{L}$) that affects the quantity v_f in the convective-diffusive model scales there as it does in the radiative model, the above argument is selfconsistent.

Finally, attention is turned to substantiation of an earlier remark concerning the parameter $\tilde{L}$, more precisely concerning the decay length of the burnt-gas temperature downwind of the firefront. The rate of loss of heat (owing to radiation) per gram of gas, if T is temperature and t is time, is expressed by

$$\frac{\partial (c_p T)}{\partial t} = - \frac{\epsilon \sigma T^4}{\rho}, \tag{4.15}$$

where ρ is gas density. With x = Ut, so

$$\frac{\partial}{\partial t} = U \frac{\partial}{\partial x}, \tag{4.16}$$

it follows that, for c_p const.,

$$c_p \frac{\partial T}{\partial x} = - \frac{\sigma \epsilon T^5}{(\rho T) U}. \tag{4.17}$$

The product (ρT) is virtually constant in the present isobaric system:

$$\rho T = \rho_o T_o, \; T_o = 300 \text{ K}, \; \rho_o \simeq 10^{-3} \text{ g/cm}^3. \tag{4.18}$$

While (4.17) is readily integrable, we simply note the following. For the temperature, assigned the value T_f, to decrease to the value (T_f/α), where T_f characterizes the peak (flame) temperature and the factor $\alpha > 1$, requires a streamwise span $\Delta x = \tilde{L}$, where

$$\frac{c_p T_f}{\alpha \tilde{L}} \simeq \frac{\sigma \epsilon T_f^5}{(\rho T) U}, \tag{4.19}$$

or, if $a_o^2/(\gamma-1) = c_p T_o$, where a_o is the speed of sound in the gas at temperature T_o and γ is the ratio of specific heats, then

$$\alpha \tilde{L} = \frac{U \rho_o a_o^2/(\gamma-1)}{\sigma \epsilon T_f^4}. \tag{4.20}$$

For typical values ($U = 100$ cm/s, $a_o^2 = 1.2 \times 10^9$ cm/s), $\alpha \tilde{L} \simeq 31$ cm, or, for $\alpha = 2^{1/4} \simeq 1.2$, $\tilde{L} \simeq 26$ cm. This value for $\tilde{L}$, derived here on the basis of radiative cooling, is quite comparable to the value of 30 cm adopted earlier on the basis of observation for a firespread inferred to have a convective-diffusive mechanism for preheating.

SECTION 5

EXPERIMENTAL RESULTS

5.1 RESULTS FROM THE TRW FIRETUNNEL FACILITY.

5.1.1 The Effect of Wind Speed and Fuel Loading on the Rate of Firespread.

Perhaps the most practically significant result of the experimental testing is that the quasisteady rate of firespread v_f varies as $U^{1/2}$ for fixed m (Figure 9), and as $m^{-1/2}$ for fixed U (Figure 10), where U is the speed of the aiding ambient wind and m is the area-averaged thin-element fuel loading. The results are from tests with 55-cm-wide fuel beds loaded with white-pine toothpicks. Below, these data (and others) are replotted to indicate the adequacy of the fit $v_f \sim (U/m)^{1/2}$.

In Figure 11 the result for a single test, in which a few combustible thermoplastic fuel elements (Table 1) are added to the white-pine toothpicks [in a 55-cm-wide bed, with wood loading of 0.011 g/cm^2, for a test at U = 2.5 m/s], is juxtaposed with the results for two toothpick-only (but otherwise identical) tests. The slower spread with the heavier, plastic-augmented loading is consistent with the test interpretation that the synthetic-polymer elements partially volatilized, though much plastic melted into a small pool of very viscous fluid near each hole into which a plastic element was placed. That is, a fraction of the plastic mass served to enhance the fuel loading. In another comparison, a black roofing cement, a mixture of petroleum asphalt and mineral filters (manufactured by Gardner Asphalt Corporation, Tampa, FL), was coated on the above-described white-pine-toothpick elements, such that the nominal fuel loading was raised from 0.011 g/cm^2 (toothpicks only) to 0.033 g/cm^2 (toothpicks plus coating). While only 30% of the coating proved volatile, the flame-propagation speed was again retarded (owing to the enhanced loading of the bed) from the coating-free-test result. Specifically, v_f decreased from 6.4 cm/s to 3.8 cm/s, for tests with U = 3.4 m/s.

In Table 7, firespread-rate results are presented for fuel beds sparsely loaded with white-pine toothpicks; schematic drawings of most of the fuel-loading patterns pertinent for Table 7 are given in Figure 12.

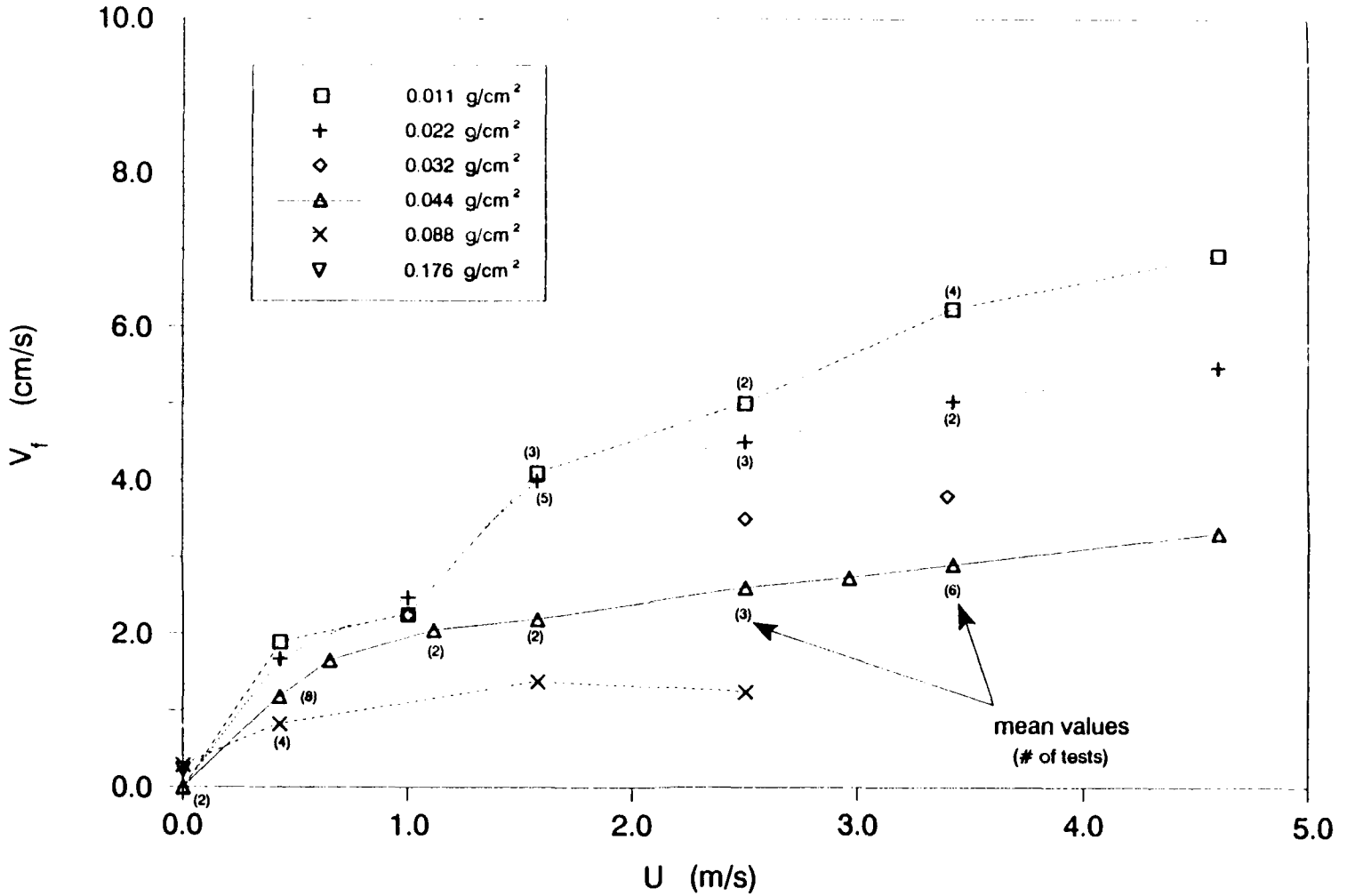

Figure 9. A compilation of test results for the quasisteady firefront propagation speed v_f (as inferred from streamwise-centerline, near-bed-surface thermocouples) as a function of wind speed U, for several values of the (white-pine-toothpick) loading m. Some data points are the mean of several tests, as noted. There is a small but finite rate of spread in the absence of wind, for heavier fuel loading.

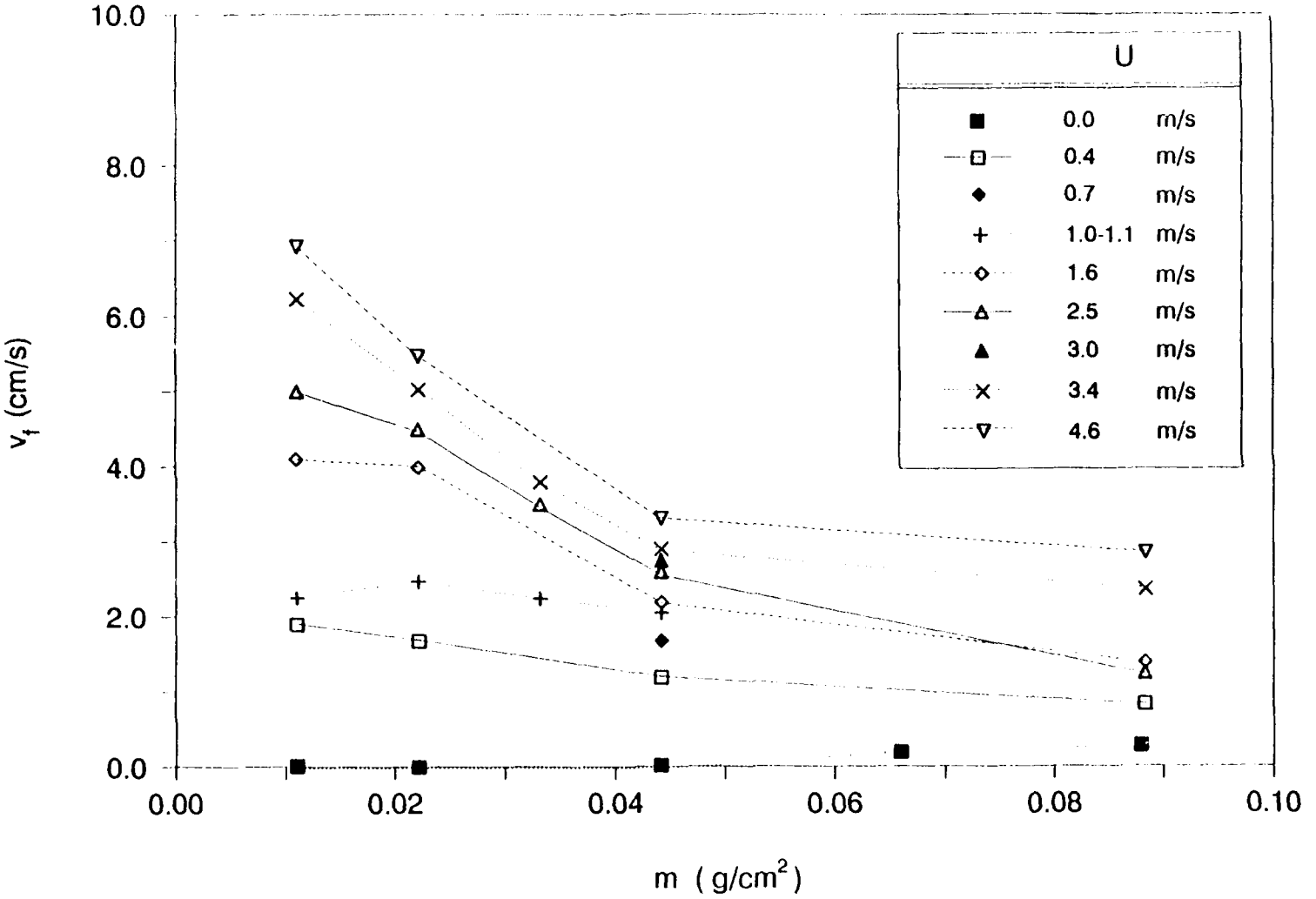

Figure 10. A replotting of the data of Figure 9, with the firespread rate v_f presented as a function of the fuel loading m, for several values of the wind speed U.

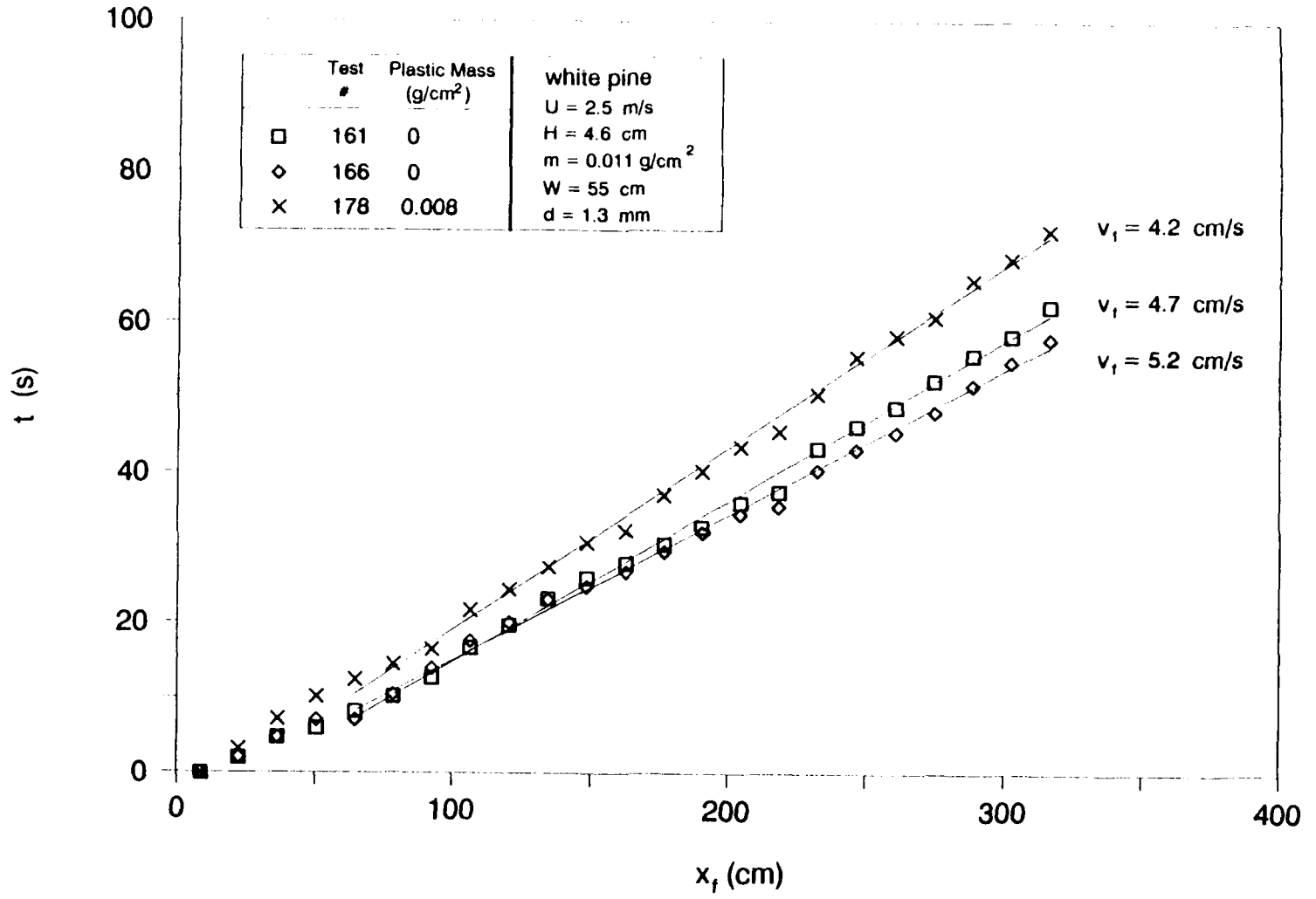

Figure 11. The streamwise position of the firefront (downwind from the leading edge of the fuel bed), x_f, as a function of time t since ignition of the upwindmost row at x = 0, for three tests executed with the stated wind speed U, wooden-element fuel loading m (where the elements have effective diameter d and height H), and fuel-bed width W. For test 178 (of Table 2), an additional loading of 0.008 g/cm^2 in the form of thermoplastic, hollow-core, tubular elements was added to the bed.

Table 7. Flame propagation as a function of wind speed and fuel loading for 55-cm-wide fuel beds: test results.

Fuel: White Pine d = 1.3 mm, h = 4.6 cm		Wind Speed 0.0 m/s	0.7 m/s	1.6 m/s	2.5 m/s
Loading g/cm cm	0.005	No	No	No	No (d)
	0.007	No	Cond (c)	Cond (c)	Cond (c)
	0.011	No	Yes (a)	Yes (4.2)	Yes (4.9)
	0.022	No	Yes (a)	Yes (4.0)	Yes (4.5)
	0.044	No	Yes (1.4)	Yes (2.2)	Yes (2.6)
	0.066	Yes (0.21)	Yes (b)	Yes (b)	Yes (b)
	0.088	Yes (0.3)	Yes (a)	Yes (1.4)	Yes (1.3)
	0.176	Yes (0.23)	Yes (b)	Yes (b)	Yes (b)

Notes:

Firespread rates, given in parentheses after some "yes" entries, are in units of cm/s;

(a) = firespread rate not measured;
(b) = test not conducted, but propagation is expected;
(c) = firespread nonsustainable;
(d) = test not conducted, but propagation is not expected;
d signifies fuel-element effect diameter;
h signifies fuel-element height.

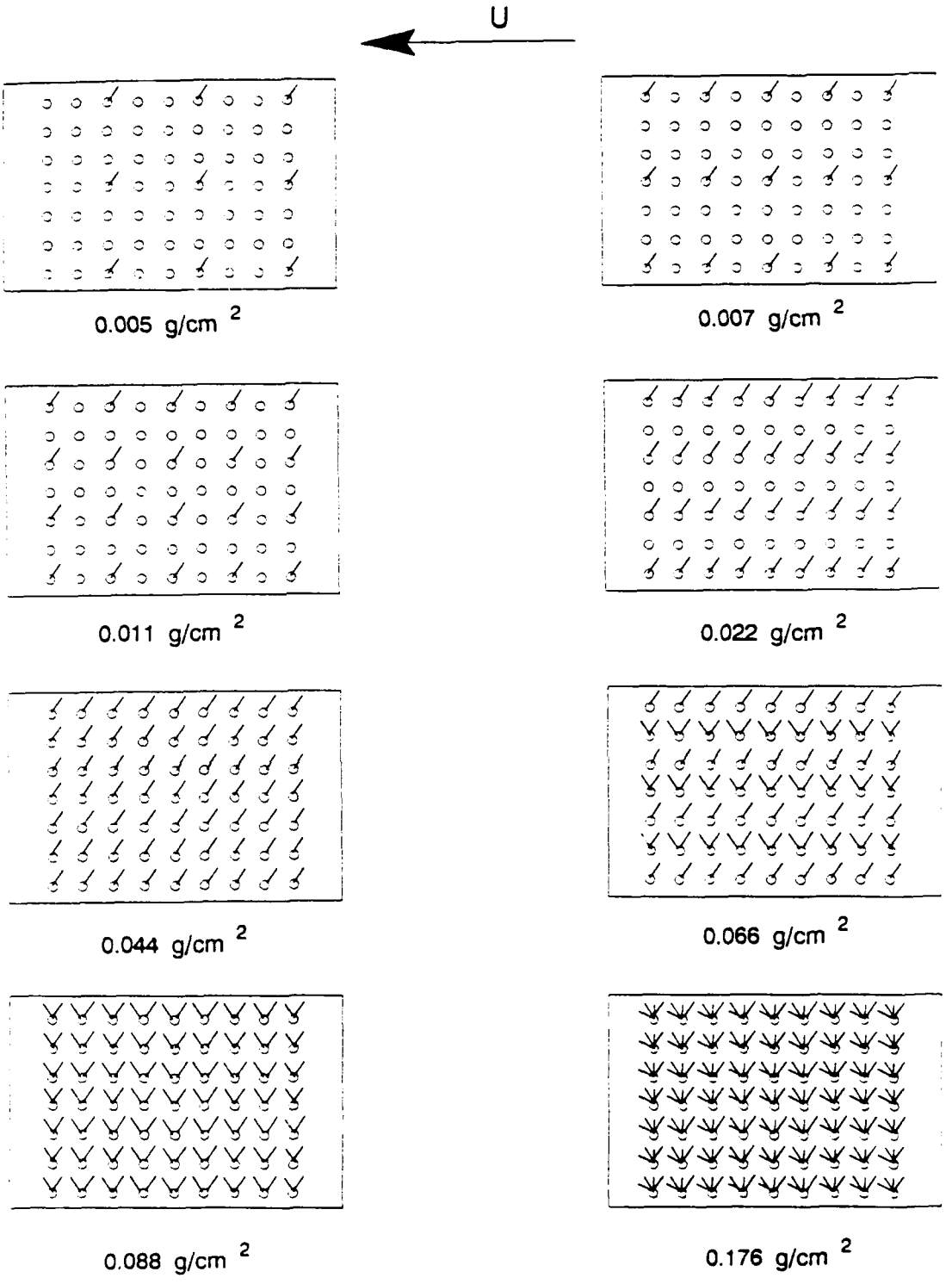

Figure 12. A schematic of the fuel-element placement for the fuel-bed loadings (designated by fuel mass per planform area, m) cited in Table 7.

The purpose is to identify the minimal loading for which fire propagates. These tests begin to identify the limits of the domain in the (U,m) parametric space for which the relation $v_f \sim (U/m)^{1/2}$ holds. Firebreaks arising because of the large distance from fuel element to fuel element might be modified locally because of ignition-inducing firebrands. Firebrands did not occur during the firespread testing in the laboratory facility. We conjecture that ignitions owing to firebrands are often a random event, and, for a modest amount of branding, we would expect the test results reported for the rate of spread, or for nonpropagation of fire, to be only locally and transiently modified by branding.

5.1.2 The Effect of Ceiling Movement on the Rate of Firespread.

Figure 13 presents comparative test results that relate to the provision for a moving test-section ceiling, so that there is unimpeded ascent of buoyant product gases (as well as an invariant wind speed at the firefront, such that a quasisteady rate of firespread can be achieved, if a quasisteady rate exists for the test conditions). For a fully extended ceiling at the test initiation, so that the ascent of buoyant product gases is impeded, and the buoyant gases are turned downwind by the oncoming stream, no steady rate of propagation is achieved. For a ceiling translated such that the buoyant ascent is unimpeded, but such that the flow arriving at the firefront is effectively invariant with firefront movement, a quasisteady rate is achieved (Figure 13). If the ceiling is not translated at all, but instead is left fully retracted at its upwind position, the rate of spread tends to be slightly slower than with the rate observed with ceiling translation.

5.1.3 The Effect of Fuel-Bed Width on the Rate of Firespead.

Because of lateral radiative heat loss at the fuel-bed edges, and because, during preheating, the downwind fuel elements near the lateral edges do not receive heat from upwind-fuel-element burning to each side (as much as the near-centerline fuel elements do), the firefront develops a curvature (Figure 14). The centerline-firefront position, used to obtain the spread rate, lies further downwind than the firefront position near the fuel-bed edges. Since only the component of the oncoming wind normal to the local-firefront locus aids spread, once the spread rate at the flanks lags, it

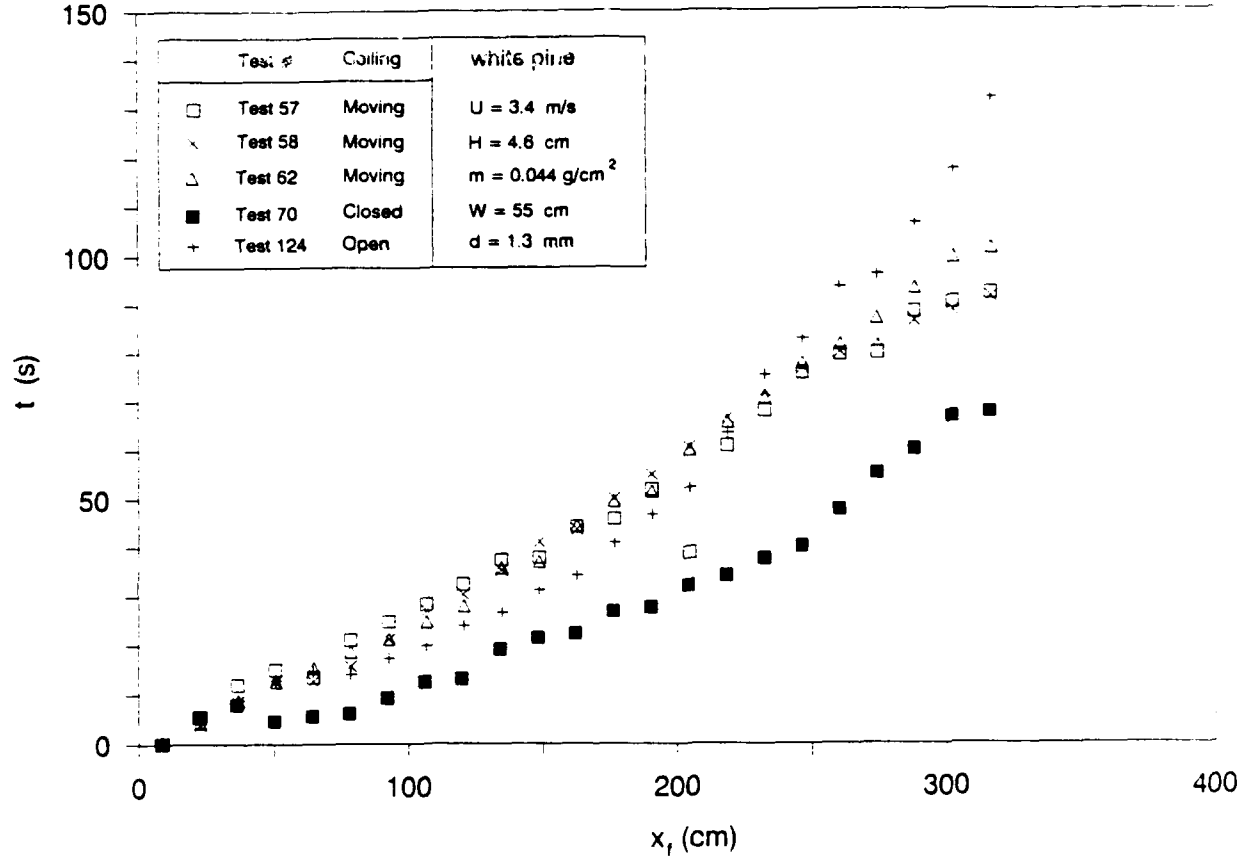

Figure 13. The streamwise position of the firefront (as indicated by the near-bed-surface thermocouples on the streamwise centerline), x_f, as a function of time t (since ignition of the upwindmost row at x = 0), for the specified aiding wind speed U, bed width W, fuel-element effective diameter d, fuel-element height H, and fuel loading m. In tests 57, 58, and 62 (of Table 2), a ceiling is translated (in its own plane) downwind during a test, such that its leading edge is just upwind of the buoyant firefront gases; in test 70, the ceiling is fully extended downwind at ignition; in test 124, the ceiling remains fully retracted throughout the test, so that the entire test section remains lid-free ("open").

Figure 14. A photograph of the firefront curvature for wind-aided firespread across a bed of discrete fuel elements. Here (for test 1 of Table 2) the loading m = 0.011 g/cm^2 (of white-pine toothpicks), the wind U = 1.6 m/s, and the bed width W = 100 cm. Whereas the near-centerline fuel elements are preheated by the burning of upwind fuel elements to each side, near-edge elements receive heat from one side only. Once lateral heat losses result in a firefront lag at the fuel-bed edges, the reduced wind aiding at the flanks precludes restoration of a planar firefront. The aiding wind is blowing from right to left, and the streamwise position is several meters downwind from the upwindmost row.

continues to lag, perhaps even more so with time under a constant wind. Testing with a wider and wider fuel bed removes the near-fuel-bed-centerline fuel elements even further from edge effects, and hence a faster rate of firespread for wider fuel beds is observed (Figure 15), although achievement of an asymptotic value for the centerline spread rate may entail a prohibitively large facility. Also, if there is any tendency for the oncoming wind to be more easily diverted around (rather than over or through) the buoyant product gases at the firefront, such diversion becomes impeded as the fuel-bed width approaches the test-section width of the facility; this phenomenon would also contribute to a faster rate of spread for a wider fuel bed. Comparison of test results for other parameters is meaningful if the tests are all executed at the same width of bed.

One may achieve somewhat more planar firefronts by decreasing the fuel-bed width with distance downwind from the leading edge. Both the lateral heat loss, and the asymmetric preheating of off-centerline fuel elements, are seemingly reduced by such tapering of the bed width with increasing downwind position. Indeed, for tapered beds, the rate of firefront propagation is enhanced sufficiently that a bed locally can support flame propagation as rapid as that for a wider, constant-width fuel bed (Figures 16 and 17). Of course, for the sufficiently narrow bed at the end of a firefront transit of a sufficiently tapered fuel bed, a propagation mechanism different from that holding upwind may predominate, simply because the bed is too narrow (Miller 1970). In fact, the rate of spread typically slows dramatically for a sufficiently small bed width, and often extinction quickly ensues.

5.1.4 The Effect of the Presence of Inert Matter in the Fuel Bed on the Rate of Firespread.

In seven tests, vertically oriented common nails were regularly distributed in the midspan (only) of a fuel bed with regularly arranged, thin, upright, wooden toothpicks (Figure 18). The objective was to ascertain the (relatively small) heat-sink and (relatively large) wind-retardation effects arising owing to the presence of noncombustible material in the fuel bed. The oxygen-deprivation effect that may inhibit vigorous burning (and may lead to copious smoke production) when inert

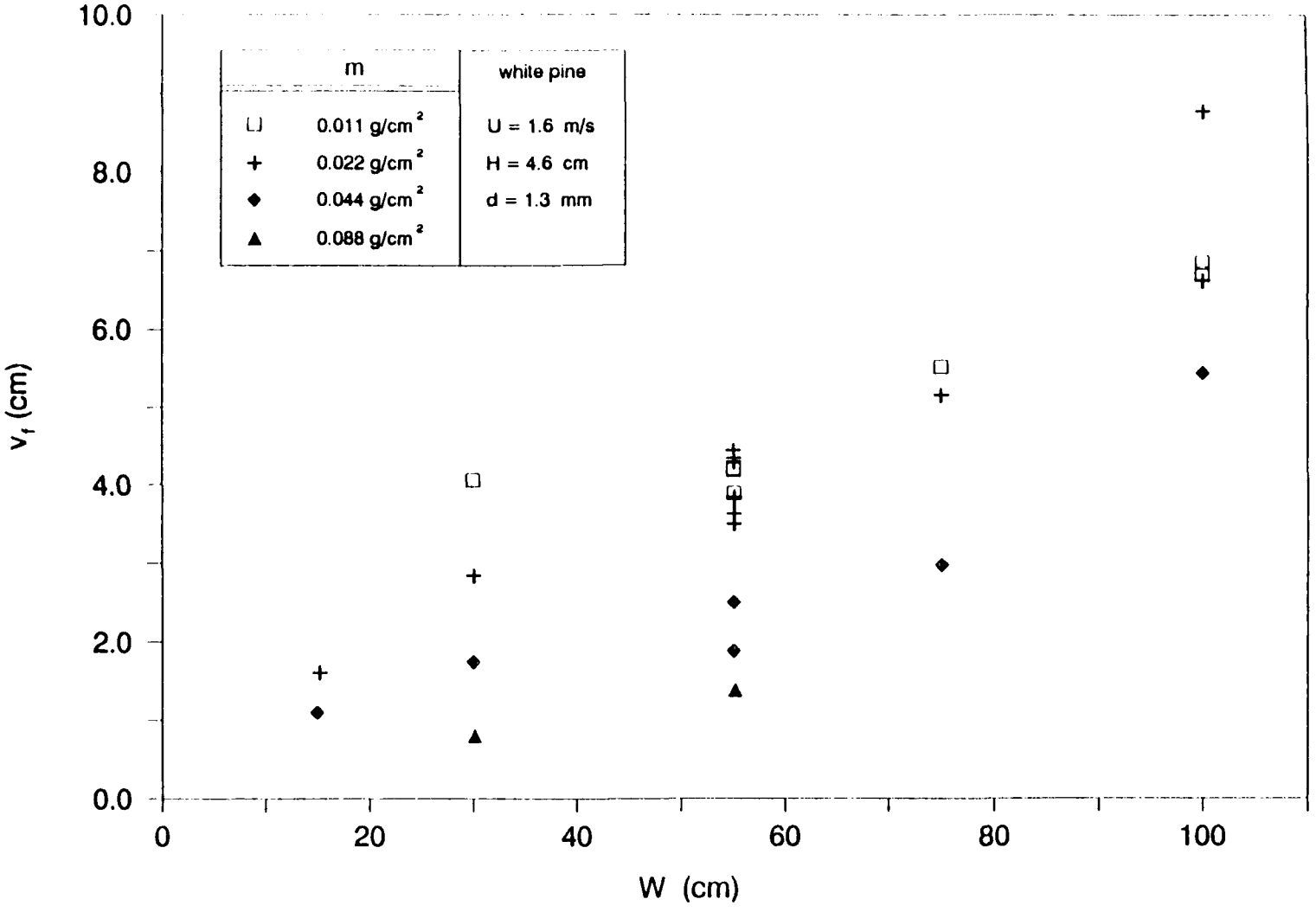

Figure 15. The rate of firespread, v_f, as a function of fuel-bed width W, for three different values of fuel loading m, from tests executed with the cited fixed values of the spread-aiding ambient wind U, (white-pine-toothpick) fuel-element effective diameter d, and fuel-element height H. The width of the test section of the firespread facility is 110 cm.

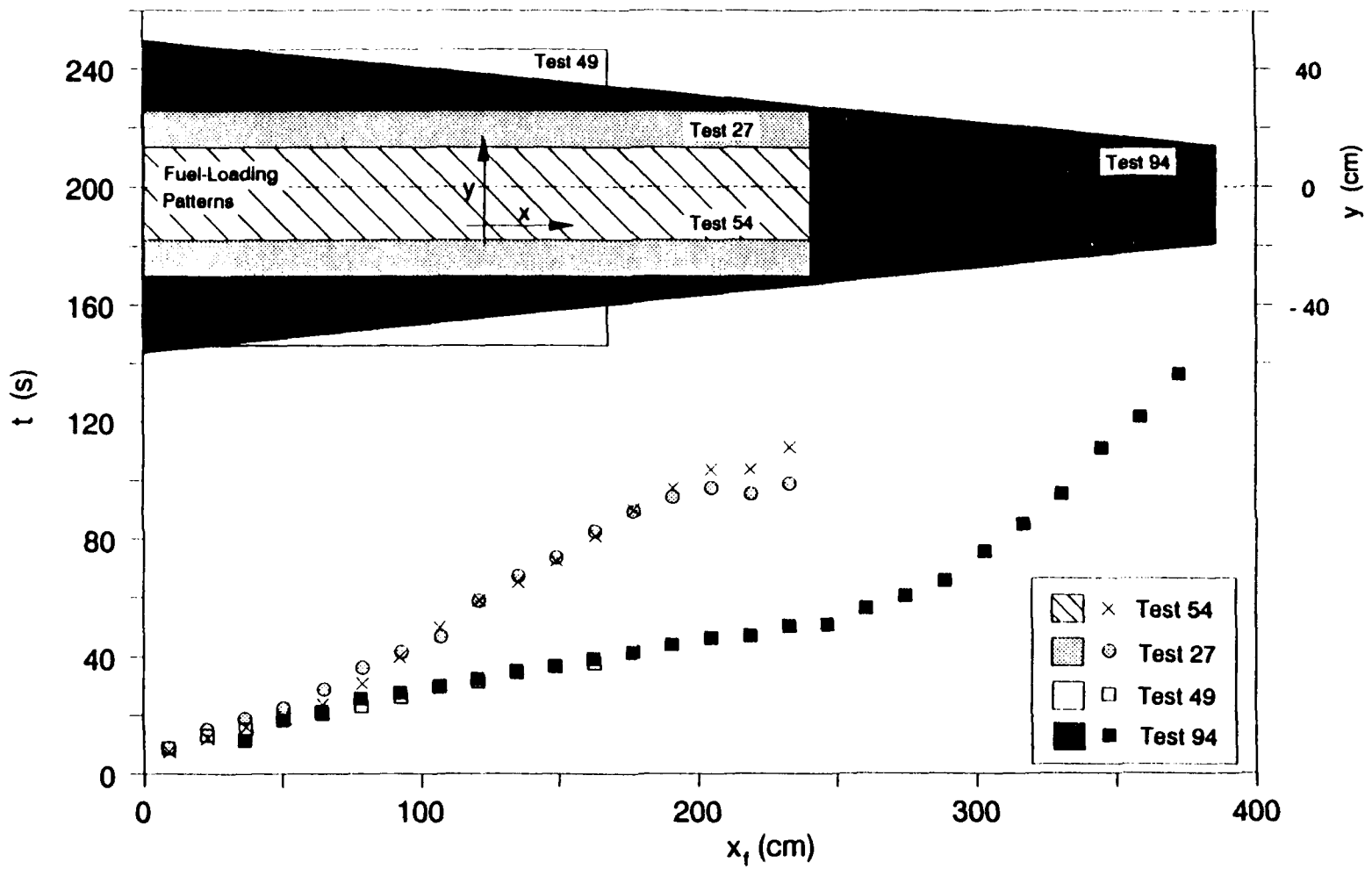

Figure 16. Below, the streamwise position (downwind of the fuel-bed leading edge) of the firefront, x_f, as a function of time t since ignition of the upwindmost row of fuel elements at x = 0, for four tests, all executed with fuel loading m = 0.044 g/cm^2 and ambient wind speed U = 1.6 m/s. Above, the distance, ±y (where y = 0 is the streamwise center-line), indicating the width of the fuel bed for streamwise position x at test initiation; for purposes of the upper portion of the figure, the abscissa is labelled more properly x than x_f.

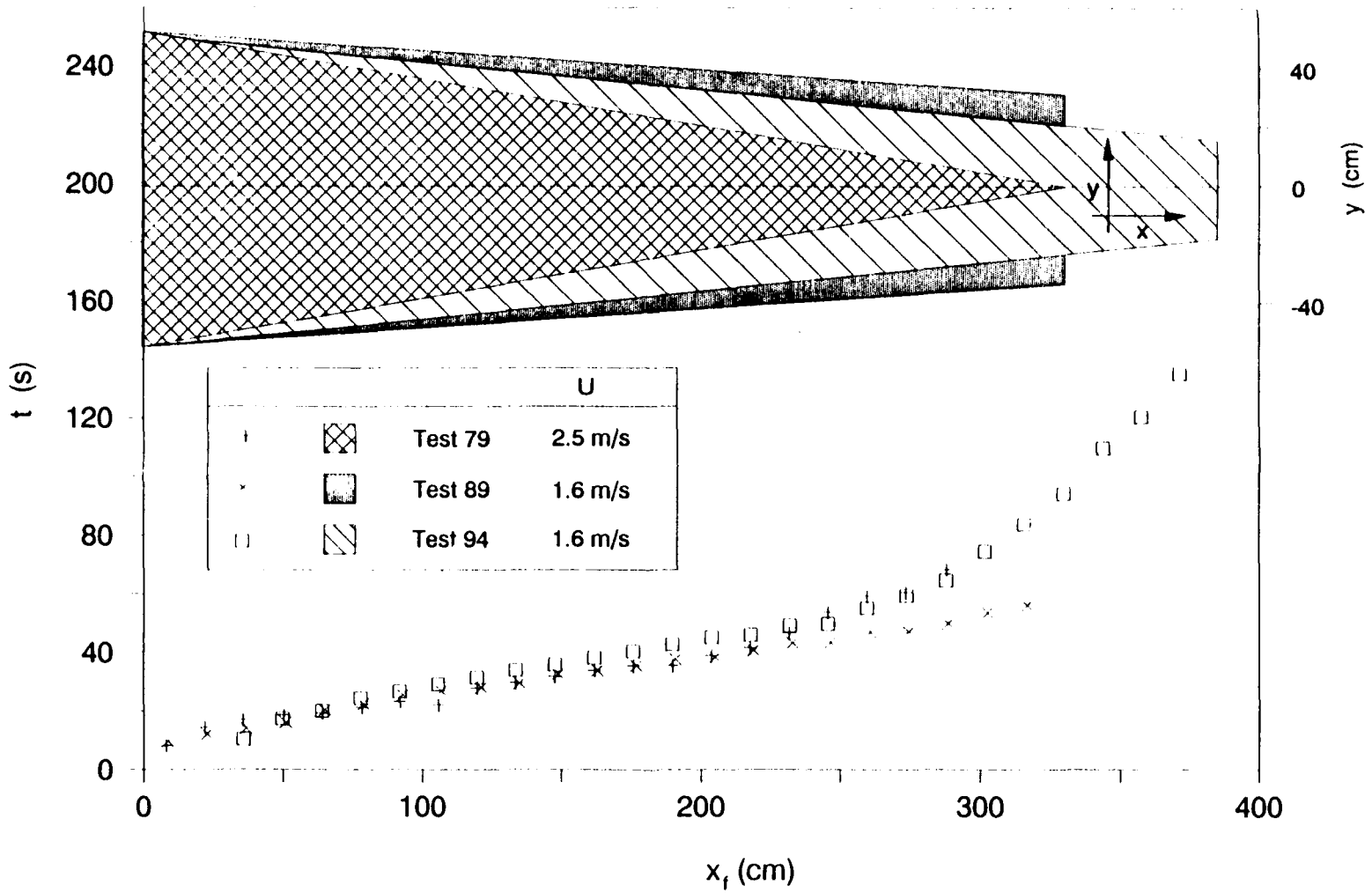

Figure 17. Same as Figure 16, but for three tests executed at different wind speeds U for the same fuel loading m = 0.044 g/cm^2.

Figure 18. A side view of a pretest fuel bed consisting of common nails interspersed regularly amid white-pine toothpicks; the inert and combustible elements are positioned in shallow holes drilled in a checkerboard pattern (1-cm sides) in a ceramic substrate. Table 1 presents the properties of the bed elements.

material is well mixed with combustible polymers cannot be investigated by the study of such arrangements, but the arrangements investigated here do meet the criterion of fuel-bed reproducibility adopted in this study.

Upwind and downwind of the midspan are expanses in which the fuel-element loading is identical to that of the midspan, but no nails are present. Properties of the nail and white-pine-toothpick elements used in the tests are listed in Table 1; it may be useful to note that the presence of one nail in every drilled hole results in an planform-area-averaged inert loading of 1.28 g/cm^2, whereas the presence of one toothpick in every drilled hole results in a planform-area-averaged fuel loading of 0.044 g/cm^2.

Figures 19-21 present the results; the insets symbolize the loading of the midspan, with a darker mark denoting a nail-filled hole, a lighter mark denoting a toothpick-filled hole, and a circle with no mark denoting an empty hole (the shallow holes being drilled into the substratum). In Figure 19, the ratio R of the number of nails to the number of toothpicks in the midspan is unity in the three presented tests, but the rates of firespread (inferred, per usual, from near-bed-surface-thermocouple data) differ. The preheating capacity of a fuel element is strongest on a neighbor immediately downwind; to the extent that the neighbor is inert, firespread is slowed. Figure 20 examines alternate arrangements for which $R = 0.25$, with $m = 0.22$ g/cm^2, the same loading as in Figure 19. The small change in firespread rate with a variance in microstructure within macroproperty invariance ("nail crystallinity") is noteworthy. Figure 21 presents results for $R = 0$, 0.33, 0.5 and 1, with m and U held invariant; it is found that v_f increases monotonically as R decreases. It appears as if there may be no finite value of R for which v_f is effectively unaltered despite the presence of nails; i.e., there seems no noteworthy threshold value before the nail content alters v_f.

Of curiosity is the juxtaposition of results from tests 87 and 93 (see Table 2), both with nail-filled midsections (Figure 22). Whereas the flamespread was more rapid with greater aiding-wind speed for the upwind and downwind nail-free sections, the flamespread for the nail-containing midsection was more rapid by a factor of two for the smaller of the two

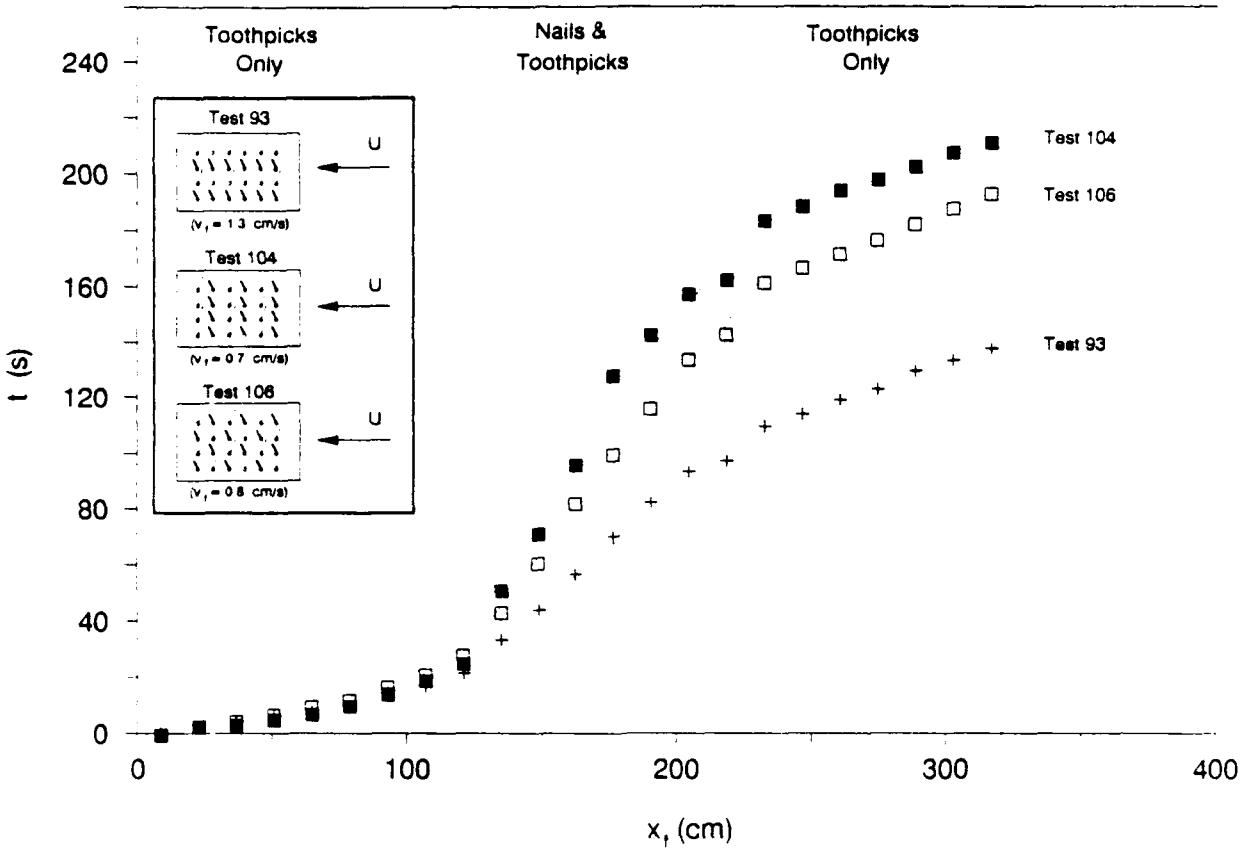

Figure 19. The firefront position x_f (downwind from the leading edge of the fuel bed) vs. time t (since ignition of the upwindmost row of fuel elements at x = 0). The tests involve a fuel loading of white-pine toothpicks, with m = 0.022 g/cm^2, a wind speed U = 2.5 m/s, and a fuel-bed width W = 55 cm. The ratio R (of the number of nails to the number of toothpicks) is unity for the midspan of the fuel bed. Upwind and downwind of the midspan nail-and-toothpick arrangement (which is indicated in the inset, with a darker mark signifying that a nail occupies a shallow hole in the substratum, a lighter mark signifying that a toothpick occupies a hole, and a circle without marks signifying that the hole is empty), R = 0 for all cases; i.e., upwind and downwind, the toothpicks are present, without any nails.

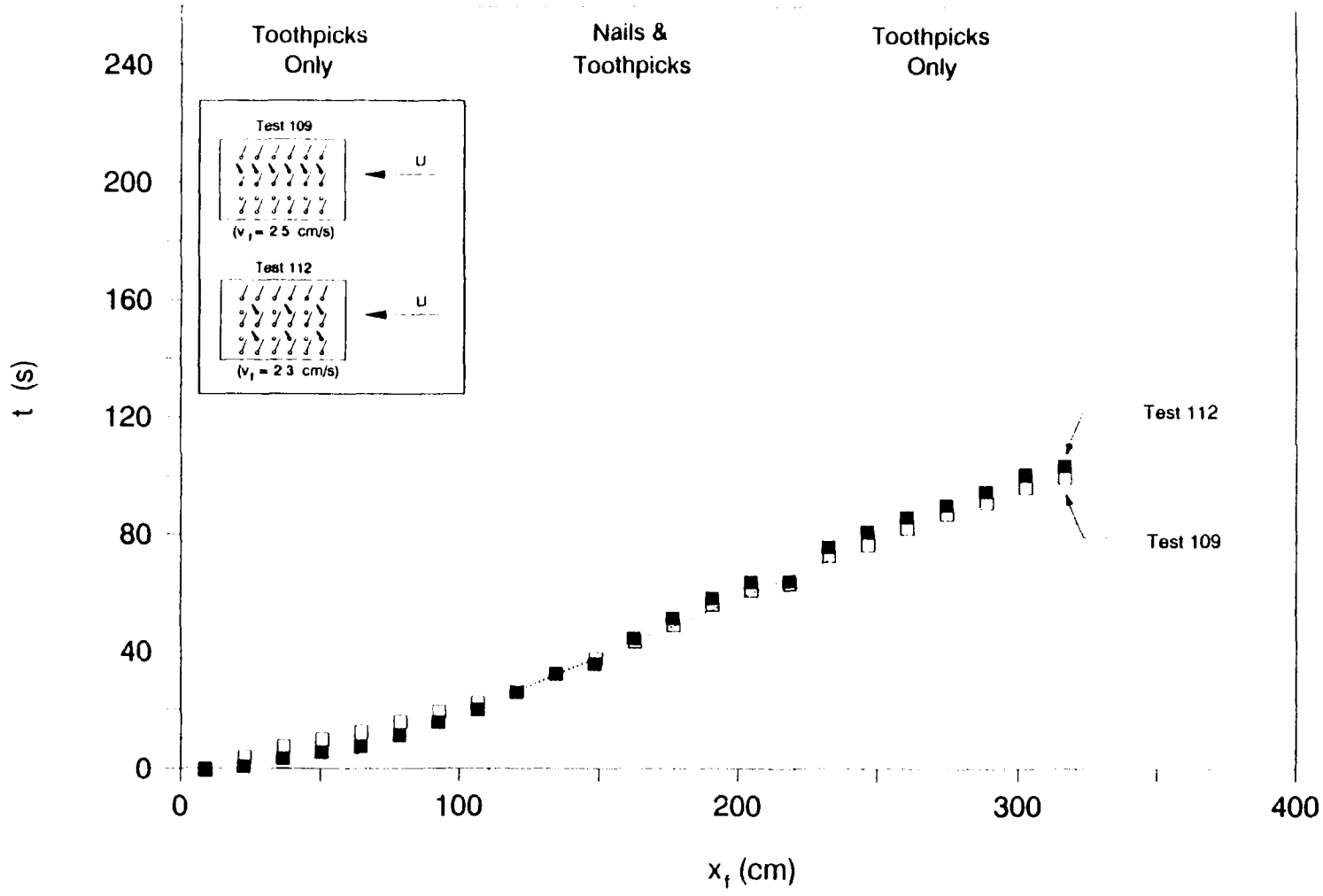

Figure 20. Same as Figure 19, except, for both cases, R = 0.5 for the midspan (only).

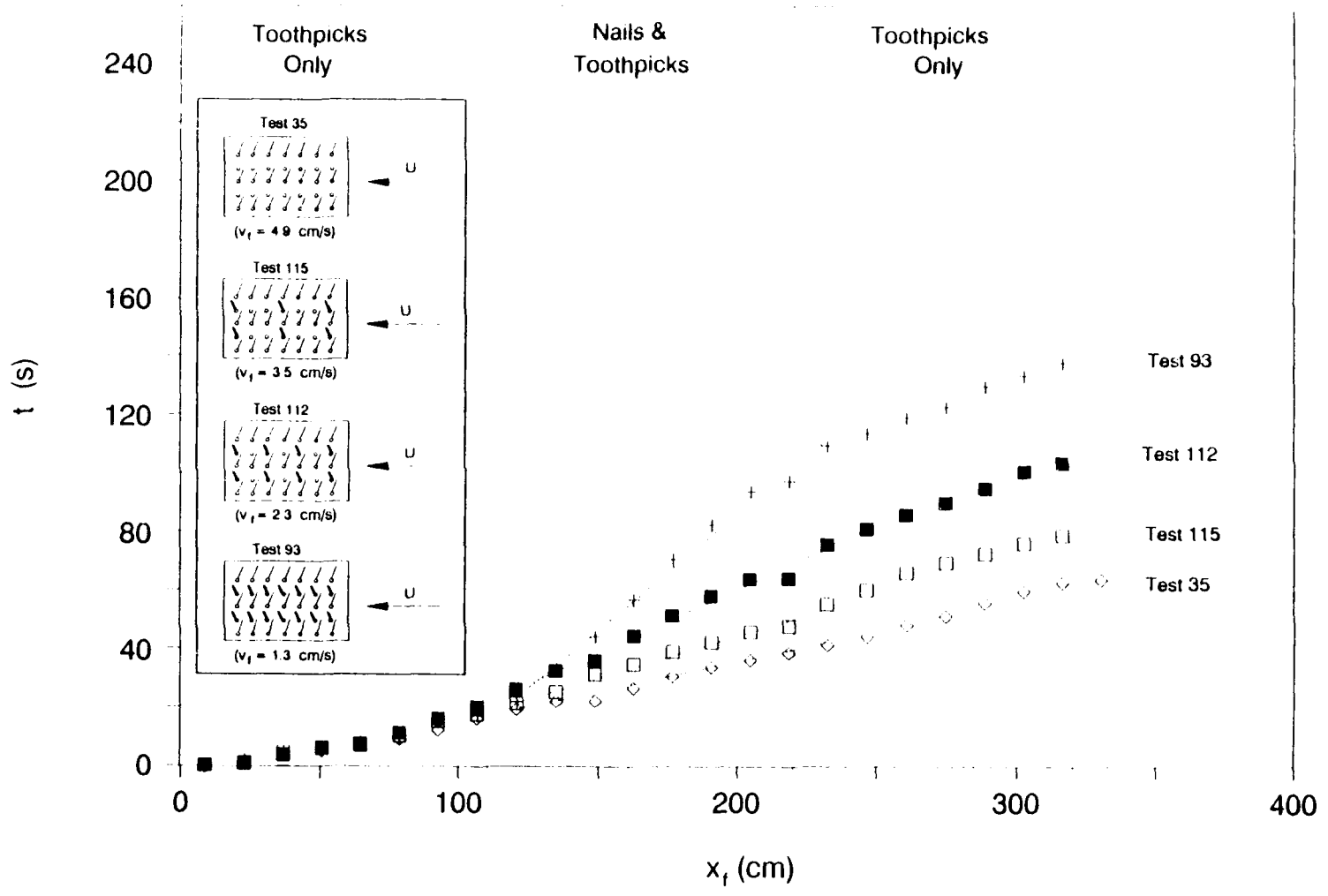

Figure 21. Same as Figure 19, except R takes on the successive values 0, 0.33, 0.50, and 1.0 (for the midspan only) for the four cases tested.

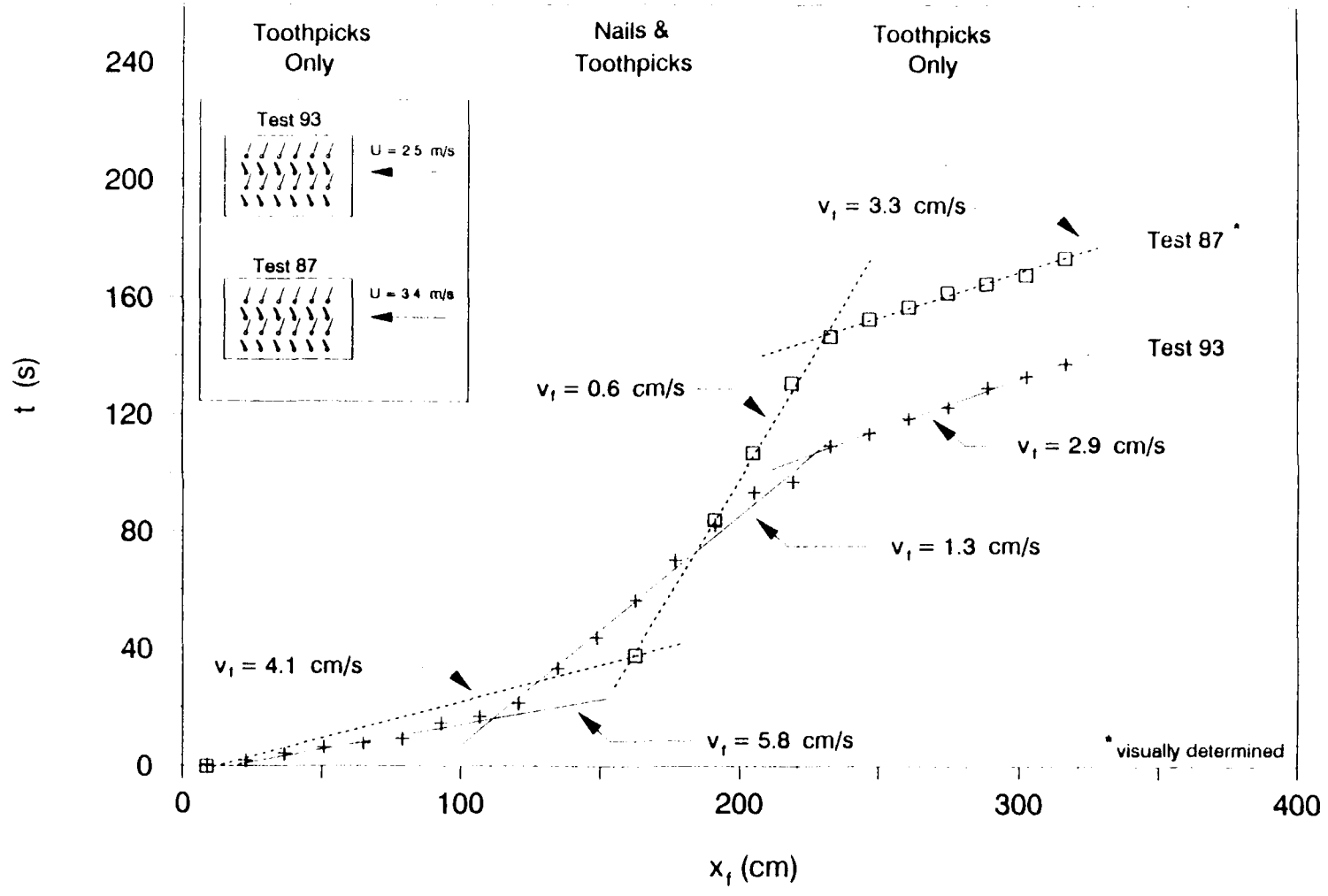

Figure 22. Same as Figure 19, but with R = 0.5 and with two values of the wind, U = 2.5 m/s and U = 3.4 m/s. For test 87 (see Table 2) the thermocouple-output-recording device failed, but the slow propagation speed permitted visual estimation of the firefront position.

aiding-wind speeds. This observation concerning the midsection behavior may be evidence of a so-called finite-Damkohler-number effect in firespread across discrete fuel elements, where Damkohler number is defined to be a dimensionless ratio of a characteristic reaction rate to a characteristic flame rate. If the Damkohler number is sufficiently small, the chemical reaction is extinguished ("chemically frozen" flow); if the Damkohler number is sufficiently large, the chemical reaction proceeds at chemical-equilibrium rates; at intermediate-Damkohler-number conditions, transport rates and reaction rates are competitive, and a faster flow implies a slower rate of chemical reaction. Upwind and downwind, presumably the Damkohler number was sufficiently large for the flow to be in chemical equilibrium, and the faster flow is responsible for a faster rate of spread under rate-of-preheating-controlled considerations. In the midsection the temperature is reduced owing to the presence of a heat sink (the nails), and the chemical-reaction rate typically decreases exponentially as the temperature is reduced; then, rather than being under preheating-mechanism control, the spread rate is under reaction-rate control, and an enhanced wind speed implies a reduced spread rate.

5.1.5 The Effect of Fuel-Element Height on the Rate of Firespread.

On the basis of the limited testing carried out in this program, only the general guidance is suggested that the effect of fuel-element height on the rate of firespread seems to be represented by the relation

$$v_f \sim \left(\frac{U}{m}\right)^{1/2} \left(\frac{H}{d}\right)^{p}, \quad 0.25 < p < 1.0. \tag{5.1}$$

Some plausibility for such a dependence is suggested by the results presented in Figure 23.

5.1.6 The Effect of Fuel-Element and Substratum Moisture on the Rate of Firespread.

If the water content exceeds very roughly 30% of the ovendry weight of toothpick-type fuel elements, liquid water tends to accumulate on the elements; for the time scales and exothermicity associated with firefront passage for the test conditions typical of Table 2, fire propagation tends

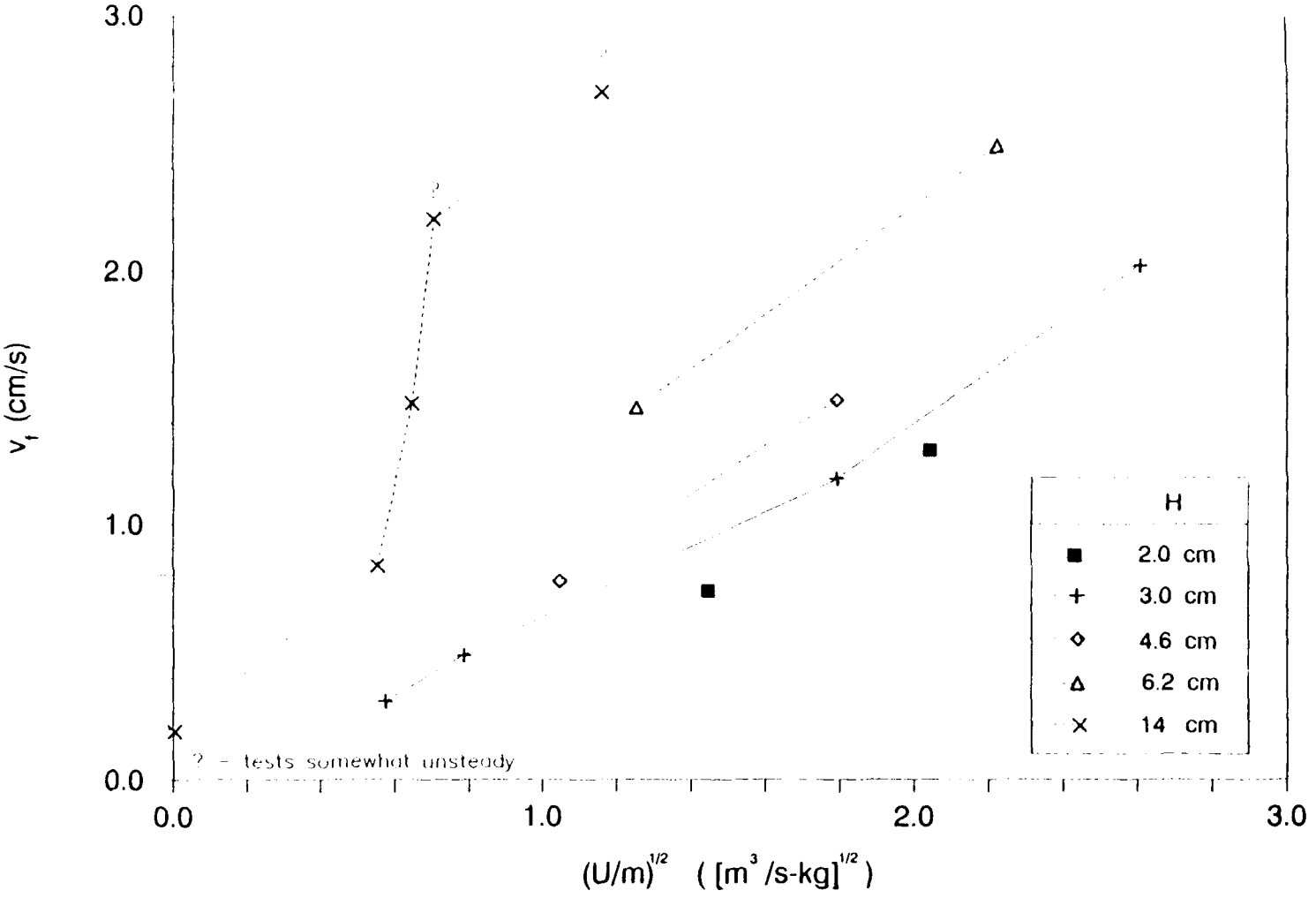

Figure 23. The rate of quasisteady firespread, v_f, as a function of the ratio (U/m), where U is the wind speed and m is the initial mass of fuel per unit planform area of the bed, for tests with birch 1-type fuel elements, 33 mm in diameter (see Table 1). The height H of fuel elements, uniform in any one test, is varied from test to test.

to be precluded. For water content below 30% or so, the rate of firespread is uncertain relative to the rate for the same test conditions for modest water content (say, 6-8% of ovendry weight) (Figures 24-25): a rigorous correlation of the amount of firespread-rate retardation with the amount of water content (up to the above-discussed level of crudely 30%) was not obtained in the limited number of tests dedicated to the phenomenon. A plausible explanation seems to involve the role of the (usually concomitant) moisture content of the substratum supporting the combustible fuel elements. Water tends to accumulate on and just below the surface of the porous ceramic, and the total amount of any such water content can readily exceed the total water content of the fuel elements (for the fuel loadings investigated in the testing). Thus, the retardation of the rate of firespread owing to moisture content of the substrate seems attributable to the reduction of the flame temperature T_f in (4.11).

Although the humidity of the air stream was not controlled in the testing, an effort was made to minimize the amount of pretest convective drying by rapid test initiation.

5.1.7 The Role of Substratum Composition on the Rate of Firespread.

The rate of firespread appears to be independent of the substrate composition, at least for the clay and ceramic materials tested (Figure 26). The ceramic had density of 425 kg/m^3, heat capacity of 1130 J/(kg K), and thermal conductivity of 0.080 W/(m K) at 447 K, 0.223 W/(m K) at 1255 K; the respective properties of a clay are 1750 kg/m^3, 1000 J/(kg K), and 0.585 W/(m K) at room temperature. Thus, at 1255 K, the square root of the conductance of the clay is but about three times that of the ceramic, and the two inert materials might be expected not to yield different results. However, we point out that retention of even residual liquid water by either material can lead to distinctly different firespread-rate results from those given in Figure 26.

5.1.8 The Effect of Mixed Fuel Elements on the Rate of Firespread.

Figure 27 juxtaposes results for fuel beds (1) with different fuel loadings of the same thin fuel elements; (2) with virtually equal fuel loadings constituted by fuel elements of different diameters, and (3) with equal fuel-element loadings but different inert-element content. It has

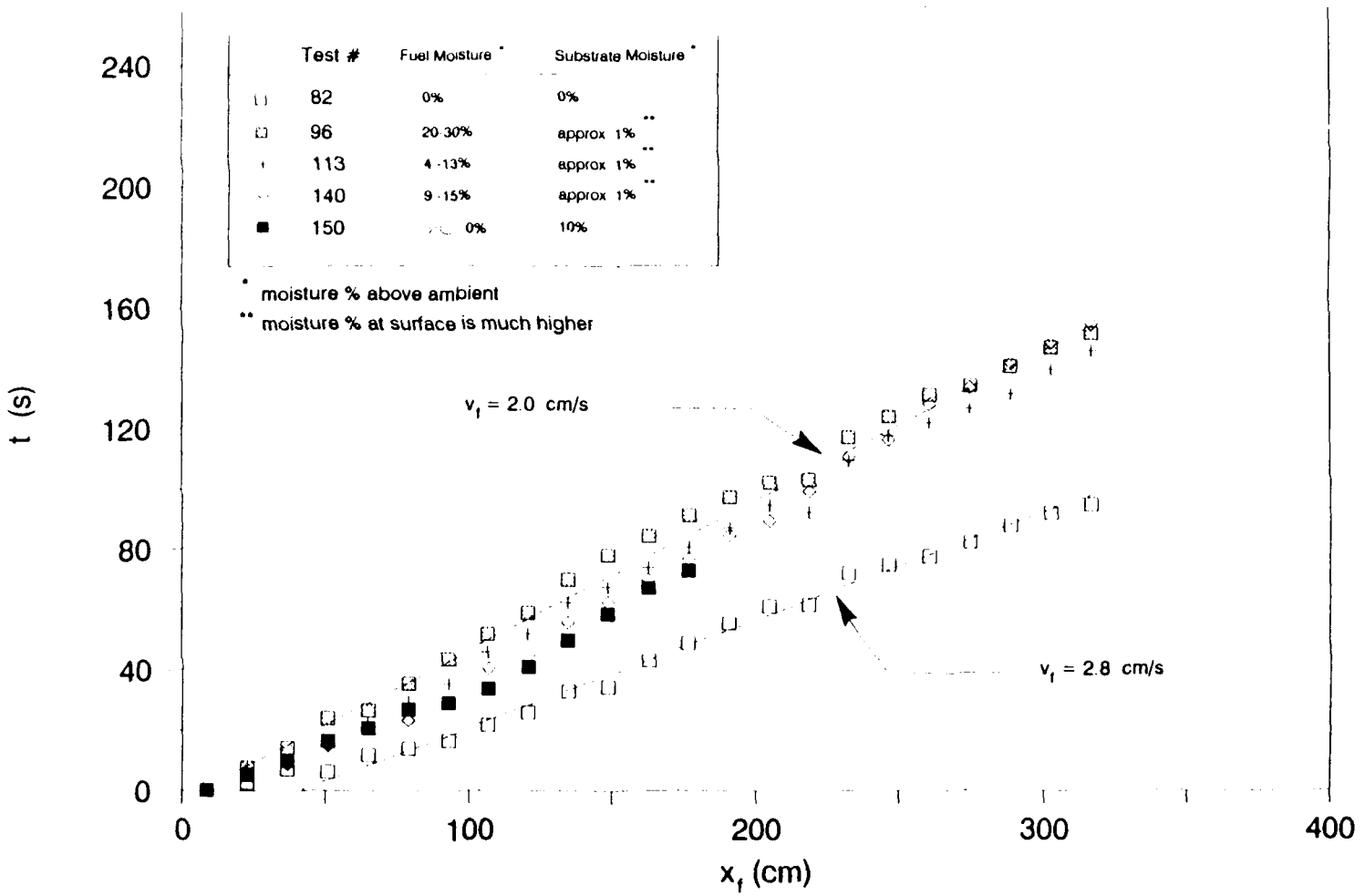

Figure 24. The streamwise centerline firefront position, x_f, as a function of time t since ignition of the upwindmost row of fuel elements at x = 0, for tests with 55-cm-wide beds of 4.6-cm-high white-pine toothpicks with pretest fuel loading of 0.044 g/cm^2, at a wind speed of 2.5 m/s. Further detail on test conditions is available from Table 2; the moisture enhancement is achieved by pretest confinement in a saturated environment.

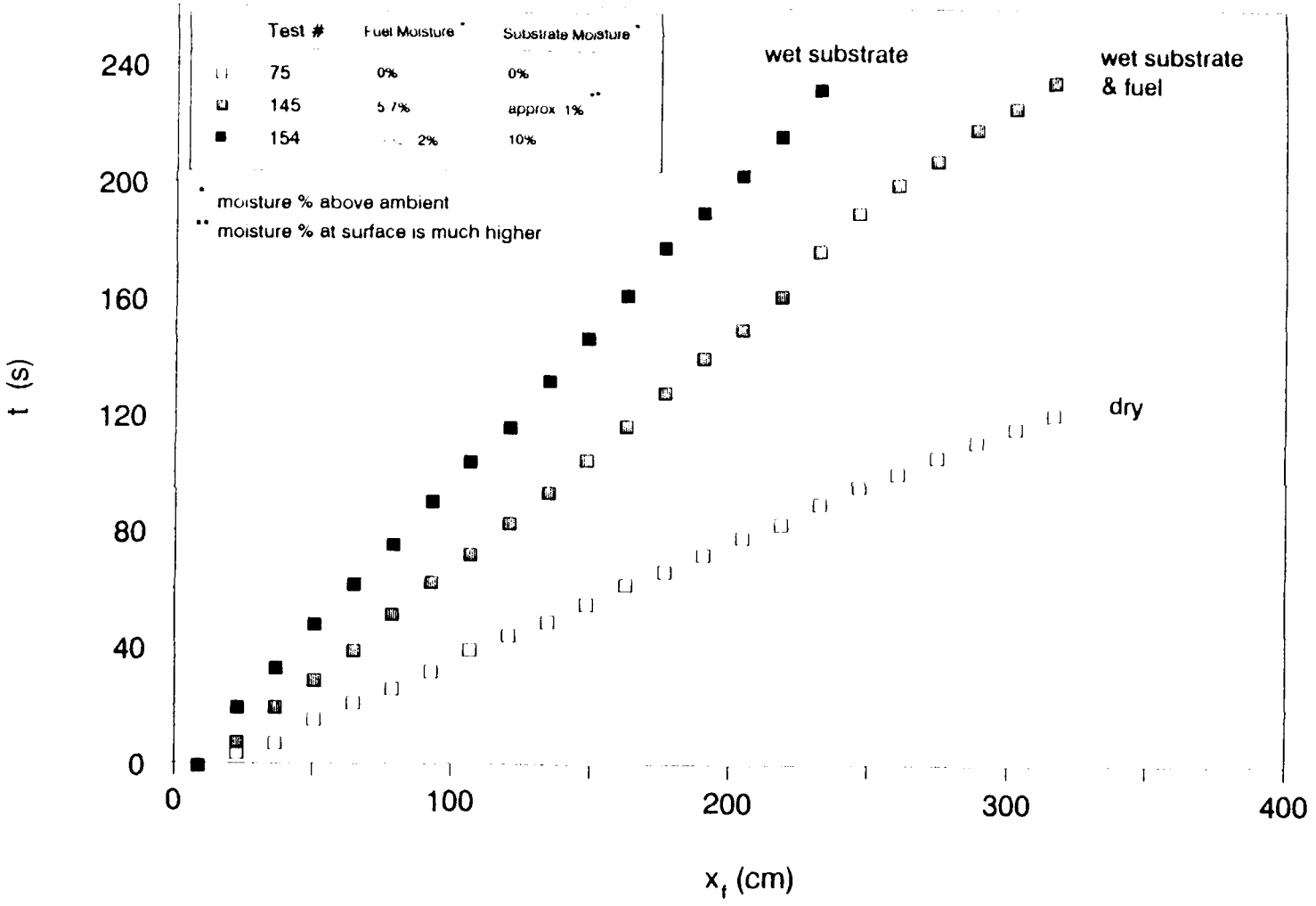

Figure 25. The same as Figure 24 but for tests at fuel loading of 0.022 g/cm^2 and for a wind speed of 1.0 m/s. Here a differentiation is undertaken of the retardation of the rate of firespread owing to substrate moisture from any retardation owing to fuel moisture content.

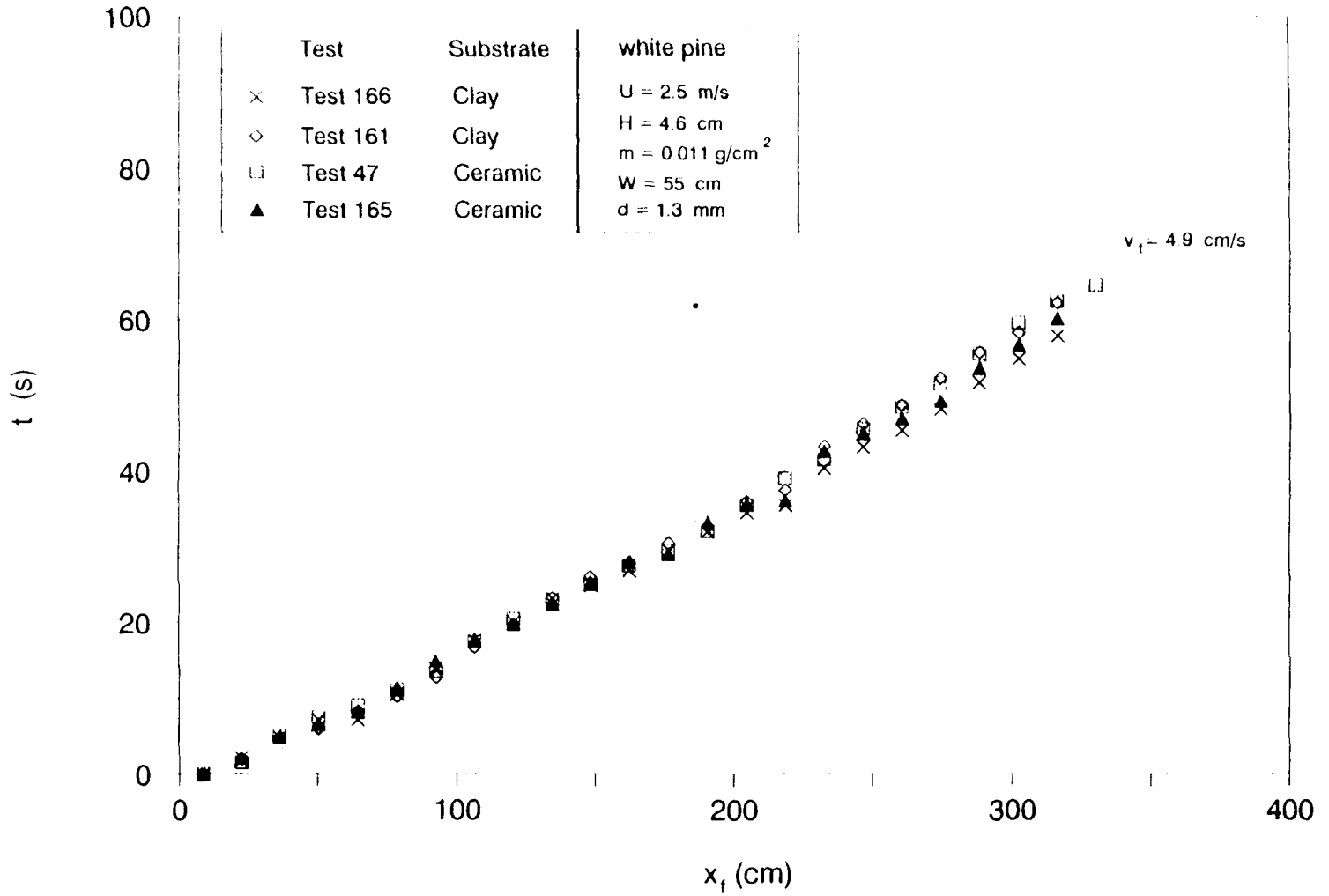

Figure 26. For tests with white-pine toothpicks at the cited wind speed U, fuel-element height H and effective diameter d, fuel-bed width W, and areal-averaged fuel loading m, the firefront position x_f is presented as a function of time t, for tests (see Table 2) with different substrate composition.

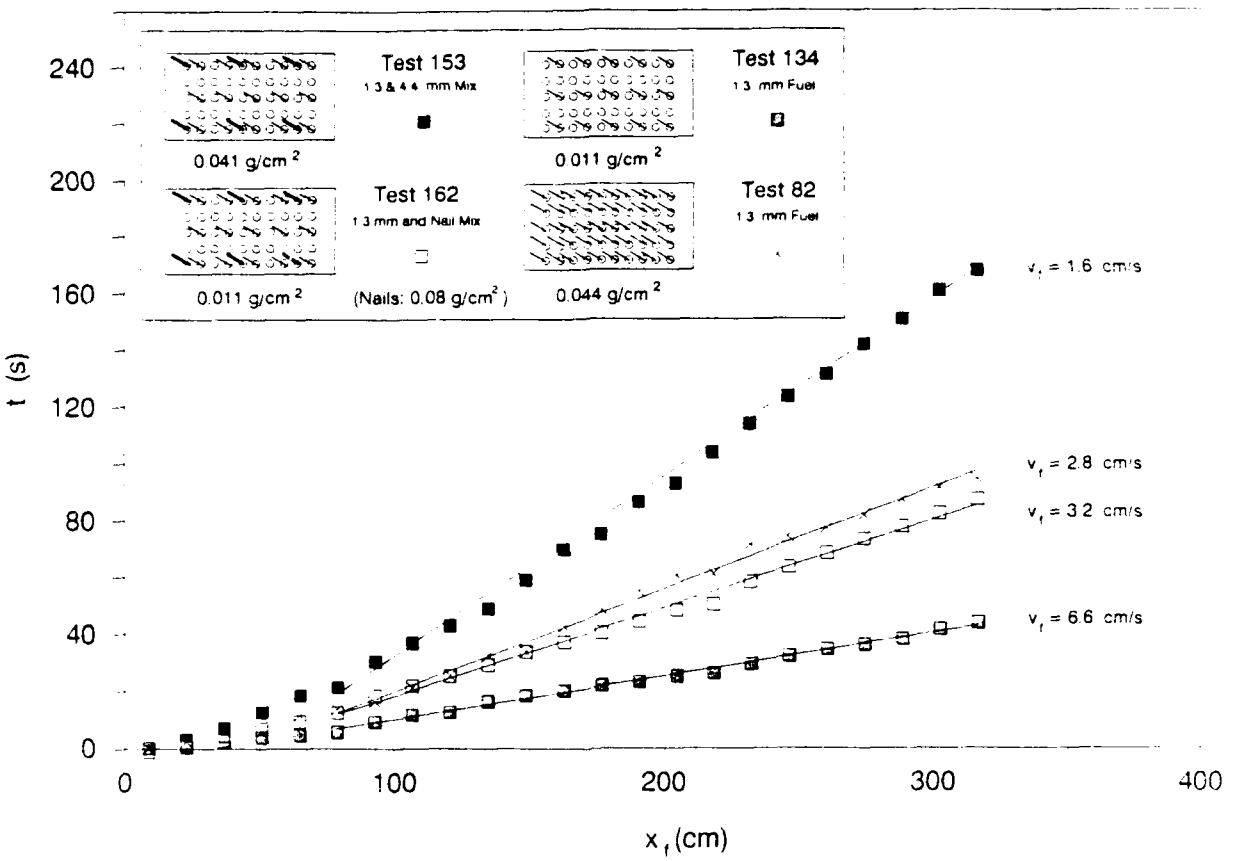

Figure 27. The firefront position x_f as a function of time t, for tests with a 55-cm-wide bed composed of 4.6-cm-high elements under a wind of 2.5 m/s. In the inset, an empty circle designates an empty hole drilled in the ceramic substrate; a dark mark signifies a hole occupied by a 4.4-mm-diameter birch dowel; and a light mark signifies a hole occupied by a 1.3-mm-diameter white-pine toothpick. The only exception is for test 162, in which a dark mark signifies a hole occupied by a common nail. The loadings under the sketches refer to the combustible elements only.

already been noted that inert elements serve as a wind obstruction and retard the rate of firespread that would occur in their absence. It also has already been established that a greater loading of the same type of thin-fuel element retards the rate of firespread. However, Figure 27 contributes the additional insight that if a substantial fraction of the fuel mass is constituted by thicker fuel elements, even if those elements burn to completion with the thinner ones during firefront passage, the rate of firespread is significantly retarded. The proportionality factor in the relation $v_f \sim (U/m)^{1/2}$ is altered by this change in fuel-element properties.

Whereas elements of diameter 3.4 times those of the thinner elements burned simultaneously with the thinner ones under a wind speed of 2.5 m/s (test 153, presented in Figure 27), at a higher wind speed of 4.6 m/s the thicker, 4.4-mm-diameter birch II elements did not burn as the firefront propagated through (and fully consumed) the 1.3-mm-diameter, white-pine-type toothpicks (test 179). In test 179, the thicker elements either burned slowly to completion well upwind of the firefront, or did not burn much at all. The fuel loading was 0.041 g/cm^2 just as in test 153; in fact, the loading in test 179 was exactly as in test 153 except that all the thin thoothpicks were moved to one column (that had every hole occupied) and only a few thicker dowels populated the parallel occupied column--between these two (at least partly occupied) columns was left an entirely empty, parallel column, just as in test 153. Thus, in the testing, at least one condition was defined at which the firefront propagation entailed the thinner elements only, in a fuel bed with multidiameter elements.

5.2 COMPARISON WITH OTHER EXPERIMENTAL DATA.

5.2.1 Summary of Results from the Present Testing.

It seems useful to recall that in the present investigation testing with previously described flat-sided white-pine 4.6-cm-high toothpicks was carried out primarily for beds of 55-cm width. The wind speed U was varied mostly from 0.0 to 4.6 m/s, and the loading was varied from 0.11 to 0.88 kg/m^2; hence, (U/m) varied from 0.00 to 41.7 m^3/(kg s), and 0.0 cm/s $\leq v_f \leq$ 6.9 cm/s. Least-squares curve fitting of the data (Figure 28) gives, if σ is the standard deviation, with v_f in cm/s,

$$v_f = 1.13\ (U/m)^{1/2},\ \sigma = 0.42\ \text{cm/s}. \tag{5.9}$$

Thus, a model with convective preheating of a finite-thermal-conductivity fuel bed seems compatible with the data.

5.2.2 The Nelson-Adkins Data.

Nelson and Adkins (1986, p. 1296, table 1) present flamespread data (Figure 29) taken for fire propagation across fresh slash-pine needles set in a tray 0.91 m in width and 4.88 m in length, after conditioning to a moisture content of 11% (ovendry basis); the dry fuel loading averaged 0.54 kg/m^2, and the layer thickness of moist needles was estimated to be 2.5 cm. The wind-tunnel test section was 21.3 m in length with a 2.44 x 2.44-m cross section. The fuel bed was placed in the tunnel with the fuel surface approximately 20 cm above the floor and with its long dimension parallel to the direction of flow. A quasisteady state was achieved usually within a quarter to a half of the total test time.

Nelson and Adkins (1988) suggest that, in the present notation,

$$v_f = 0.39\ m^{0.25}\ U^{1.50}/t_r, \tag{5.10}$$

where t_r is a flame-residence time in seconds, v_f is in m/s, m is in kg/m^2, and U is in m/s; this empirical fit is taken to describe a wide range of laboratory (and field) data. Since the residence time t_r itself depends on

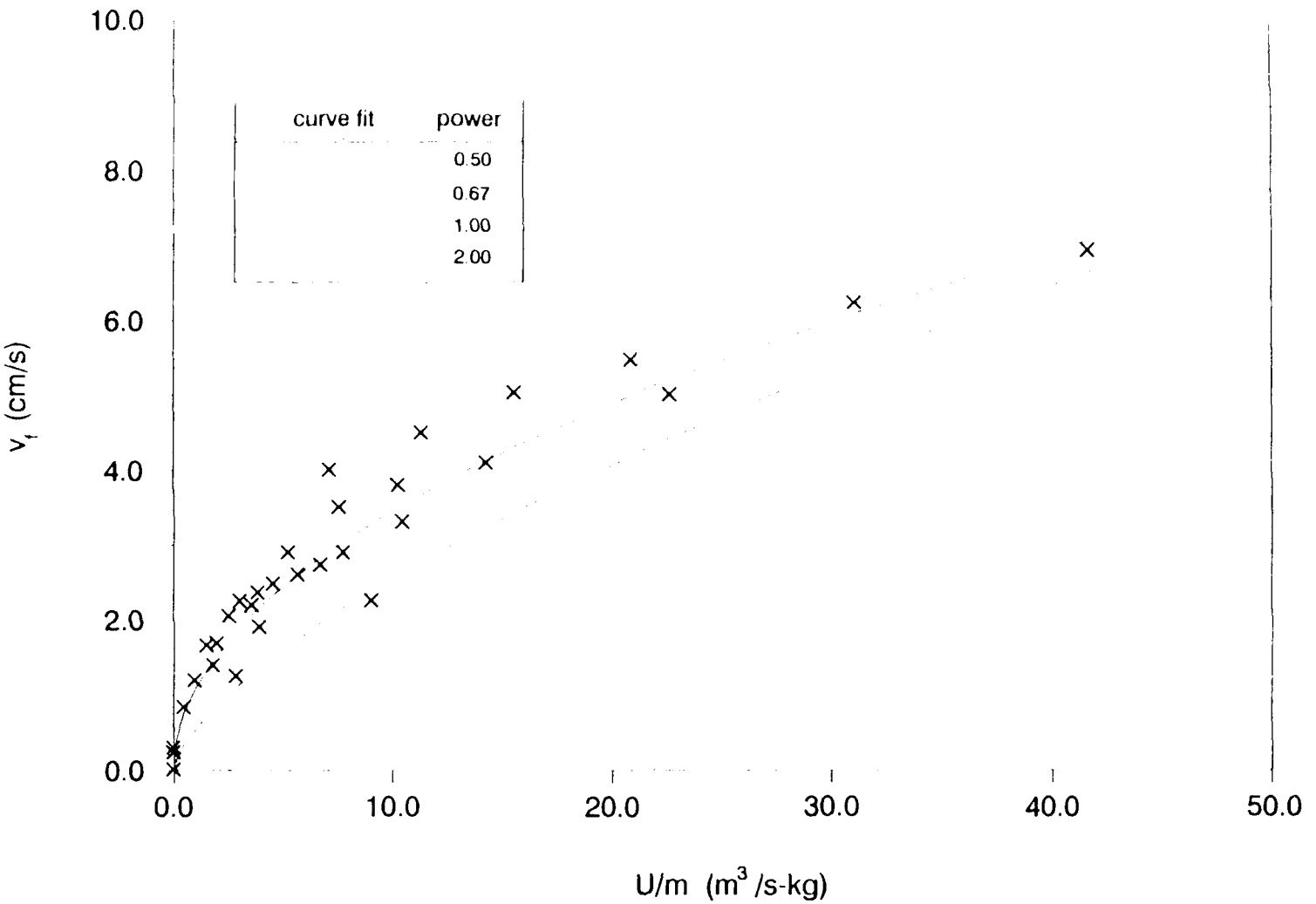

Figure 28. For data obtained in the TRW firetunnel for a 55-cm-wide bed of 4.6-cm-high white-pine toothpicks, the firespread rate v_f is presented as a function of the ratio of the wind speed U to the fuel loading m. Several power-law curve fits are also plotted.

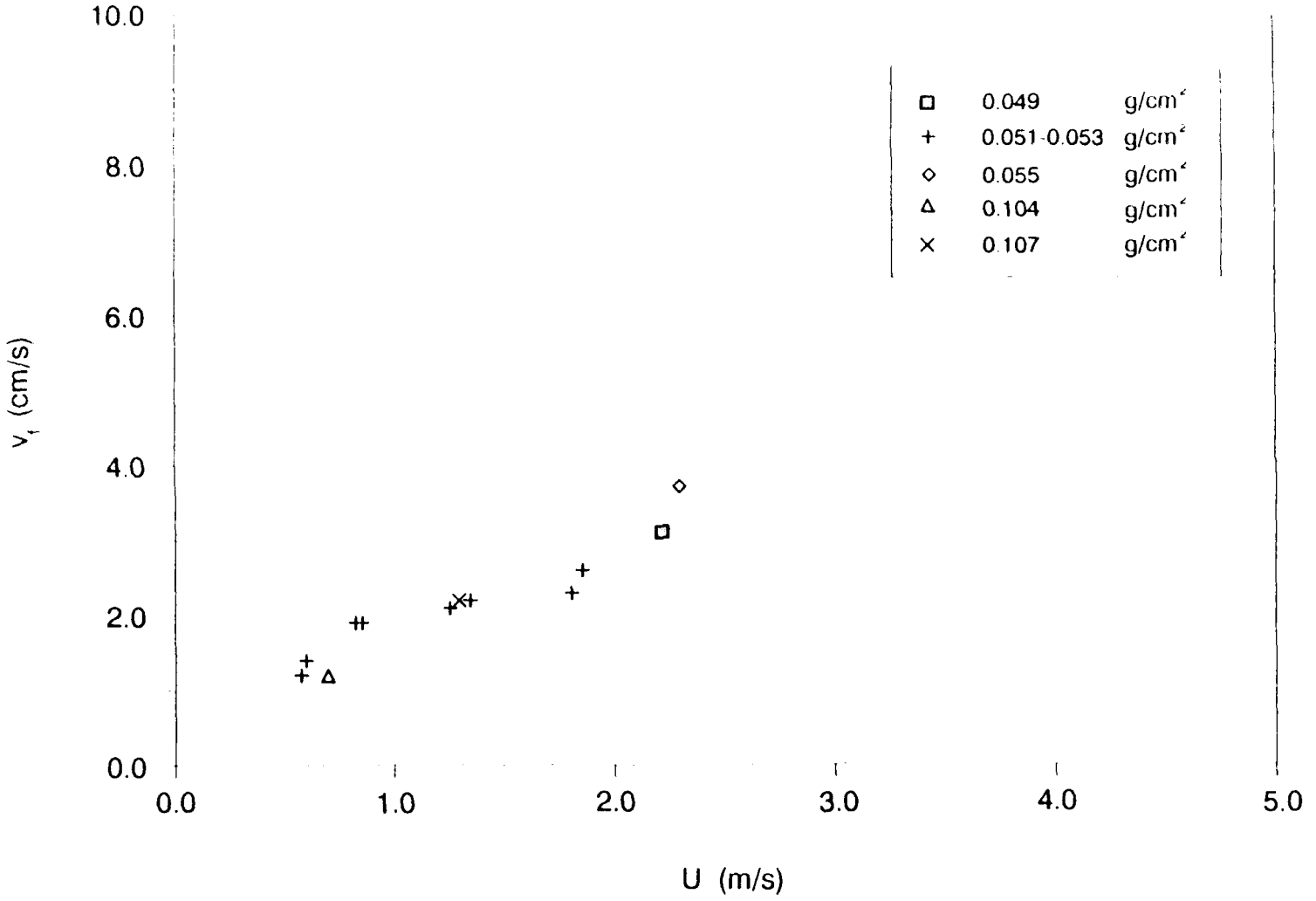

Figure 29. For the data of Nelson and Adkins (1986) for a 6.4-cm-high, 91-cm-wide bed of dry slash-pine needles, the firespread rate v_f is plotted against the wind speed U, for several values of the loading m.

m, U, and possibly other parameters in an unidentified way, the fit is of limited utility in its present form; an expression more tied to quantities measurable prior to the test is preferred here, although admittedly for mixed-size-fuel beds the fraction of the total fuel loading burned during firefront passage is unknown prior to test execution. While a least-squares fit to the twelve cases reported by Nelson and Adkins gives

$$v_f = 1.7 \frac{U^{0.17}}{m^{0.39}} \tag{5.11}$$

with a standard deviation of 0.66 cm/s, where v_f is in cm/s, U is in m/s, and m is in kg/m^2, more generally it appears that the data of Nelson and Adkins are obtained from experiments in which convective preheating is a reasonable inference (Figure 30). In these data, m varies from 0.49 to 1.07 kg/m^2, while U varies from 0.2 to 2.3 m/s, so (U/m) varies (fairly modestly) from 0.45 to 4.19 m^3/(kg/s). The observed flame speed varied from 1.2 to 3.7 cm/s.

5.2.3 The Fons Data.

Fons (1949 p. 112, table 1) tabulates experimental data (Figure 31) for 49 tests with vertically oriented, equally spaced, uniform twigs of ponderosa pine, about 19 cm in height and either 0.15, 0.30, or 0.45 cm in diameter. The bed was 3.6 m in length and quasisteady propagation was taken to have been achieved after propagation of 1.2 m along the bed. Wind speed U was varied from 1.8 to 3.6 m/s, and fuel loading was varied from 0.33 to 1.27 kg/m^2, so that (U/m) was varied from 2.03 to 10.7 m^3/(kg s) and the observed flame speed from 1.3 to 5.2 cm/s. One finds that, if σ is the standard deviation, curve fitting to a prescribed power via a least-squares criterion gives

$$v_f = 0.92\ (U/m)^{2/3},\ \sigma = 0.56 \text{ cm/s}. \tag{5.12}$$

Here again U is in m/s, v_f is in cm/s, and m is in kg/m^2. From Figure 32, plausibly, the mode of preheating in Fons's twig-fire experiments is

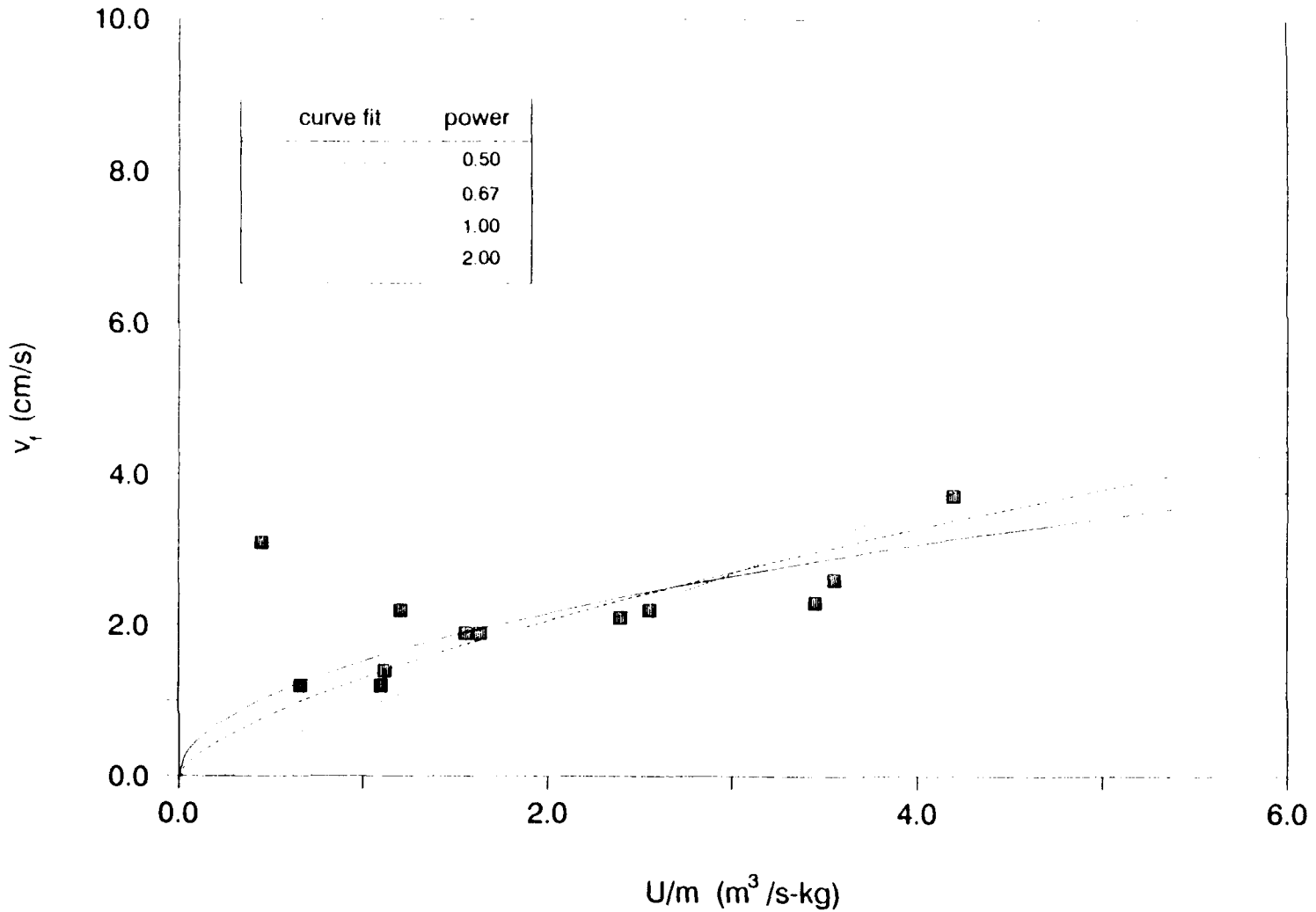

Figure 30. A replotting of the Nelson-Adkins data of Figure 29, with the firespread rate v_f presented as a function of the ratio of the wind speed U to the fuel loading m. Several power-law curve fits are plotted as well.

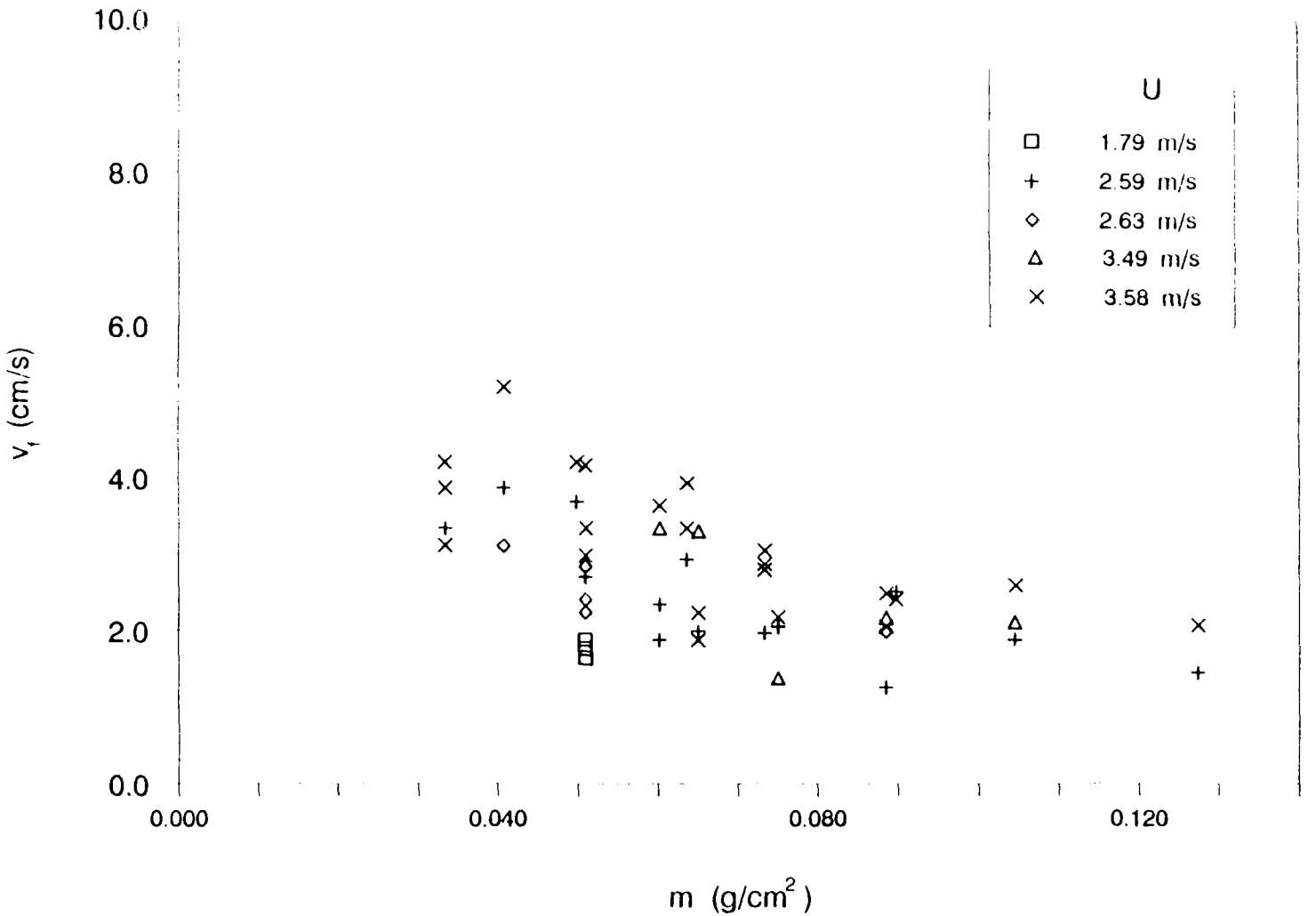

Figure 31. For the data of Fons (1946) for a 91-cm-wide bed of 19-cm-high ponderosa-pine twigs, the firepsread rate v_f is plotted against the fuel loading m, for several values of the wind speed U.

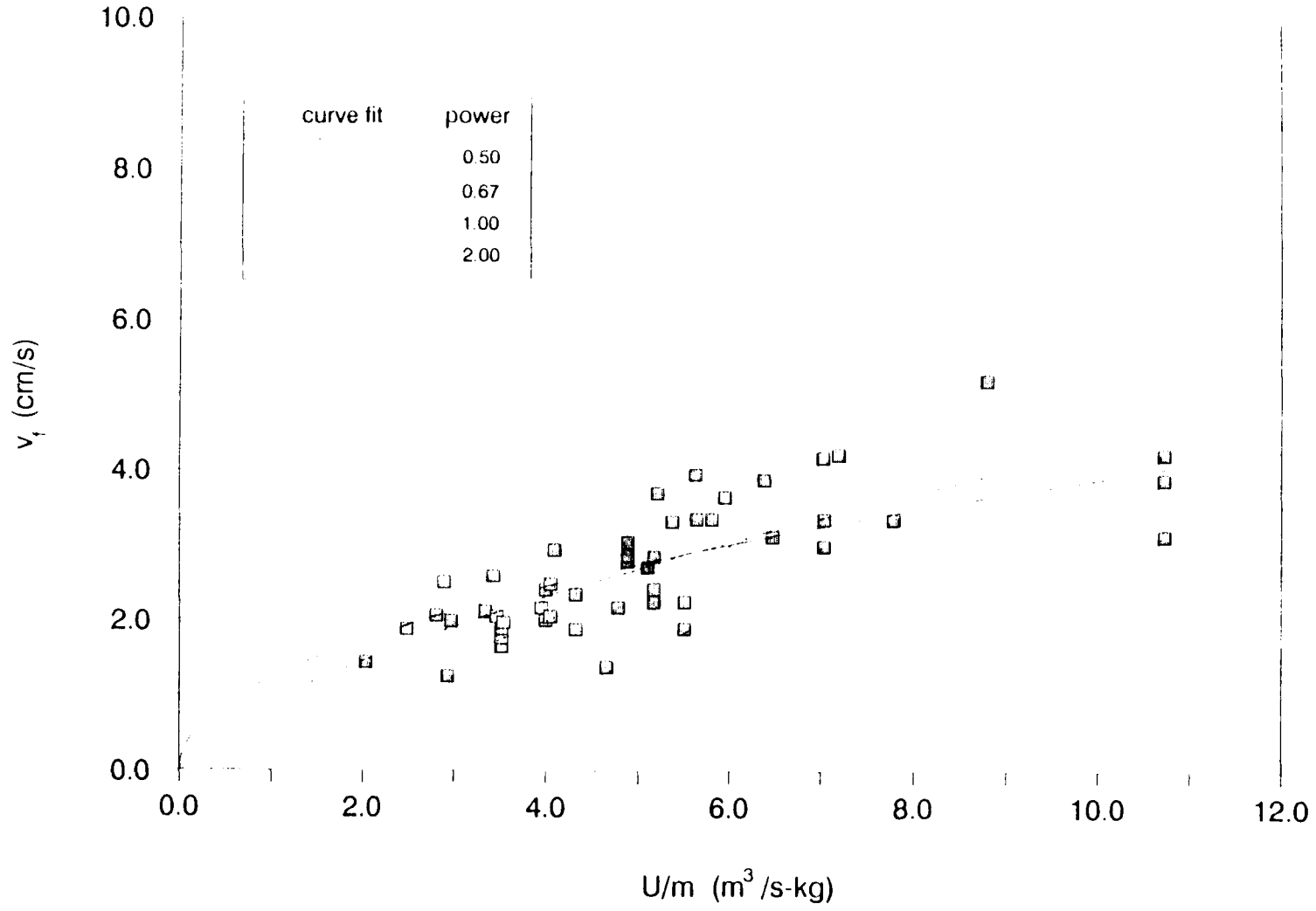

Figure 32. A replotting of the Fons data of Figure 31, with the firespread rate v_f presented as a function of the ratio of the wind speed U to the fuel loading m. Several power-law curve fits are plotted as well.

convection, and the finite-thermal-conductivity model (with nonuniform temperature in the fuel bed) may be particularly suitable.

5.2.4 The Steward Match-Splint and Wood-Shavings Data.

Steward (1974b, table 4) reports a dozen tests (Figure 33) with prone poplar match splints in a fuel bed with 0.81 voidage and either 6.5% or 8.3% (ambient) moisture content. The fuel beds were 1.8 m in length and 0.4 m in width. These dimensions seem somewhat limited for ensuring that a steady rate of propagation is achieved. The fuel loading m was fixed at 2.15 kg/m^2 in all tests, while the wind speed U was varied from 0.6 to 3.5 m/s, so that (U/m) was varied but from 0.28 to 1.63 m^3/(kg s). It may be noted that the fuel loading is well above the peak values used by either Fons or Nelson and Adkins in experiments discussed above. One finds from least-squares fitting that $v_f \sim U^{1.32}$ serves well, but the absence of any variation of the fuel loading limits the drawing of strong conclusions. Tests with poplar wood shavings (0.92 voidage) gives $v_f \sim U^{0.81}$ (Figure 33); in these tests, $0 < (U/m) < 3.75$ m^3/(kg s).

5.2.5 The Steward-Tennankore Birch-Dowel Data.

Vertically oriented, circular-cross-section birch dowels, arranged in a uniform matrix via holes drilled in a steel plate and having about 5% (ambient) moisture content, were burned in a wind tunnel 1.22 m in width and 1.19 m in height and 7.1 m in length (Steward and Tennankore 1979, figure 10).

Thirteen experiments (Figure 34) were carried out with 2.5-mm-diameter, 67-mm-long dowels with center-to-center distance of 25.4 mm. The wind speed U varied from 0.4 to 3.5 m/s, with the fuel loading held fixed at 0.21 kg/m^2. One finds from least-squares fitting that $v_f \sim U$ serves fairly well, but again the absence of any variation of the fuel loading limits the drawing of strong conclusions.

Twelve experiments were carried out with 2.5-mm-diameter dowels with 25.4-mm-separated centers, but with the dowel length slightly more than doubled (to 140 mm) (Figure 34). The wind speed was varied from 0.31 to 2.28 m/s, with the fuel loading held fixed at 0.437 kg/m^2. One finds that roughly $v_f \sim U^{3/2}$, but again it is difficult to draw strong conclusions.

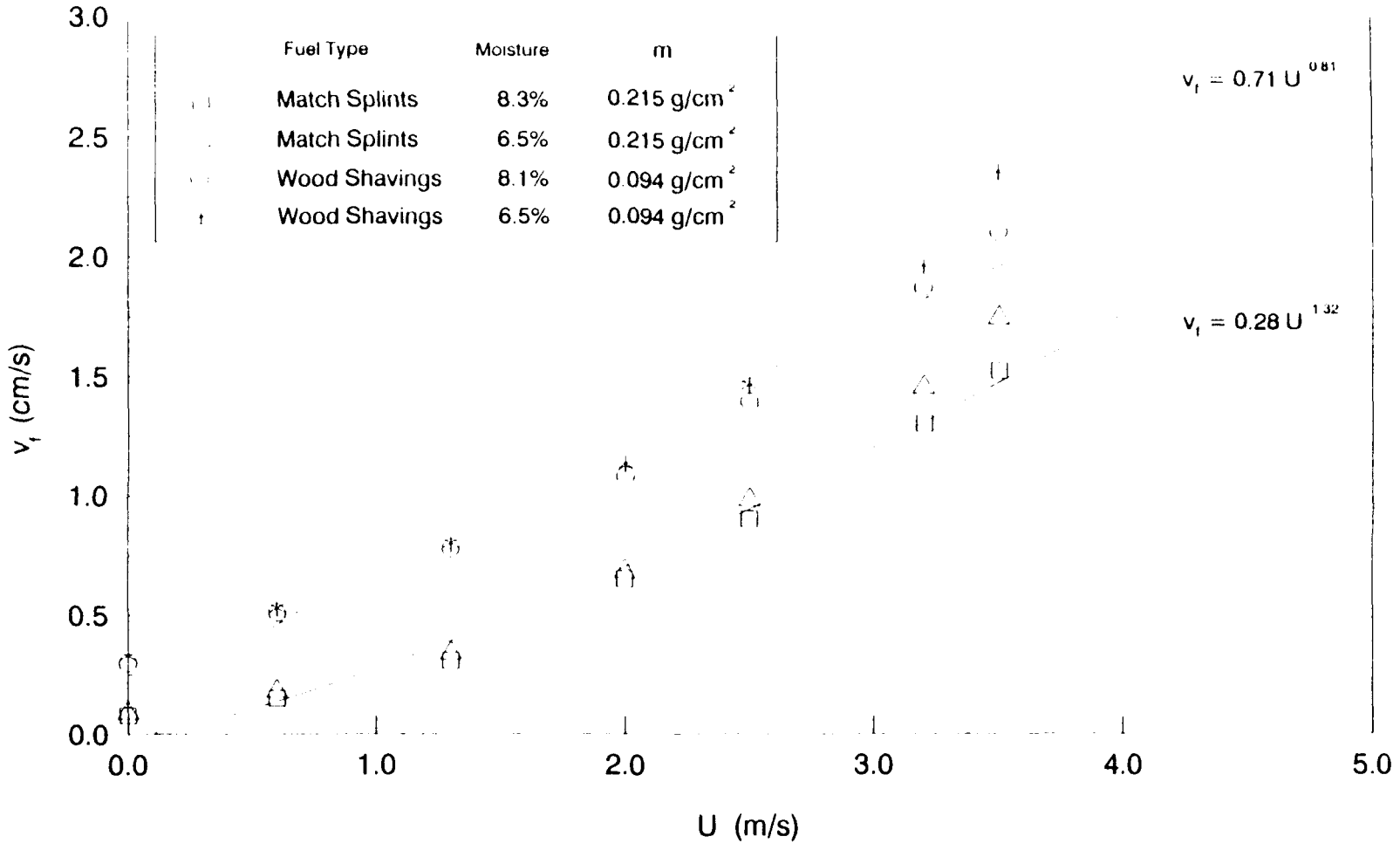

Figure 33. For the Steward (1974b) data for a 41-cm-wide, 4.3-cm-high bed of prone poplar match splints, the firespread rate v_f is plotted against the wind speed U. The fuel loading is constant for all tests at 0.215 g/cm^2 [computed on the basis of a somewhat small value for the wood density, 0.41 g/cm^3--for assignment of a different wood density ρ_S (in g/cm^3), the loading m is given by $(\rho_S/0.41)$ (0.215) g/cm^2]. Also shown are spread rates for beds of poplar wood shavings.

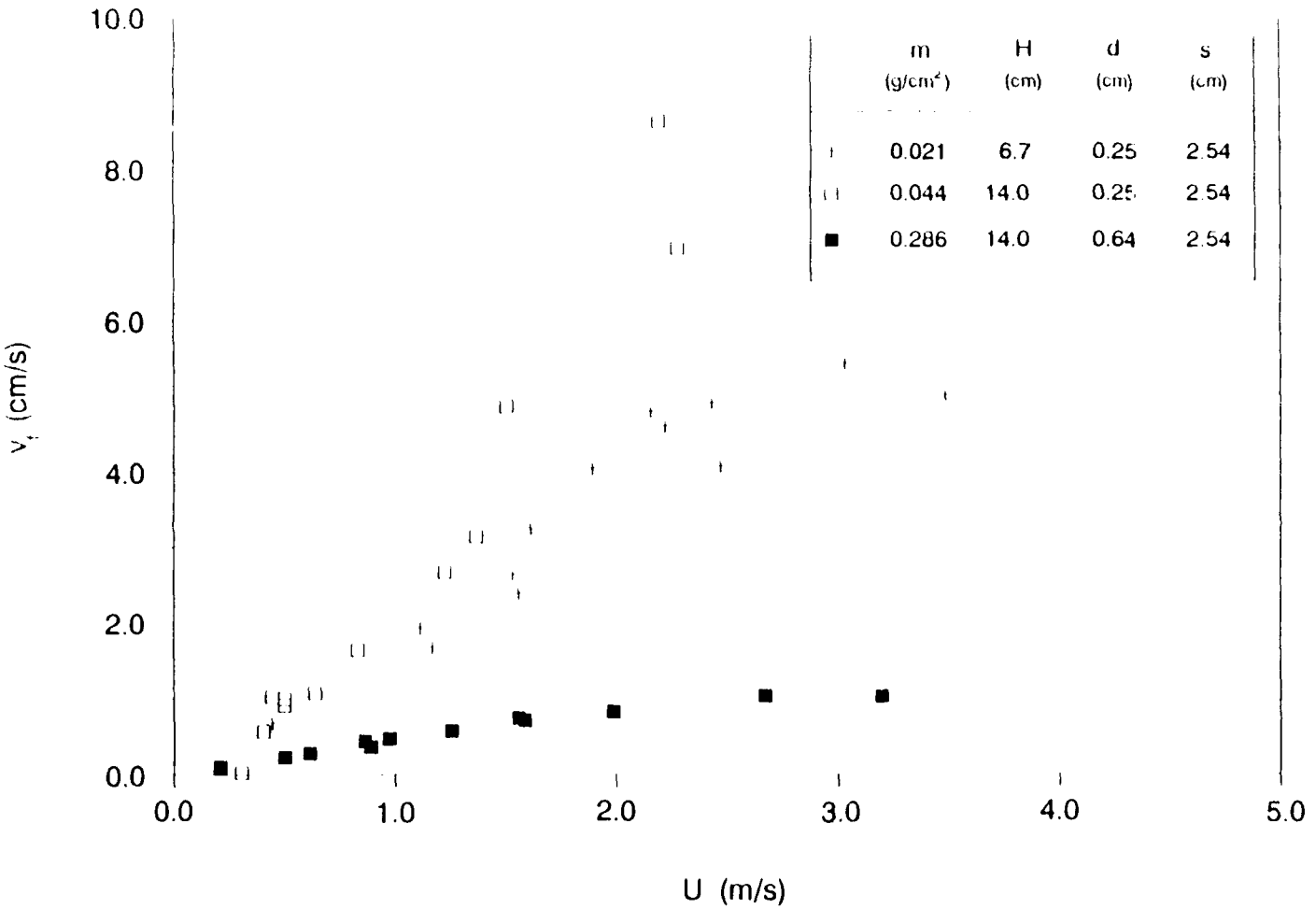

Figure 34. For the data of Steward and Tennankore (1979) for birch dowels spaced at 2.54-cm intervals in a bed of 35-cm-or-greater width, the firespread rate v_f is plotted against the wind speed U. In these data, the fuel loading m is held fixed as the wind speed is varied, for each of three types of dowels (of variable height H and/or diameter d). For dowel-center-to-dowel-center spacing s, for a checker board arrangement, the loading m is calculated on the basis of a somewhat small value for the wood density, 0.41 g/cm^3; for assignment of a different wood density ρ_s (in g/cm^3), the revised value of the loading is given by the product of (ρ_s/0.41) times the values of m appearing in the inset of the figure.

Twelve experiments were carried out (Figure 34) with 6.4-mm-diameter, 140-mm-high birch dowels on 25.4-mm-separated centers, such that the fuel loading was increased to 2.86 kg/m^2. The wind speed U varied from 0.21 to 3.2 m/s, with the fuel loading fixed at the relatively large value of 2.86 kg/m^2. One finds that roughly $v_f \sim U^{2/3}$, but the previously stated reservation is again cited.

If attention is limited to experiments with 2.5-mm-diameter dowels, in addition to the previously discussed dozen cases with 140-mm length and 25.4-mm separation and the previously discussed dozen cases with 67-mm length and 25.4-mm separation, Steward and Tennankore also present four cases with 67-mm length at 12.8-mm separation and one case with 140-mm length and 12.8-mm separation. One finds from Gauss-Markov iterative fitting that, if H denotes fuel-element length, $v_f \sim H$.

5.2.6 The Thomas Field-Burn Data.

The applicability of the laboratory-test results obtained here to wind-aided-firespread rates in the field requires an extensive experimental program. As a preliminary step, Thomas (1971, p. 159, table 1) presents data from nine head fires in heather and gorse; Thomas himself suggests, in present notation, that $v_f \sim (1 + U)/\rho_b$. Since $\rho_b = \rho_s(1 - \phi)$, and Thomas presents the fuel-bed height H, by (3.1) we are able to replot his results (Figure 35) in the form $v_f = C(U/m)^{1/2}$, in which the proportionality factor C appears to take on different values for tests with gorse and heather, values somewhat larger than that given in (5.9) for the present laboratory tests. Two very marginally propagating fires, for which only estimated input values are available and for which relights were necessary, deviate from the fits.

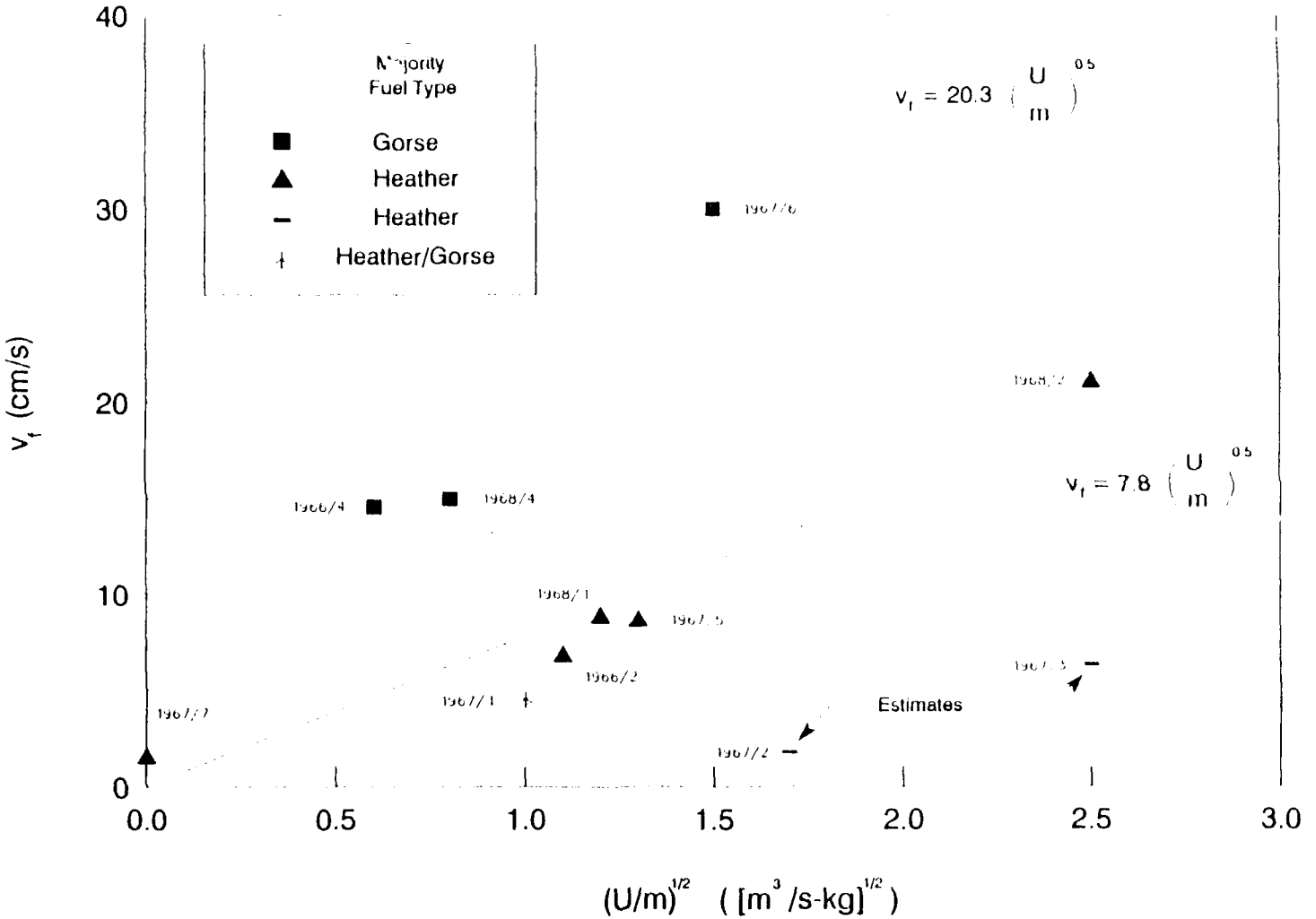

Figure 35. A replotting of the field-test results tabulated by Thomas (1971) for the rate v_f of firespread across gorse and heather beds for which the burned-fuel loading was m and the aiding wind was U. The year/case designation of each data point is that of Thomas. Two tests with marginal propagation and requiring relights are segregated from the other cases.

SECTION 6

FUTURE DIRECTIONS

About 195 tests of wind-aided firespread across regular two-dimensional arrays of vertically oriented thin fuel elements have been conducted. The primary output reported from these experiments is the rate of firespread v_f, under quasisteady conditions, as a function of key input parameters, such as the wind speed U and the fuel loading m. The thickness (streamwise depth) of the burning zone d_t is the product of the spread rate v_f and the duration of burning of a single fuel element t_{burn}. But observationally (for the parametric values investigated to date), for thin fuel elements, v_f varies directly with the square root of the wind speed and inversely as the thickness of an individual fuel element, and t_{burn} varies as the three-halves power of the thickness, independently of the wind speed (Steward and Tennankore 1981). The upshot is that the burning-zone thickness $d_t \sim (Ud)^{1/2}$. For quasisteady spread, it is recalled that we require a burned-out upwind expanse and a still-unburned downwind expanse, between which is sandwiched a flaming front that is observed to propagate at a constant speed. For a range of wind speeds of practical interest, we have found that an approximately 6-m-long test section affords a propagating, burning zone of finite width within the facility if the thickness of an individual fuel element does not exceed about 4 mm or so. For a test section (say) six times greater in length, one ought to be able to accommodate a burning-front thickness six times as great, and still be able to confirm a quasisteady rate of firespread. The above relation suggests that a bed of fuel elements, each of which is 36 times as thick, or about 15 cm in diameter, might be burned informatively in a firespread facility of the enhanced length. A somewhat different dependence of t_{burn} on fuel-element thickness is inferred from the current experiments (Figure 36). Specifically, the time of burn, t_{burn}, is found to vary as the loading m, and hence as d^2, so $d_t \sim U^{1/2}\, d$. Hence, a test section six times as long might permit investigation of quasisteady fire propagation across beds of fuel elements only six times as thick, or only about 2.4 cm in diameter. In fact, one can replot (Figure 37) the results of Steward and Tennankore (1981) themselves, and those of Fang (1969), to obtain

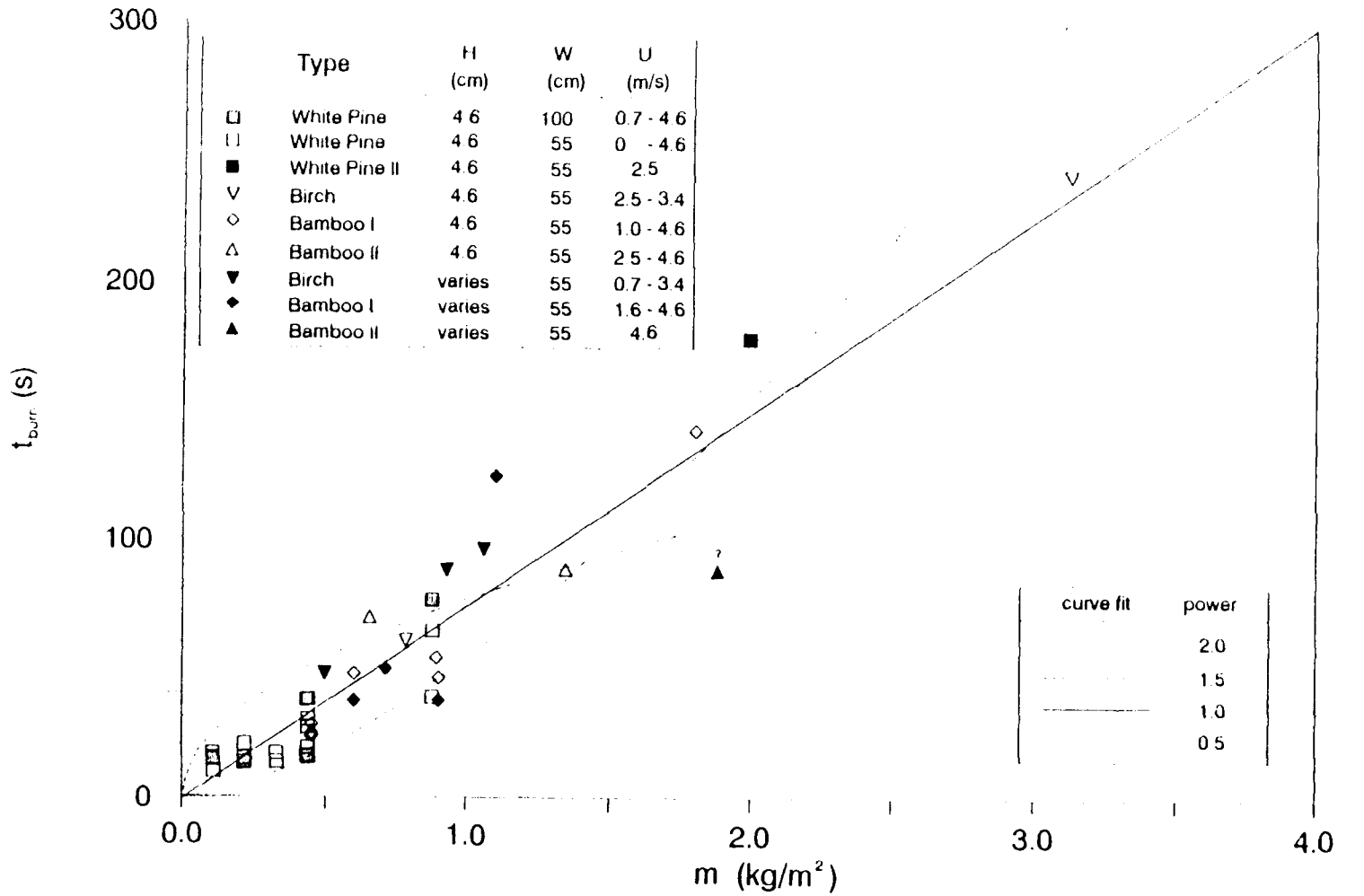

Figure 36. From results of the current testing, the duration of the fuel-element burning time, t_{burn}, as a function of the fuel loading m, during quasisteady firespread, for a variety of test conditions, where H is the fuel-element height, W is the bed width, and U is the speed of the spread-aiding ambient wind. The interval t_{burn} is taken to be the temporal span over which the thermocouples, situated near the fuel-bed surface on the streamwise centerline, record readings in excess of about 500 K. The quantity $t_{burn} \sim m^p \sim d^{2p}$, where d is the effective fuel-element diameter and, apparently, $1 < p < (3/2)$.

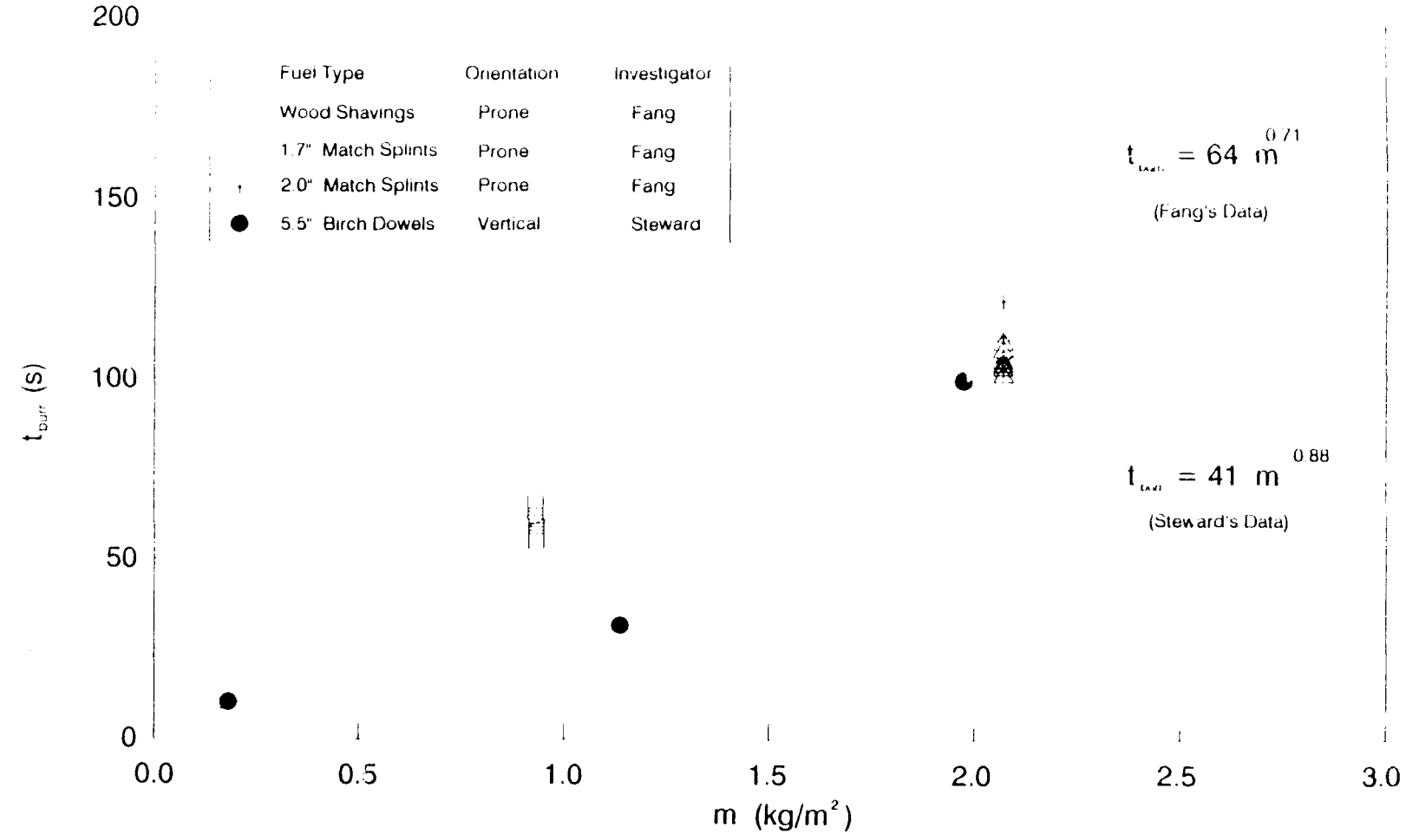

Figure 37. Results calculated from data on the time for (wind-aided) burn, t_{burn}, as a function of the fuel loading m for beds of prone poplar matchsplints and of poplar wood shavings; t_{burn} is defined here as the time in which "a fuel particle is submerged in the flames [as measured by] the time taken between the rise and the drop of the output signal of a thermocouple" (Fang 1969, p. 61). Results are also calculated from data for t_{burn} for an array of upright birch dowels by Steward and Tennankore (1981); t_{burn} is then defined to be the time over which the weight of a dowel decreases from 80% to 20% of its pretest value, during a wind-aided burn. The quantity t_{burn} is effectively invariant to the wind U over the range tested.

approximately, $t_{burn} \sim m$. Thus, the alternative, conservative estimate of the fuel-element thickness compatible with achieving a quasisteady spread in the lengthened chamber may be the more plausible estimate.

In any case, a direction for future research on firespread might concern thicker, more isolated fuel elements; as one motivation, such elements characterize the less-blast-damaged scenario holding at lateral distances further from the hypocenter in a thermonuclear aftermath. However, the above facility of enhanced length is not proposed here as a high-priority future direction for the discrete-element-firespread research. The reservation is that if one proceeds over a sequence of ever increasing spatial scales in the form of beds of dowels of ever larger radius, one is moving efficiently toward a data bank on firespread (if any) across a "field of telephone poles". Seemingly of higher priority is obtaining insight on the rate of flow-assisted firespread between buildings. Buildings are characterized by internal structure, with a floor, ceiling, walls, and contained combustible matter; in contrast, a dowel has no internal structure.

An optimal agenda for obtaining insight on the rate of firespread through arrays of houses is difficult because there exist no known scaling laws that permit extrapolation from laboratory-scale observations to full-scale observations. Currently, if one wants definitive information about firespread through an array of houses, one must burn many arrays of houses. Hopefully, just as simple interpretation of data and use of similitude arguments have permitted highly plausible conjectures to be made concerning the burning of thicker dowels from experimental observations on thinner dowels, so one hopes that highly plausible extrapolations to larger scale will evolve from testing on smaller scale for the rate of firespread under wind aiding through discrete fuel elements with internal structure.

We suggest that flow-assisted firespread across regular arrangements of wooden boxes with covers be examined, with the fuel apportioned among the outer sheath, the rafters, and the internal combustible contents to match the apportioning in structures (homes and/or buildings) of interest. At first, a single dimension ℓ is to characterize the (cubic) boxes, but in later tests, the width, height, and depth of the outer sheath may be

unequal. A plausible succession of values for the dimension ℓ may be 12.5 cm, 25 cm, 50 cm, 120 cm, and 240 cm. It may be noted that the test-section width in the current firetunnel facility is 110 cm, so the last two values (at least) would require a larger indoor facility or outdoor testing. It is emphasized that what is being suggested is a program that proceeds to the testing on scales comparable to those of actual structures.

It is also useful to introduce the spatial dimension L, the distance between wooden boxes. At first, the streamwise and transverse separations between wooden boxes might be equal, so a single dimension suffices for description; later, the consequences of unequal separations may be investigated. In a typical envisioned test, a regular arrangement of wooden boxes is placed in the test section of the firetunnel, the blower is turned on to produce a preselected wind speed (unless spread in the absence of an ambient wind is being investigated), and a gas-jet-diffusion-flame igniter is used to ignite simultaneously and identically the burning of all boxes in the upwindmost row (Figure 38). Photographic recording and thermocouples are then used to record the subsequent fire event.

After testing at each value within the range of wind speeds, it will be interesting to inquire how the spread rate v_f varies with wind speed U and fuel loading m; in particular, it will be interesting to ascertain whether it is sufficient to seek v_f in terms of U and m (only), and, if so, whether $v_f \sim (U/m)^q$, where $q \simeq 0.5$.

It is reiterated that testing is to be repeated for different values of the wooden-box dimension ℓ, so that ℓ takes on a succession of values $\ell_1, \ell_2, \ell_3, \ldots$ Clearly a purpose of this agenda is to develop a predictive capability, with the aid of theoretical modeling, that can be extrapolated to larger scales $\ell_4, \ell_5, \ldots$.

As a preliminary example of the tests just outlined, the results are discussed for three tests with regular arrays of small empty paper boxes (2.8 cm x 2.4 cm x 3.8 cm), each box pierced with eight round toothpicks with an average diameter of 2 mm. The toothpicks, 6.5 cm in length and protruding from the sides of the boxes, constituted 50% of the box-assembly mass of 3.255 g. The char remaining after burning was rough 0.173 g (Figure 39). In the tests to be described, the upwindmost 15-20 cm of the

(a) Overhead View

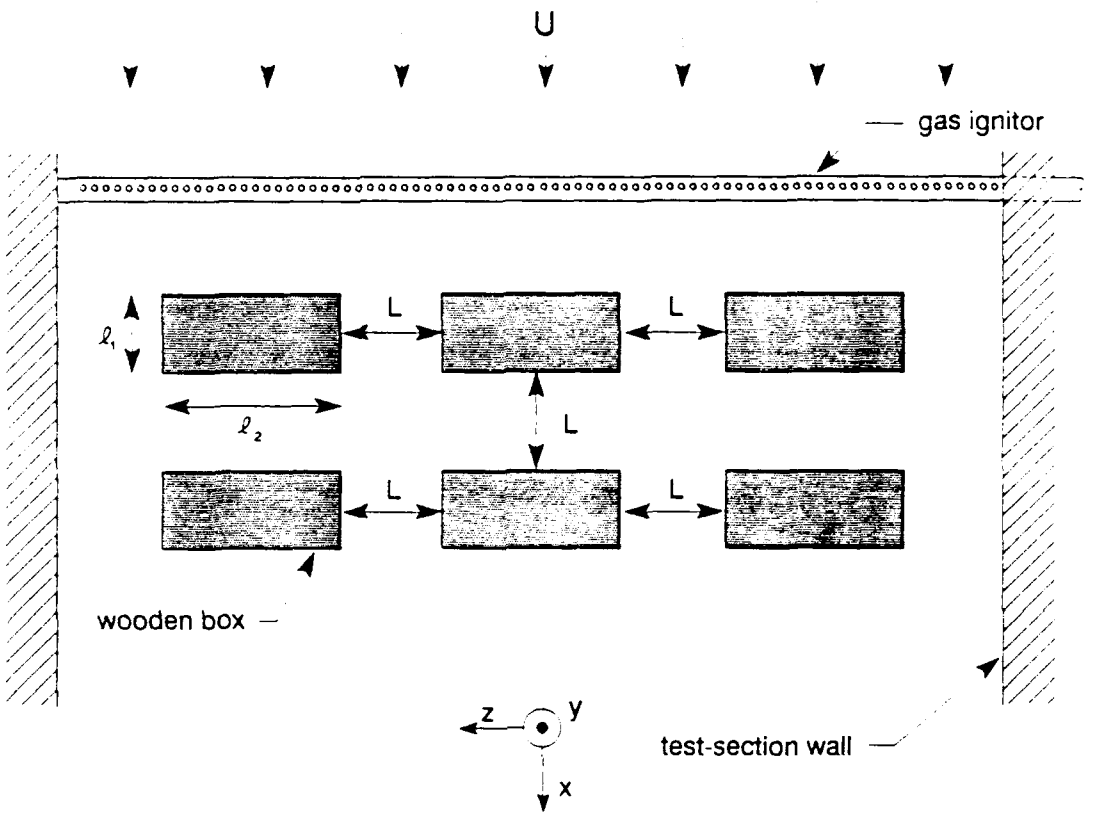

(b) Side View

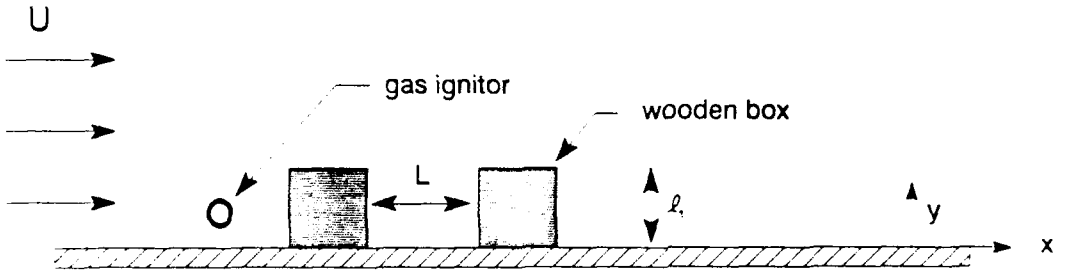

Figure 38. (a) A planform sketch is presented of a firetunnel experiment to study the wind-aided firespread across a regular array of identical wooden boxes of length and height ℓ_1, width ℓ_2, and separation distance L. The boxes, which have "roofs", may contain an internal fuel loading. This experiment is to be repeated for various dimensions (and wind speeds U), to assist in the evolution of urban-firespread scaling laws, with the aid of dimensional analysis and analytic modeling. (b) A side-view sketch of the same configuration is presented.

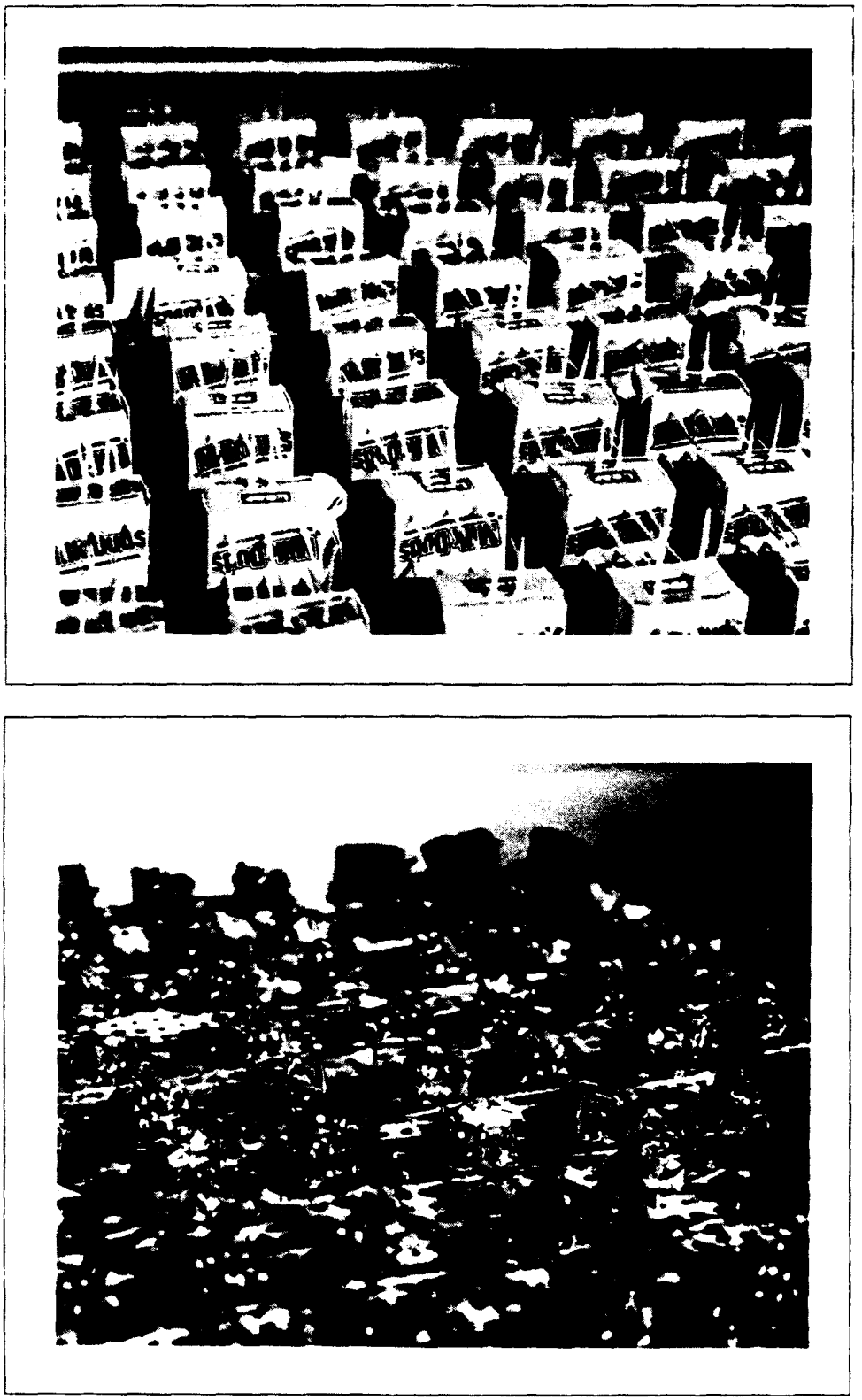

Figure 39. Photographs of the fuel bed before and after test 194, involving a regular arrangement on a 6-cm x 6-cm grid of small paper boxes (2.8 cm x 2.4 cm x 3.8 cm), each pierced with eight protruding toothpicks. The 55-cm-wide bed was burned in a wind of 1.6 cm/s. Each box assembly initially had 3.255 g, of which half was contributed by the toothpicks; about 0.173 g remained as char after the test.

fuel bed was loaded with round white-pine toothpicks, for ease of ignition (Figure 40). This figure also presents the packing arrangements for each of the three tests. For a 10-cm x 10-cm grid (box-center-to-box-center distance), the fuel loading $m = 0.31$ kg/m^2; for an 8-cm x 8-cm grid, $m = 0.48$ kg/m^2; for a 6-cm x 6-cm grid, $m = 0.86$ kg/m^2. Since only the unshaded boxes burned, inspection of Figure 40 indicates that sustained firespread occurred only for the heaviest of the three loadings; since the measured burned time was roughly 100 seconds and the flame speed was roughly 1 cm/s, a minimum test length of about 100 cm is required to achieve a quasisteadily propagating structure, and the results are of marginal credibility. On the basis of results obtained from testing with 1.3-mm-diameter plain white-pine toothpicks [for which $v_f = 1.13\ (U/m)^{1/2}$, where U is in m/s, m is in kg/m^2, and v_f is in cm/s], a spread rate of 1.5 cm/s would have been expected for the conditions of the test. While the result of about 0.8 cm/s was much slower, presumably owing to the nature of the fuel loading, the possible pertinence of a relation of the form $v_f \sim (U/m)^q$, perhaps even with $q = 0.5$, is not prejudiced by the result.

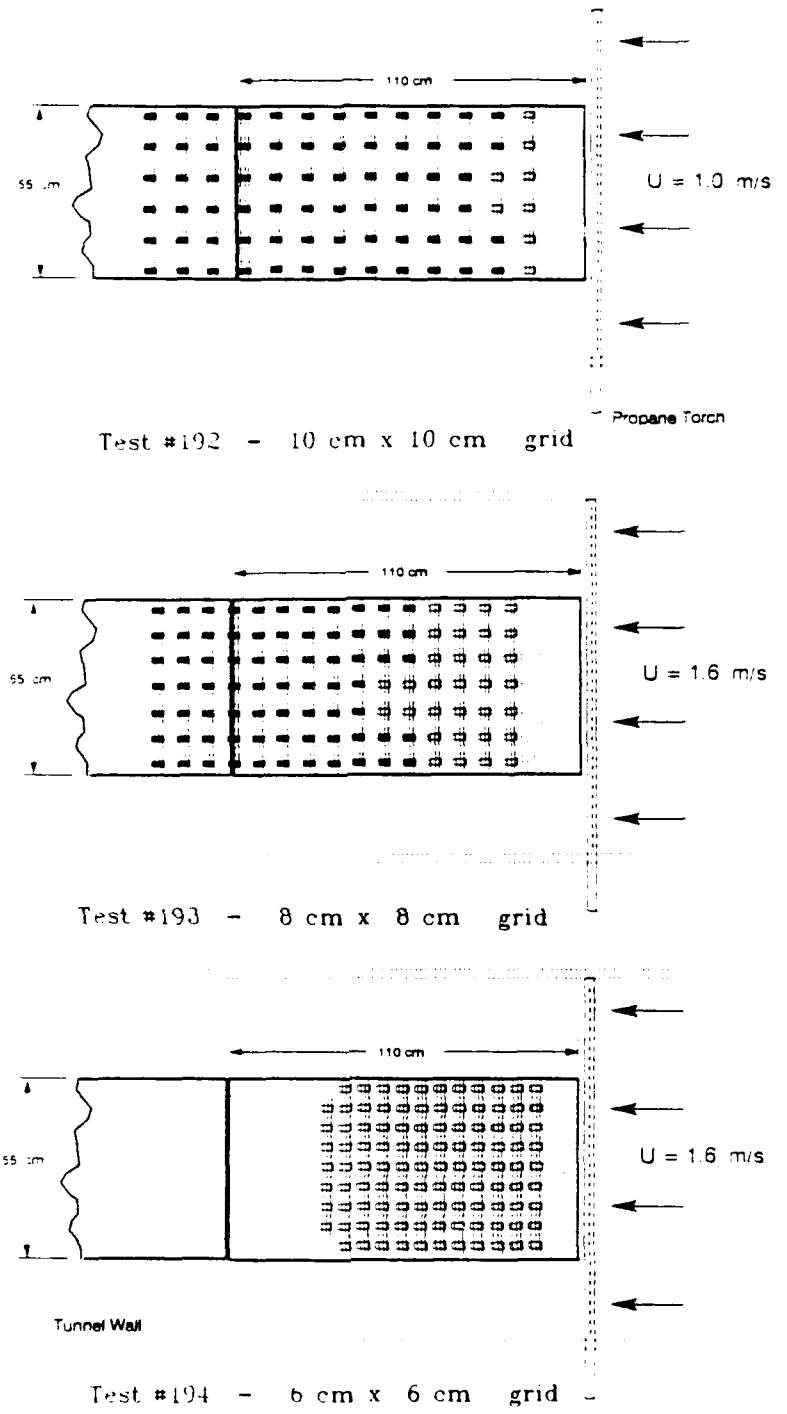

Figure 40. A schematic of the fuel-bed loading for each of three tests with regular arrangements of small paper boxes, each with protruding toothpicks. The boxes are designated by small shaded squares with associated line segments. The upwindmost portion of the fuel bed was loaded with regularly arranged vertical white-pine toothpicks, the leading row of which was ignited by a propane torch to initiate a test in the noted wind U. An unshaded box indicates one which burned in the ensuing firespread.

SECTION 7

LIST OF REFERENCES

Anderson, H. E., and Rothermel, R. C. 1965 Influence of moisture and wind upon the characteristics of free-burning fires. Tenth Symposium (International) on Combustion, 1009-1019. Pittsburgh, PA: Combustion Institute.

Beach, K. L., Carrier, G. F., Fendell, F. E., Gat, N., Hsu, C. T , Kwoh, D. S. W., Lake, B. M., Wagner, R. N., and Wolff, M. F. 1986 Laboratory fire modeling. 1. Wind-aided flame spread. 2. Wet coagulation of smoke. Technical report DNA-TR-86-248. Washington, DC: Defense Nuclear Agency.

Byram, G. M., Clements, H. B., Bishop, M. E., and Nelson, Jr., R. M. 1966 An experimental study of model fires. Macon, Georgia: Southern Forest Fire Laboratory, Forest Service.

Caidin, M. 1960 A Torch to the Enemy--The Fire Raid on Tokyo. New York, NY: Ballantine.

Carrier, G. F., Fendell, F. E., and Hsu, C. T. 1985 Modeling of aspects of large-area fires. Technical report DNA-TR-85-100. Washington, DC: Defense Nuclear Agency.

Carrier, G. F., Fendell, F.E., and Feldman, P. S. 1985 Firestorms. Journal of Heat Transfer 107, 19-27.

Carrier, G. F., and Fendell, F. E. 1986 Firestorms--the thermohydrodynamics of destruction. Mechanical Engineering 108 (12), 50-54.

Carslaw, H. S., and Jaeger, J. C. 1959 Conduction of Heat in Solids, 2nd edition. Oxford, England: Clarendon.

Cheney, N. P. 1981 Fire behavior. Fire in the Australian Biota, 151-175. Canberra, Australia: Australian Academy of Science.

Davison, C. 1931 The Japanese Earthquake of 1923. London, England: Thomas Muirby.

Emmons, H. W. 1965 Fundamental problems of the free burning fire. Tenth Symposium (International) on Combustion, 951-964. Pittsburgh, PA: Combustion Institute.

Emmons, H. W., and Shen, T. 1971 Fire spread in paper arrays. Thirteenth Symposium (International) on Combustion, 917-926. Pittsburgh, PA: Combustion Institute.

Fang, J. B. 1969 An investigation of the effect of controlled wind on the rate of fire spread. Ph.D. thesis, Department of Chemical Engineering. Fredericton, Canada: University of New Brunswick.

Fang, J. B., and Steward, F. R. 1969 Flame spread through randomly packed fuel particles. Combustion and Flame 13, 392-398.

Fendell, F. E. 1965 Ignition and extinction in combustion of initially unmixed reactants. Journal of Fluid Mechanics 21, 281-303.

Fendell, F. E. 1986 Crown streets. Combustion Science and Technology 45, 311-315.

Fleeter, R. D., Fendell, F. E., Cohen, L. M., Gat, N., and Witte, A. B. 1984 Laboratory facility for wind-aided firespread along a fuel matrix. Combustion and Flame 57, 289-311.

Fons, W. L. 1946 Analysis of fire spread in light forest fuels. Journal of Agricultural Research 72, 93-121.

Glasstone, S., and Dolan, P. J. 1977 The Effects of Nuclear Weapons, 3rd ed. Washington, DC: U.S. Department of Defense and U.S. Department of Energy.

Luke, R. H., and McArthur, A. G. 1977 Bushfires in Australia. Canberra, Australia: Australian Government Printing.

Miller, R. A. 1970 Flame propagation in two-dimensional matchstick arrays. Report, Department of Aerospace and Mechanical Sciences. Princeton, NJ: Princeton University.

Mushan, H. A. 1941 The great Chicago fire, October 8-10, 1971. Papers in Illinois History and Transactions for the Year 1940, 69-189. Springfield, IL: Illinois State Historical Society.

Nelson, Jr., R. M., and Adkins, C. W. 1986 Flame characteristics of wind-driven surface fires. Canadian Journal of Forestry Research 16, 1293-1300.

Nelson, R. M., Jr., and Adkins, C. W. 1988 Flame characteristics of wind-driven fires in surface fuels. Canadian Journal of Forestry Research 18, 391-397.

Noble, W. S. 1977 Ordeal by Fire--The Week a State Burned Up. Melbourne, Australia: Hawthorn.

Prahl, J. M., and T'ien, J. S. 1973 Preliminary investigation of forced convection on flame propagation along paper and matchstick arrays. Combustion Science and Technology 7, 271-282.

Pyne, Stephen J. 1982 Fire in America--A History of Wildland and Rural Fire. Princeton, NJ: Princeton University.

Rothermel, R. C., and Anderson, H. E. 1966 Fire spread characteristics determined in the laboratory. Research Paper INT-30. Ogden, UT: Intermountain Forest & Range Experiment Station, Forest Service.

Simpson, R. W. 1989 The Fires of '88--Yellowstone Park and Montana in Flames. Helena, MT: American Geographic.

Spalding, D.B. 1955 Some Fundamentals of Combustion. New York, NY: Academic.

Steward, F. R. 1974a Fire spread through a fuel bed. Heat Transfer in Fires: Thermophysics, Social Aspects, Economic Impact, 315-378. Washington, DC: Scripta.

Steward, F. R. 1974b Fire spread through various types of fuel beds. Report, Fire Science Centre. Fredericton, Canada: University of New Brunswick.

Steward, F. R., and Tennankore, K. N. 1981 The measurement of the burning rate of an individual dowel in a uniform fuel matrix. Eighteenth Symposium (International) on Combustion, 641-646. Pittsburgh, PA: Combustion Institute.

Steward, F. R., and Waibel, R. T. 1973 Flame spread through uniform fuel matrices. Report, Fire Science Center. Fredericton, Canada: University of New Brunswick.

Steward, F. R., Wuest, L. J., and Waibel, R. T. 1977 Some characteristics of fires within uniform fuel matrices. Heat Transfer Division Paper 77-HT-71. New York, NY: American Society of Mechanical Engineers.

Taylor, G. I. 1961 Fire under influence of natural convection. International Symposium on the Use of Models in Fire Research, 10-28. Washington, DC: National Academy of Sciences--National Research Council (Publication 786).

Telisin, H. P. 1974 Flame radiation as a mechanism of fire spread in forests. Heat Transfer in Flames, 441-449. Washington, DC: John Wiley.

Thomas, P. H. 1971 Rates of spread of some wind-driven fires. Forestry 44, 155-175.

Van Wagner, C. E. 1968 Fire behaviour mechanisms in a red pine plantation: field and laboratory evidence. Publication 1229. Chalk River, Ontario Canada: Petawawa Forest Experiment Station, Department of Forestry and Rural Development.

Vogel, M., and Williams, F. A. 1970 Flame propagation along matchstick arrays. Combustion Science and Technology 1, 429-43.

Wells, R. W. 1968 Fire at Peshtigo. Englewood Cliffs, NY: Prentice-Hall.

APPENDIX A

ALTERNATE APPROXIMATIONS FOR THE MODELING

We now develop alternative approaches to the simple analytic modeling of quasisteady wind-aided firespread across a bed of discrete fuel elements. These alternatives involve different physical approximations (e.g., here we consider, inter alia, a well-mixed, isothermal fuel bed) and different methods (e.g., here we consider a semi-empirical approach) from those adopted in Section 4, in which there was developed a first-principles-based approach, based on convective/diffusive preheating (with comments on radiational preheating) for a nonisothermal bed with finite thermal conductivity. The material below is included for contrast only; it is relegated to an appendix because we regard the approach in the main text as <u>superior</u> for the present study.

A major distinction between the approach in Section 4 and the present approach is that here we adopt <u>two</u> spatial scales for the downwind preheat region (Figures 7 and 8): the vertical scale Y (defined as before) is joined by a horizontal scale X. Together with the key output sought, the rate v_f of firespread, we now require three equations to ascertain these three unknowns. It is emphasized that X pertains to the preheat zone, and is distinct from the length L characterizing the streamwise expanse of the pyrolysis zone:

$$mv_f = \int_{-L}^{0} \dot{m}\, dx, \quad \dot{m}(x) = \rho_b v_b(x), \tag{A.1}$$

where $v_b(x)$ is the speed in the y direction with which the substratum beneath the fuel bed approaches an observor fixed on the bed surface. Actually, identifying L is not required for finding v_f.

From the conservation of energy [see (4.3)]

$$YU\rho_o \sim mv_f\left(\frac{Q}{c_p T_f}\right), \tag{A.2}$$

where the notation is defined in Section 4.

Empirically (Figures 41, 42, and 43),

$$A \sim \left(\frac{m}{U}\right)^{\alpha}, \tag{A.3a}$$

where A is the angle of inclination (of the gas-phase isotherms at the pyrolysis front x = 0 with respect to the ray in the direction of propagation), as inferred from thermocouple-rake data obtained in the experimental facility. [The angle A is to be distinguished from the function of integration A(s) introduced in (4.7).] For small values of A, and, in any case for present purposes,

$$\frac{Y}{X} \sim \left(\frac{m}{U}\right)^{\alpha}, \tag{A.3b}$$

where $1 \gg \alpha > 0$ for $m = 0(0.05\ g/cm^2)$, and $U = 0(1\ m/s)$.

Conservation of energy in the preheating portion of the fuel bed, for an observor in the steady frame of reference of the propagating firefront (Figures 7 and 8), is given by (again, T denotes the temperature above ambient temperature, which is taken to be the same for both air and fuel bed)

$$k_b T_{yy} + \frac{\rho_b c_b v_f}{X} T_{\chi} = 0,\ 0 < y < H,\ 0 < \chi < \infty. \tag{A.4}$$

As in Section 4, for the analysis, the vertical coordinate y has been taken positive downward, in contrast to the convention adopted in the just-cited figures; however, the streamwise coordinate x is still positive downwind (in contrast to the procedure for the analysis in Section 4), and $\chi = x/X$, with X still to be identified. If one adopts the Fourier transform over the domain $-\infty < \chi < \infty$ (although the results of interest are limited to nonnegative values of χ), then the transform and its inversion are here defined to be

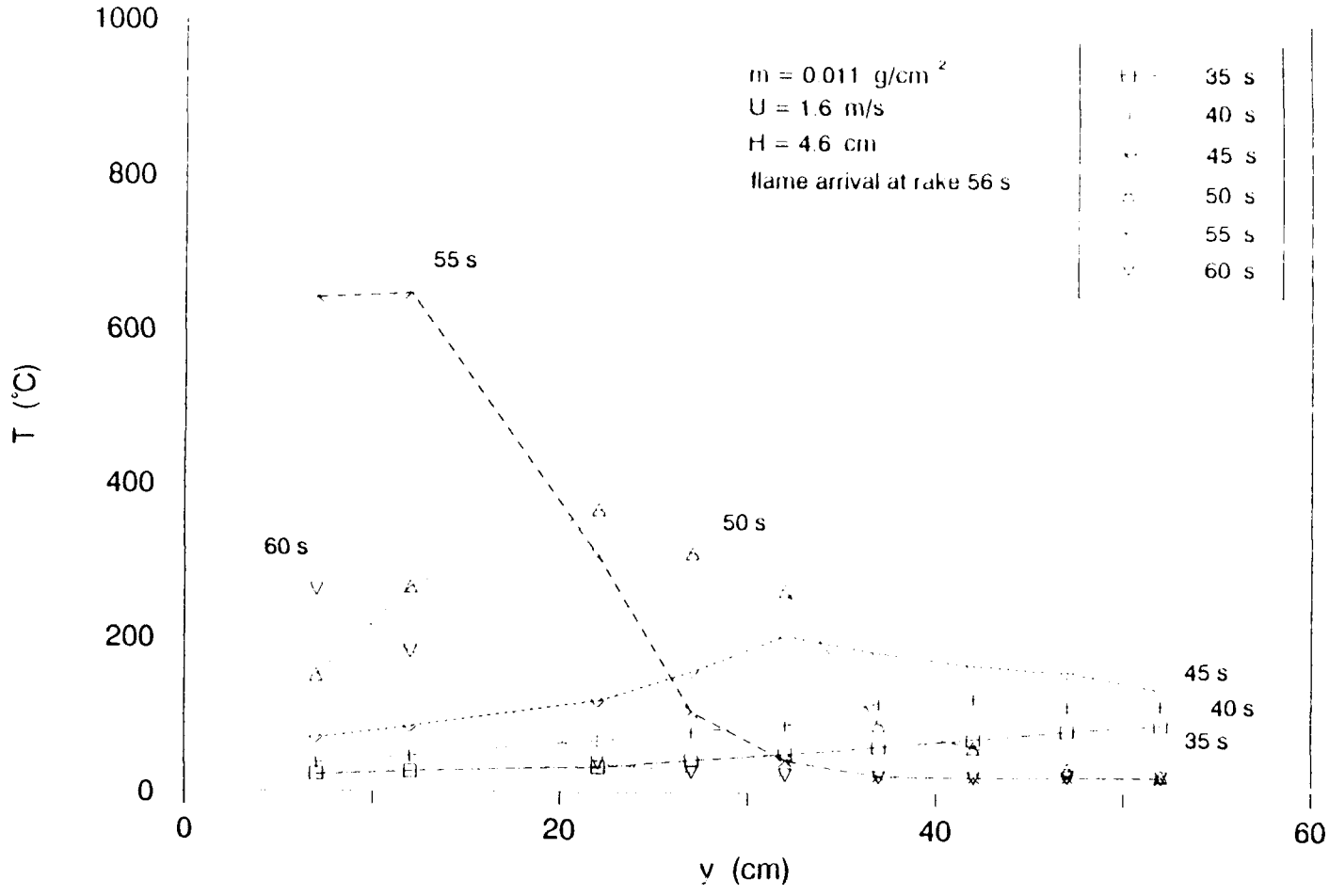

Figure 41. Gas temperature T as a function of height y above the surface of a fuel bed (composed of flat-sided white-pine toothpicks), for various times during firefront passage. The fuel loading m, the wind speed U, and the fuel-element height H are cited on the figure. The temperatures are inferred from the output of thermocouples distributed at heights signified by the data points. The rake itself is situated at the fuel-bed (streamwise) centerline, about 2 m downwind from the leading edge of the bed.

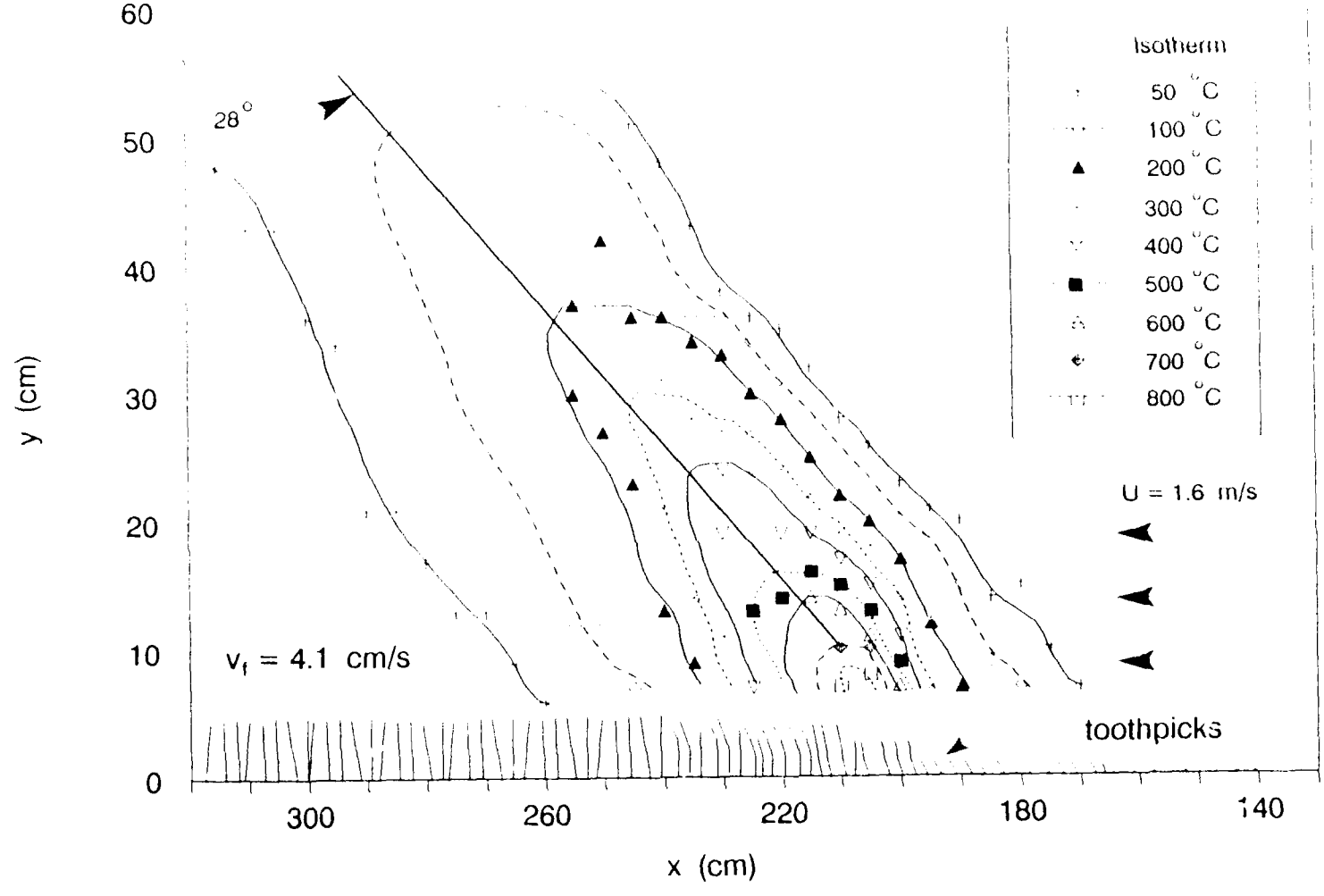

Figure 42. On the basis that the flamefront is propagating downwind at the known quasisteady speed v_f = 4.1 cm/s [inferred from the output furnished by other, near-fuel-bed-surface thermocouples, distributed along the streamwise centerline of the bed], the data of Figure 41 yield the above-plotted isotherms. An angle of inclination A with respect to the downwind horizontal is inferred for the isotherms; 0° implies isotherms blown flat onto the downwind bed, whereas 90° implies isotherms symmetric with respect to the perpendicular to the fuel-bed surface.

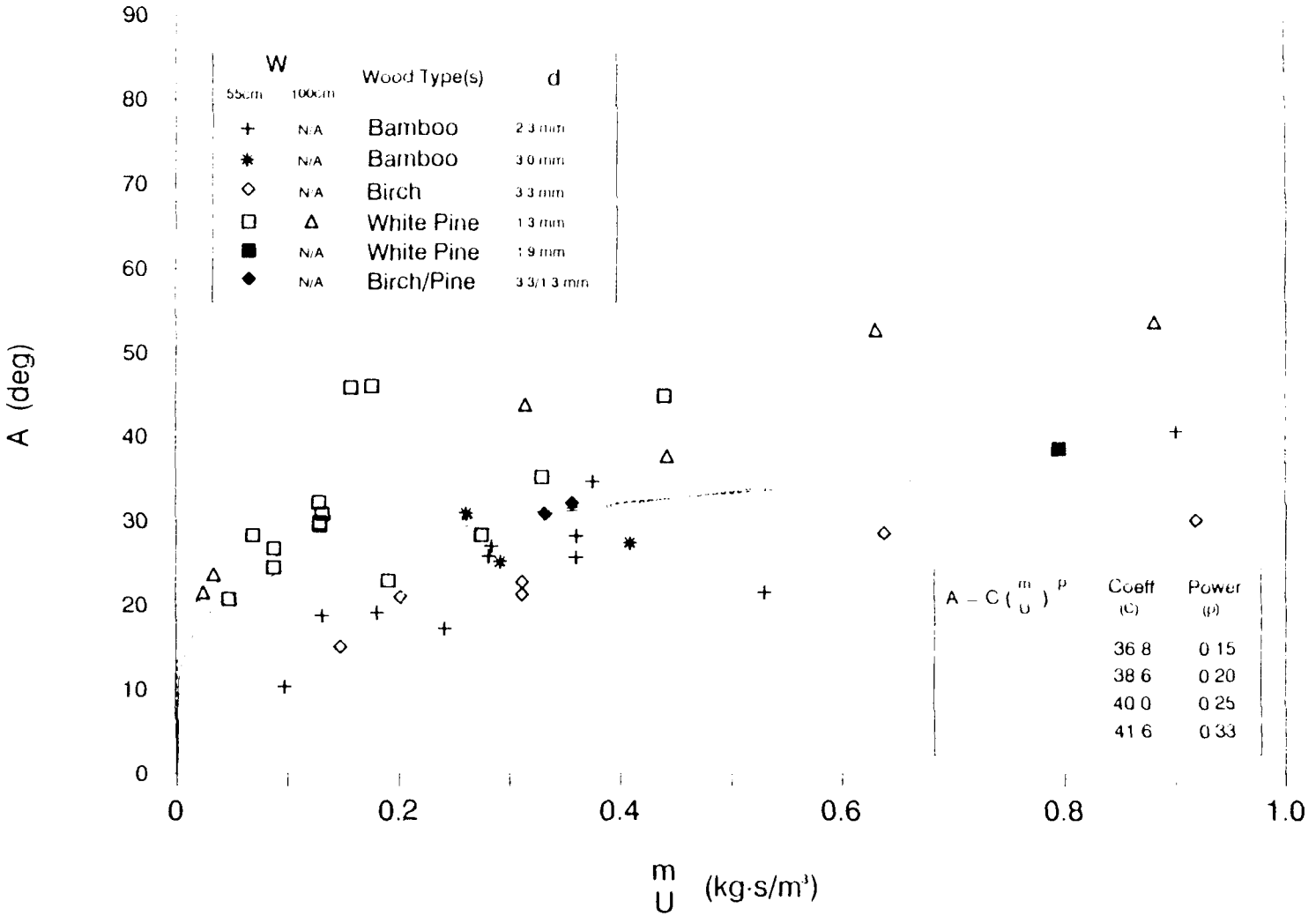

Figure 43. A compilation of results (obtained by the procedures described by Figures 41 and 42) for the isotherm-tilt angle A as a function of the ratio of the fuel loading m to the wind speed U. The experiment involves beds of width W with fuel elements of effective diameter d. Several power-laws curve fits are plotted as well.

$$\bar{T}(\xi,y) = \int_{-\infty}^{\infty} T(\chi,y) \exp(-i\chi\xi)\, d\chi, \tag{A.5a}$$

$$T(\chi,y) = \frac{1}{2\pi} \int_{-\infty}^{\infty} \bar{T}(\chi,y) \exp(i\xi\chi)\, d\xi. \tag{A.5b}$$

Hence, (A.4) becomes

$$\bar{T}_{yy} + \frac{\rho_b c_b v_f}{\chi} (i\xi)\, \bar{T} = 0, \tag{A.6a}$$

$$\bar{T}(\xi,y) = \tilde{A}(\xi) \exp\left[-\left(\frac{i\xi\rho_b c_b v_f}{k_b \chi}\right)^{1/2} y\right], \tag{A.6b}$$

for $H \to \infty$. But, since T_f is constant, for a convective-conductive mode of heat transfer from the gas phase to the fuel bed, for $\chi > 0$, if $f(\chi)$ is a function that decreases monotonically to zero (as its argument increases) at least rapidly enough to ensure boundedness,

$$k_b T_y(\chi,0) = -f(\chi)/Y, \text{ or } k_b \bar{T}_y(\xi,0) = -\bar{f}(\xi)/Y. \tag{A.7}$$

Hence, from (A.5b), (A.6b), and (A.7),

$$T(\chi,0) = \frac{1}{2\pi Y} \left(\frac{k_b \chi}{\rho_b c_b v_f}\right)^{1/2} \int_{-\infty}^{\infty} \frac{\bar{f}(\xi) \exp(i\xi\chi)}{(i\xi)^{1/2}}\, d\xi. \tag{A.8}$$

But, by definition, $T(0,0) = T_{pyr}$, the pyrolysis temperature, a given constant. Hence, from (A.8),

$$Y \sim \left(\frac{\chi}{v_f}\right)^{1/2}. \tag{A.9}$$

From (A.2), (A.3b), and (A.9), for preheating primarily by convective diffusion, with a finite value for the effective thermal conductivity k_b,

$$v_f \sim \left(\frac{U}{m}\right)^{(1+\alpha)/2}, \quad Y \sim \left(\frac{U}{m}\right)^{(\alpha-1)/2}, \quad X \sim \left(\frac{U}{m}\right)^{(3\alpha-1)/2}. \tag{A.10}$$

The appearance of $(\alpha/2)$ in the expressions for v_f and Y reduces the sensitivity to the (somewhat uncertain) value of α. For $\alpha = 0$, the square-root dependence obtained in (4.11) for v_f on the ratio (U/m) for convective/diffusive preheating is recovered. In fact, $\alpha = o(1)$; although the data are somewhat scattered, the assignment $\alpha \simeq 0.15$ is plausible (Figure 43). Intuitively, the result that the horizontal scale X decreases as (U/m) increases seems anomalous, but the dependence is rather weak (the exponent $\simeq -0.28$).

If one considers a fuel bed of finite depth H with no heat transfer to the substratum, then for preheating one considers (A.4) subject to (A.7) and

$$T(\infty,y) = 0, \quad T(0,0) = T_{pyr}, \quad k_b T_y(\chi,-H) = 0. \tag{A.11}$$

For a uniformly mixed fuel bed (i.e., for the case in which k_b increases as T_y decreases, such that the product is finite and the fuel-bed temperature approaches invariance with depth), one may integrate over $0 < y < H$ to obtain

$$-k_b T_y(\chi,0) + \frac{\rho_b v_f c_b H}{X} T_\chi = 0, \tag{A.12}$$

or

$$T_\chi = -\frac{X f(\chi)}{\rho_b v_f c_p H Y}. \tag{A.13}$$

Since $\rho_b H = (m + m_o)$ by definition, where m_o is the mass of air per unit planform area of the bed (and $m \gg m_o$ except for very light fuel loading),

$$T(\chi) = T_{pyr} - \frac{X \int_0^{\chi} f(x_1)\, dx_1}{c_b v_f Y (m + m_o)} , \tag{A.14}$$

or

$$T_{pyr} = \frac{X \int_0^{\infty} f(x_1)\, dx_1}{c_b v_f Y (m + m_o)} , \text{ or } Y \sim \frac{X}{v_f (m + m_o)} . \tag{A.15}$$

This relation, together with (A.2) and (A.3b), yields

$$v_f \sim \left(\frac{U}{m}\right)^{\alpha} \frac{1}{m + m_o} , \; Y \sim \left(\frac{U}{m}\right)^{\alpha - 1} \frac{1}{m + m_o} , \; X \sim \left(\frac{U}{m}\right)^{2\alpha - 1} \frac{1}{m + m_o} . \tag{A.16}$$

For $1 \gg \alpha > 0$, these results are at odds with observation.

For radiative transfer as the dominant mode of preheating [compare (4.4a) and (4.4b)], (A.7) becomes (g decreases monotonically to zero as its argument increases)

$$k_b T_y(\chi, 0) = - g(\chi) Y , \tag{A.17}$$

so (A.2) and (A.3b) are complemented by

$$Y \sim \left(\frac{v_f}{X}\right)^{1/2} . \tag{A.18}$$

Hence,

$$v_f \sim \left(\frac{U}{m}\right)^{(3-\alpha)/2}, \quad Y \sim \left(\frac{U}{m}\right)^{(1-\alpha)/2}, \quad X \sim \left(\frac{U}{m}\right)^{(1+\alpha)/2}. \tag{A.19}$$

Again, as $\alpha \to 0$, one recovers the corresponding results for v_f in Section 4, explicitly, (4.12). It may be noted as a check that indeed, for radiative preheating, an increase in the Y scale implies a comparable increase in the X scale, especially as $\alpha \to 0$.

For uniform mixing over the fuel-bed depth, but with radiative transfer from the gas phase as the mechanism for fuel-bed preheating, so that (A.7) is replaced by (A.17) when substituting into (A.12), then (A.15) is replaced by

$$Y \sim \frac{v_f(m + m_o)}{X}, \tag{A.17}$$

or, with (A.2) and (A.3b),

$$v_f \sim \left(\frac{U}{m}\right)^{2-\alpha} (m + m_o), \quad Y \sim \left(\frac{U}{m}\right)^{1-\alpha} (m + m_o), \quad X \sim \left(\frac{U}{m}\right) (m + m_o). \tag{A.18}$$

For $1 \gg \alpha > 0$, again the results are at odds with observations.

APPENDIX B

PARTIAL LIST OF SYMBOLS

English Symbols

A	angle of ascent of the buoyant gases, measured from the downwind horizontal
a_o	speed of sound at ambient conditions
$A(s)$	function of integration
c_b	specific heat capacity of the gas at constant pressure
d	effective diameter of fuel elements
d_t	burning-zone thickness
f	fraction of the horizontal area occupied by fuel (dimensionless)
H	height of the fuel elements; also, depth of the fuel bed
k	thermal conductivity of the gas
k_b	effective thermal conductivity of the fuel bed
k_o	thermal conductivity of the gas near the flame at the pyrolysis front
	box dimension
L	streamwise length of the fuel bed; also, the distance between boxes
$\tilde{L}$	effective streamwise (horizontal) distance over which radiative preheating is received (cm)
m	mass of thin fuel per unit planform area of the bed (g/cm^2)
m_o	mass of air per unit planform area of the bed; also, a reference fuel loading
M	positive real constant which characterizes the radiative-heat-transfer profile
n	number of elements per unit planform area; also, a constant (typically, an exponent)
N	number of toothpicks; also, a positive real number which characterizes the convective-heat-transfer profile

PARTIAL LIST OF SYMBOLS

English Symbols

p	constant (typically an exponent)
q	downward heat flux
Q	heat released per unit mass of fuel burned, after subtraction of the sensible and latent preheating required to bring the mass from the ambient to the pyrolysis condition
$\tilde{Q}$	total (time-integrated) heat incident on the fuel (erg/g)
R	ratio of the number of nails to the number of toothpicks
s	spacing of toothpicks, also, the integration variable in the Laplace transform
t	time
t_{burn}	time during which the fuel-bed temperature exceeds 473 K
t_r	flame-residence time (s)
T_f	flame temperature
T_∞	ambient temperature
T_{pyr}	pyrolysis temperature
U	ambient wind speed
v_f	rate of firespread (cm/s)
V	product of V_1 and f
V_1	fuel-geometry and orientation portion of the view factor (dimensionless)
W	width of the fuel bed
x	coordinate in the streamwise direction, positive downwind
X	characteristic horizontal scale
y	axis perpendicular to x and to the gas/fuel-bed interface (typically positive into the gas phase)
Y	stand-off distance of the flame from the gas-solid interface at the pyrolysis front

PARTIAL LIST OF SYMBOLS

Greek Symbols

α	constant (dimensionless)
β	constant used in the Laplace-transform-inversion integral
ϵ	absorption coefficient of the hot gas (cm^{-1})
γ	ratio of specific heats; also, the tilt angle of the buoyant gases, measured from the vertical axis (the complementary angle of A)
θ	width of the test section of the fire tunnel
κ	thermal diffusivity of the gas phase
κ_b	bulk thermal diffusivity of fuel bed
ξ	x/Y
ρ	gas density
ρ_b	mass of bed per unit volume of bed
ρ_s	solid-fuel density
σ	Stefan-Boltzmann constant, 5.67×10^{-5} erg/(s cm^2 K^4); also, standard deviation
ϕ	porosity
χ	x/X

Superscripts

-	Laplace-transformed variable

Subscripts

b	Pertaining to the fuel bed
f	Pertaining to the flame

DISTRIBUTION LIST

DNA-TR-89-193

DEPARTMENT OF DEFENSE

DEFENSE INTELLIGENCE AGENCY
ATTN: DB-6E2 C WIEHLE
ATTN: RTS-2B
ATTN: WDB-4CR

DEFENSE NUCLEAR AGENCY
ATTN: COL G GIDDINGS
ATTN: OPNS
ATTN: RAAE
2 CYS ATTN: TDTR
4 CYS ATTN: TITL

DEFENSE NUCLEAR AGENCY
ATTN: TDNM
2 CYS ATTN: TDTT W SUMMA

DEFENSE TECHNICAL INFORMATION CENTER
2 CYS ATTN: DTIC/FDAB

THE JOINT STAFF
ATTN: JKCS

DEPARTMENT OF THE ARMY

DEPARTMENT OF THE ARMY
ATTN: DAMO-SWS

DEPARTMENT OF THE AIR FORCE

STRATEGIC AIR COMMAND/XRFS
ATTN: XRFS

DEPARTMENT OF ENERGY

LAWRENCE LIVERMORE NATIONAL LAB
ATTN: J PENNER
ATTN: J BACKOVSKY
ATTN: R PERRETT
ATTN: M MACCRACKEN

LOS ALAMOS NATIONAL LABORATORY
ATTN: M GILLESPIE

SANDIA NATIONAL LABORATORIES
ATTN: B ZAK, ORG 6321

OTHER GOVERNMENT

DEPARTMENT OF TRANSPORTATION
ATTN: S F SINGER

DIRECTOR, FFASR
ATTN: C CHANDLER

FEDERAL EMERGENCY MANAGEMENT AGENCY
ATTN: OFC OF CIVIL DEFENSE, J F JACOBS

NASA
ATTN: O TOON
ATTN: T ACKERMAN

NATIONAL BUREAU OF STANDARDS
ATTN: G MULHOLLAND

NATIONAL CENTER ATMOSPHERIC RESEARCH
ATTN: S SCHNEIDER

NATIONAL CLIMATE PROGRAM OFFICE
ATTN: A HECHT

NATIONAL INSTITUTE OF STANDARDS & TECHNOLOGY
ATTN: H BAUM
ATTN: R LEVINE

OFFICE OF SCIENCE AND TECH POLICY
ATTN: MAJ S HARRISON

USDA FOREST SERVICE
ATTN: D WARD

USDA FOREST SERVICE
ATTN: P RIGGAN

DEPARTMENT OF DEFENSE CONTRACTORS

CALIFORNIA RESEARCH & TECHNOLOGY, INC
ATTN: M ROSENBLATT

CARPENTER RESEARCH CORP
ATTN: H J CARPENTER

CHARLES SCAWTHORN
ATTN: C SCAWTHORN

COLORADO STATE UNIVERSITY
ATTN: D KRUGER

DESERT RESEARCH INSTITUTE
ATTN: J HUDSON

IIT RESEARCH INSTITUTE
ATTN: H NAPADENSKY

INSTITUTE FOR DEFENSE ANALYSES
ATTN: L SCHMIDT

KAMAN SCIENCES CORP
ATTN: D ALDERSON
ATTN: DASIAC
ATTN: E CONRAD
ATTN: J MOULTON

KAMAN SCIENCES CORPORATION
ATTN: DASIAC

MISSION RESEARCH CORP
ATTN: G MCCARTOR

MODELING SYSTEM, INC
ATTN: G BERLIN

NOTRE DAME DU LAC, UNIV OF
ATTN: T J MASON

PACIFIC-SIERRA RESEARCH CORP
ATTN: H BRODE
ATTN: R SMALL

R & D ASSOCIATES
ATTN: D HOLLIDAY
ATTN: F GILMORE

RAND CORP
ATTN: ENGR & APPLIED SCIENCES DEPT

RAND CORP
ATTN: B BENNETT

SCIENCE APPLICATIONS INTL CORP
ATTN: DR M MCKAY
ATTN: L HUNT

SCIENCE APPLICATIONS INTL CORP
ATTN: D BACON
ATTN: J COCKAYNE

SCIENTIFIC SERVICES, INC
ATTN: C WILTON

SRI INTERNATIONAL
ATTN: G ABRAHAMSON

STAN MARTIN AND ASSOCIATES
ATTN: S B MARTIN
ATTN: S MARTIN

SWETL, INC
ATTN: T Y PALMER

TRW INC
2 CYS ATTN: F FENDELL
2 CYS ATTN: G F CARRIER
2 CYS ATTN: M E WOLFF

UNIVERSITY OF NEW MEXICO
ATTN: H GLOVER

UNIVERSITY OF WASHINGTON
ATTN: L RADKE

DIRECTORY OF OTHER

HARVARD UNIVERSITY
ATTN: G CARRIER

MARYLAND UNIVERSITY OF
ATTN: A ROBOCK DEPT METEOROLOGY

UCLA
ATTN: R TURCO